(NASA-TM-X-62360) LOW SPEED AERODYNAMIC CHARACTERISTICS OF AN 0.075-SCALE F-15 AIRPLANE MODEL AT HIGH ANGLES OF ATTACK AND SIDESLIP (NASA) 118 p HC A06/MF A01 CSCL 01A G3/02

N78-10019

Unclas 50800

NASA TECHNICAL MEMORANDUM

NASA TM X-62,360

NASA TM X-62,360

LOW SPEED AERODYNAMIC CHARACTERISTICS OF AN 0.075-SCALE F-15 AIRPLANE MODEL AT HIGH ANGLES OF ATTACK AND SIDESLIP

Daniel N. Petroff, Stanley H. Scher and Lee E. Cohen

Ames Research Center
Moffett Field, California 94035

REPRODUCED BY
NATIONAL TECHNICAL
INFORMATION SERVICE
U S. DEPARTMENT OF COMMERCE
SPRINGFIELD, VA. 22161

July 1974

NOTICE

THIS DOCUMENT HAS BEEN REPRODUCED FROM THE BEST COPY FURNISHED US BY THE SPONSORING AGENCY. ALTHOUGH IT IS RECOGNIZED THAT CERTAIN PORTIONS ARE ILLEGIBLE, IT IS BEING RELEASED IN THE INTEREST OF MAKING AVAILABLE AS MUCH INFORMATION AS POSSIBLE.

1 Report No.	2. Government Accession No.	3. Recipient's Catalog No.
NASA TM X-62,360		

4. Title and Subtitle	5. Report Date
LOW SPEED AERODYNAMIC CHARACTERISTICS OF AN 0.075-SCALE F-15 AIRPLANE MODEL AT HIGH ANGLES OF ATTACK AND SIDESLIP	July 1974
	6 Performing Organization Code

7 Author(s)	8. Performing Organization Report No.
Daniel N. Petroff, Stanley H. Scher** and Lee E. Cohen*	

9. Performing Organization Name and Address	10. Work Unit No.
NASA Ames Research Center, Moffett Field, Calif. and ARO, Inc., Moffett Field, Calif. 94035	760-17-01
	11 Contract or Grant No.

12 Sponsoring Agency Name and Address	13. Type of Report and Period Covered
National Aeronautics and Space Administration Washington, D. C. 20546	Technical Memorandum
	14. Sponsoring Agency Code

15 Supplementary Notes

* ARO, Inc., Moffett Field, Calif. 94035

** Project Engineer, NASA LaRC

16 Abstract

An 0.075-scale model representative of the F-15 airplane was tested in the Ames 12-Foot Pressure Wind Tunnel at a Mach number of 0.16 to determine static longitudinal and lateral-directional characteristics at spin attitudes for Reynolds numbers from 1.48 to 16.4 million per meter (0.45 to 5.0 million per foot). Angles of attack ranged from 0 to +90° and from -40° to -80° while angles of sideslip were varied from -20° to +30°. Data were obtained for nacelle inlet ramp angles of 0 and 11° with the left and right stabilators deflected 0, -25°, and differentially 5° and -5°. The normal pointed nose and two alternate nose shapes were also tested along with several configurations of external stores.

Analysis of the results indicate that at higher Reynolds numbers there is a slightly greater tendency to spin inverted than at lower Reynolds numbers. Use of a hemispherical nose in place of the normal pointed nose provided an over-correction in simulating yawing-moment effects at high Reynolds numbers; use of an asymmetrical beveled nose provided an even larger over-correction at positive sideslip angles and an effect in the wrong direction at negative sideslip angles.

17. Key Words (Suggested by Author(s))	18. Distribution Statement
F-15 airplane Hi alpha Hi Reynolds Static aerodynamics Wind Tunnel test Spin	

19 Security Classif. (of this report)	20 Security Classif. (of this page)	21 No. of Pages	22 Price*
Unclassified	Unclassified	118	$4.75

*For sale by the National Technical Information Service, Springfield, Virginia 22161

CONTENTS

	Page
SUMMARY	1
INTRODUCTION	1
NOMENCLATURE	2
TEST FACILITY	5
MODEL DESCRIPTION	6
TESTING AND PROCEDURE	6
DATA REDUCTION	7
RESULTS AND DISCUSSION	8
REFERENCES	10
TABLES	
1. MODEL GEOMETRY	11
2. INDEX OF DATA FIGURES	13
FIGURES	
1. AXIS SYSTEMS	14
2. MODEL DRAWINGS	15
3. MODEL INSTALLATION PHOTOGRAPHS	29
4. DATA	31

(THIS PAGE INTENTIONALLY LEFT BLANK)

LOW SPEED AERODYNAMIC CHARACTERISTICS OF AN 0.075-SCALE F-15 AIRPLANE MODEL AT HIGH ANGLES OF ATTACK AND SIDESLIP

By Daniel N. Petroff, Stanley H. Scher* and Lee E. Cohen**

Ames Research Center

SUMMARY

An 0.075-scale model representative of the F-15 airplane was tested in the Ames 12-Foot Pressure Wind Tunnel at a Mach number of 0.16 to determine static longitudinal and lateral-directional characteristics at spin attitudes for Reynolds numbers from 1.48 to 16.4 million per meter (0.45 to 5.0 million per foot). Angles of attack ranged from 0 to +90° and from -40° to -80° while angles of sideslip were varied from -20° to +30°. Data were obtained for nacelle inlet ramp angles of 0 and 11° with the left and right stabilators deflected 0, -25°, and differentially 5° and -5°. The normal pointed nose and two alternate nose shapes were also tested along with several configurations of external stores.

Analysis of the results indicate that at higher Reynolds numbers there is a slightly greater tendency to spin inverted than at lower Reynolds numbers. Use of a hemispherical nose in place of the normal pointed nose provided an over-correction in simulating yawing-moment effects at high Reynolds numbers; use of an asymmetrical beveled nose provided an even larger over-correction at positive sideslip angles and an effect in the wrong direction at negative sideslip angles.

There were found to be no significant effects of changing inlet ramp angle and adding external stores on the aerodynamic characteristics. At angles of attack between 30° and 60° deflection of the stabilators provided an increase in directional stability.

INTRODUCTION

With the advent of highly maneuverable military aircraft, it was found that a large proportion of aircraft losses were caused by the aircraft entering out-of-control and spinning motions. The department of the Air Force has required the evaluation of these motions on aircraft such as the McDonnell Douglas F-15. The tests being reported in this paper were made to support theoretical analysis of F-15 upright stall/spin motions, and

* Project engineer, NASA LaRC ** Project engineer, ARO, Inc.

to support inverted spin-model tests in the spin tunnel. The model is representative of the F-15.

Upright-attitude force tests were made to provide static aerodynamic data at high angles of attack and sideslip with various control deflections and stores to support theoretical analysis of F-15 upright stall/spin motions. Inverted-attitude force tests were made to evaluate the effects of Reynolds number on the crossflow characteristics on the fuselage ahead of the wing. In some cases, these crossflow effects can cause appreciably different side forces and yawing moments on a small-scale model from those obtained at the same attitudes on the full-scale configuration (references 1 and 2). When these effects do occur, they are usually in the angle-of-attack range between 40° and 90° for upright spins and between -40° and -90° for inverted spins. In the course of conducting investigations of aircraft spin and recovery characteristics in the spin tunnel, small-scale models must necessarily be used. It has been found that for some configurations, the Reynolds number effects are so marked that model spin and recovery characteristics do not represent the spin and recovery characteristics of the full-scale airplane.

In general, a wind tunnel Reynolds number force test program is conducted on a given design to determine if spin tunnel results could be appreciably altered by Reynolds number effects. When such effects are found, various "fixes" are investigated on the wind tunnel model in an attempt to minimize these effects. Then, a similar "fix" is placed on the spin tunnel model so that its side force and yawing moment characteristics in the spin are more representative of the larger scale model.

NOMENCLATURE

The axis systems and sign conventions are shown in figure 1. Data are presented in the body-axis coordinate system. Because the data were computer plotted the corresponding plot symbol, where used, is given together with the conventional symbol.

Symbol	Plot Symbol	Definition
A_c		cavity area
b	BREF	wing span
$\bar{c}$		wing mean aerodynamic chord, M.A.C.
C_A	CA	axial-force coefficient, axial force/qS

C_D	CD	drag coefficient, drag/qS
C_L	CL	lift coefficient, lift/qS
C_ℓ	CBL	rolling-moment coefficient, rolling moment/qSb
C_m	CLM	pitching-moment coefficient, pitching moment/qS$\bar{c}$
C_N	CN	normal-force coefficient, normal force/qS
C_n	CYN	yawing-moment coefficient, yawing moment/qSb
C_Y	CY	side-force coefficient, side force/qS
L	LREF	reference length
M	MACH	freestream Mach number
p		freestream static pressure
p_c		cavity pressure
q		freestream dynamic pressure
Re/L	RN/L	unit Reynolds number, million per meter
S	SREF	wing area
α	ALPHA	angle of attack
β	BETA	angle of sideslip
δ_{a_L}	AIL-L	left aileron deflection angle, positive trailing edge down
δ_{a_R}	AIL-R	right aileron deflection angle, positive trailing edge down
δ_r	RUDDER	rudder deflection angle, positive trailing edge to the left looking forward
δ_{st_L}	STB-L	left stabilator deflection angle, positive trailing edge down

δ_{st_R}	STB-R	right stabilator deflection angle, positive trailing edge down
ρ	RHO	duct inlet ramp angle

Configuration Code

a_{15}	A15	gun bump fairing, right-hand
a_{16}	A16	wing root fairing, left-hand
B_{156}	B156	fuselage
d_{22f}	D22F	shroud/exit choke, normal flow
d_{22g}	D22G	shroud/exit choke, blocked flow
D_{41}	D41	inlet
Fa_{17}	F17	flaps
Fa_{18}	A18	ailerons
H_{36}	H36	horizontal stabilators
J_8	J8	MER 200
M_{12}	M12	radome
Mx	MX	alternate nose shape, 45° left-hand bevel
My	MY	alternate nose shape, hemispherical
T_{23}	T23	600 gallon fuel tank
T_{25}	T25	sparrows (two forward and two aft)
T_{57}	T57	QRC-249 ECM pod
T_{64}	T64	SUU-13/A

T_{66}	T66	BLU-32/B
V_{172}	V172	vertical tails
W_{118}	W118	wing
Y_{22}	Y22	inboard wing pylons
Y_{24}	Y24	centerline pylon
Yx	YX	outboard wing pylons
	BASIC	$B_{156}\ W_{118}\ D_{41}\ H_{36}\ V_{172}\ T_{25}$
	A	$J_8(3)\ T_{66}\ Y_{24}$
	B	$J_8(6)\ T_{64}(2)\ Y_{22}$
	C	$T_{57}(2)$ Yx
	D	$J_8(3)\ T_{64}\ Y_{22}$
	E	$T_{23}\ Y_{24}$
	F	T_{25}
	G	$-M_{12}$ + Mx
	H	$-M_{12}$ + My

TEST FACILITY

The Ames 12-Foot Pressure Wind Tunnel is a variable density, low turbulence wind tunnel which operates in the Mach number range of 0.1 to 0.94. The wind tunnel is powered by a two-stage, axial flow fan driven by electric motors totaling 12,000 horsepower. Airspeed in the test section is controlled by variation of the fan's rotative speed. Eight fine-mesh screens in the settling chamber together with a contraction ratio of 25 to 1, provide an airstream of exceptionally low turbulence.

MODEL DESCRIPTION

The model was an 0.075-scale F-15 airplane. The geometry of the model is given in table 1, drawings of the model are presented as figure 2, and photographs of the model installation are included as figure 3.

The model is a twin engine, mid-wing, supersonic fighter aircraft configuration with a 45° wing leading edge sweep and a compound trailing edge sweep. At the wing root the wing section is a NACA 64A(.55)0(5.9),a=0.8 mod. airfoil. Advancing further outboard the wing section changes to a NACA 64A(.55)0(4.6),a=0.8 mod. airfoil, and then to a NACA 64A-20(3.5), a=0.8 mod. airfoil. At the wing tip it is a NACA 64A-20(3.0),a=0.8 mod. airfoil. The twin vertical tails are NACA 000(5.0)-64 airfoils at the root and blend into a NACA 000(3.5)-64 airfoil at the tip. The horizontal stabilators have a NACA 000(5.5)-64 airfoil at the root and blend into a NACA 000(2.5)-64 airfoil at the tip.

Various combinations of stores and their supporting pylons were mounted on the underside of the model and are presented in figures 2 (ℓ) to 2 (n).

The model was tested with two alternate nose configurations: a hemispherical nose having a radius of curvature of 1.11cm which shortened the normal nose length by 1.824cm; and a 45° left-hand beveled nose which shortened the normal nose by .318cm.

The control surfaces utilized during the test were the ailerons and horizontal stabilators. The ailerons were 13.283cm in span with a 23.8 per cent wing chord. The horizontal stabilator was a pivoting horizontal tail in which the entire tail rotates.

The aft end of the model, between the vertical tails, was modified to accept the sting support.

TESTING AND PROCEDURE

The investigation was conducted at a Mach number of 0.16 and at Reynolds numbers of 1.48 to 16.4 million per meter (0.45 to 5.0 million per foot). Data were obtained at angles of attack from -80° to 90° and at sideslip angles from -20° to 30°.

The left and right horizontal stabilator deflections were set at 0 and 0, -25° and -25°, and 5° and -5°, respectively. The ailerons and rudder remained at zero deflection throughout the test.

The basic configuration was $B_{156}\ W_{118}\ D_{41}\ H_{36}\ V_{172}\ T_{25}$. Model configuration changes consisted of the addition of various combinations of stores including MER200, BLU-32/B, SUU-13/A, QRC-249 ECM POD and a 600-gallon fuel tank with their associated pylons. Two alternate nose configurations were also tested.

The model was provided with boundary layer transition strips. These strips were of No. 120 carborundum grit with a width of .127cm. Grit density was approximately 59/cm. The strips were located 3.81cm aft of the tip of the airplane nose and at 5 percent chord of the wings, horizontal and vertical tails, and 1.9cm from the leading edge around the engine inlet ducts. When the model was tested for the effect of the nose configurations, no transition grit was used on the model and all stores were removed.

At angles of attack from 40° to 90° and -40° to -80° the engine nacelle ducts were plugged to simulate stalled engines. At other angles of attack the ducts were flow-through simulating normal engine operation. The inlet ramp angle of the ducts was set at either 0 or 11°.

The model was sting mounted on a turntable which permitted the variation of either angle of attack or sideslip. Aerodynamic forces and moments on the model were measured using a Task internal six-component strain gage balance. The balance cavity pressure was measured using a pressure transducer. An angle of attack transducer at the base of the support system was used to measure the angle of attack and a Selsyn was used to measure the turntable rotation.

Tunnel static pressure was measured in the plenum surrounding the test section and no blockage corrections were applied. Prior calibration of the wind tunnel with large blockage models showed plenum pressure to be essentially identical to free-stream static pressure and this pressure is currently being used for all high attitude tests.

DATA REDUCTION

The six-component force and moment data were reduced about the model moment reference center in the body axis system. The axis systems are defined in figure 1 and the moment center was assumed to be at fuselage station 106.142cm and waterline 22.131cm. The angle of attack and angle of sideslip were corrected for deflection of the sting and balance under aerodynamic load. Angle of attack and appropriate aerodynamic coefficients were corrected for model weight tares and tunnel wall interference effects (reference 3). The wall correction values are as follows:

$\Delta\alpha = 0.2568\ C_L$ $\qquad$ $\Delta C_m(\text{tail on}) = 0.001343\ C_L$

$\Delta C_D = 0.004020\ C_L$ $\qquad$ $\Delta C_m(\text{tail off}) = 0.0008763\ C_L$

A stream angle of up to 2° at zero angle of attack is known to exist in the vicinity of the model due to the influence of the support system fairing on the tunnel floor (see figure 3). No stream angle corrections were applied to the data.

Three samples of all balance and tunnel static pressure data were averaged for each data point and then reduced to coefficient form.

The balance cavity pressure was measured and the body axial force coefficient was corrected as follows:

$$C_A = C_{A_{\text{uncorrected}}} + \frac{(p_c - p)A_c}{qS}$$

Data repeatability was estimated by reviewing repeat points and is as follows:

C_N	± 0.025	C_ℓ	± 0.003
C_A	± 0.002	α	$\pm 0.04°$
C_Y	± 0.014	β	$\pm 0.04°$
C_m	± 0.010	Re/L	$\pm 0.07 \times 10^6$ per m
C_n	± 0.003	M	± 0.001

RESULTS AND DISCUSSION

Computer plotted data are presented in figures 4 through 9. An index to the plotted data is given in table 2.

The effects of Reynolds number on the aerodynamic coefficients of the model for a given angle of attack and angle of sideslip are presented in figure 4. The effects of angle of attack and angle of sideslip on the aerodynamic characteristics at a Reynolds number of 13.1 million per meter (4 million per foot) for two values of nacelle inlet ramp angle are presented in figures 5 and 6, respectively. The effects of sideslip angle on the aerodynamic characteristics at a Reynolds number of 13.1 million per meter (4 million per foot) are presented in figure 7 for several stabilator angles and in figure 8 for several configurations of external stores. The

effects of sideslip angle on the aerodynamic characteristics at Reynolds numbers of 1.48 and 16.4 million per meter (0.45 and 5.0 million per foot) for three fuselage nose shapes are presented in figure 9.

Analysis of the results presented in figure 4 indicate that at angles of attack of -80°, -70°, -60° the model adequately simulates full scale when comparing the lateral-directional coefficients, especially C_n which is an important parameter in its effects on spin characteristics (reference 1 and 2). At an angle of attack of -50°, there was a Reynolds number effect in that a positive value of C_n at 10° of sideslip at high Reynolds number became a negative value of C_n at low Reynolds number (see page 39, and see similar effects on pages 24, 29, and 34). At an angle of attack of -40°, some Reynolds number effects were also evident, but the effects were not consistent and in some cases were opposite to the effect already discussed for an angle of attack of -50° (for example of an opposite effect, see page 40).

In general, the results presented in figure 4 indicate that the airplane may have a slightly greater tendency to spin inverted than would the small-scale spin model.

At an angle of attack of -50° use of the hemispherical nose shape as a "fix" on the model at low Reynolds number changed the C_n data to be more like the C_n data at high Reynolds number when the basic tip was on; however, an over-correction is indicated. The data showed that use of the asymmetrical beveled nose is not promising because it provided an even larger over-correction at +10° of sideslip and also because it provided an increment in the wrong direction at negative sideslips (see figure 9, page 86). The use of the hemispherical nose as a "limited fix" for full scale simulation will require further analysis.

At an angle of attack of -40° neither the hemispherical nose nor the asymmetrical beveled nose appeared useful as a Reynolds number "fix". The hemispherical nose caused little or no change and the beveled nose provided an increment in the wrong direction at positive sideslips (see figure 9, page 87).

From the data presented in figures 5 and 6 it is seen that there was little effect of changing the inlet ramp angle on the variation of the aerodynamic coefficients with angle of attack and sideslip. The only coefficient to be appreciably affected by changing the ramp angle from 0 to 11° was the axial-force coefficient.

The data presented in figure 7 show that at angles of attack between 30° and 60° deflection of the stabilators can be used to increase the directional stability. Differential deflection of the stabilators is more effective in increasing directional stability at the higher angles of attack.

The data presented in figure 8 show no significant effects of adding external stores on the aerodynamic characteristics.

Ames Research Center
National Aeronautics and Space Administration
Moffett Field, California 94035

July 3, 1974

REFERENCES

1. Neilhouse, Anshal I.; Klinar, Walter J.; and Scher, Stanley H.: Status of Spin Research for Recent Airplane Designs. NASA TR R-57, 1960. (Supersedes NACA RML 57F12).

2. Polhaums, Edward C.: Effect of Flow Incidence and Reynolds Number on Low-Speed Aerodynamic Characteristics of Several Noncircular Cylinders With Applications to Directional Stability and Spinning. NASA TR R-29, 1959.

3. Sivells, James; and Salmi, Rachel: Jet-Boundary Corrections for Complete and Semispan Swept Wings in Closed Circular Wind Tunnels. NACA TN2454, 1951.

TABLE 1. - MODEL GEOMETRY

(Dimensions Cm or Cm^2)

Fuselage (B_{156})

Length	134.247
Cavity pressure	51.936

Wing (W_{118})

Span (reference)	97.63
Area (reference)	3177.3
Root chord (theoretical)	52.070
Root chord (actual)	57.432
Tip chord	13.018
Mean aerodynamic chord (reference)	36.439
Aspect ratio	3.01
Maximum t/c	0.059
Taper ratio	0.250
Dihedral	-1.0°
Incidence	0°
Leading-edge sweep	45.0°
0.25c sweep	38.63°
Trailing-edge sweep	0.0° up to BL. 29.530cm 11.42° from BL. 29.530cm to wing tip
Section: at BL. 15.216	NACA 64A(.55)0(5.9),a=0.8 mod. airfoil
at BL. 29.530	NACA 64A(.55)0(4.6),a=0.8 mod. airfoil
at BL. 42.812	NACA 64A-20(3.5),a=0.8 mod. airfoil
at BL. 48.920	NACA 64A-20(3.0),a=0.8 mod. airfoil

Horizontal Stabilator (H_{36})

Semi span	17.916
Area	313.548/side
Exposed area	643.818
Root chord	26.137
Tip chord	8.891
Exposed M.A.C.	18.922
Exposed aspect ratio	2.05
Maximum t/c	0.055
Exposed taper ratio	0.34
Dihedral	0°
Leading-edge sweep	50.0°
0.25c sweep	43.34°
Trailing-edge sweep	12.5°

Section: at BL. 13.335: NACA 000(5.5)-64 airfoil
at BL. 31.251: NACA 000(2.5)-64 airfoil

Vertical tail (V_{172})

Exposed area	327.019/side
Root chord (2.634cm above FRP)	21.920
Tip chord	5.834
Exposed M.A.C.	15.423
Height from FRP	26.219
Exposed aspect ratio	1.7
Maximum t/c	0.050
Exposed taper ratio	0.226
Leading-edge sweep	36.57°
0.25c sweep	29.74°
Trailing-edge sweep	3.41°
Toe out	2.00°

Section: at root: NACA 000(5.0)-64
at tip: NACA 000(3.5)-64

TABLE 2. - INDEX OF DATA FIGURES

Figure	Title	Page
4	Variation of aerodynamic characteristics with Reynolds number at various angles of attack.	1
5	Effect of ramp angle on aerodynamic characteristics, Reynolds number equals 13.1 million per meter.	41
6	Effect of ramp angle on aerodynamic characteristics, Reynolds number equals 13.1 million per meter.	51
7	Effect of stabilators on aerodynamic characteristics, Reynolds number equals 13.1 million per meter.	59
8	Effect of stores on aerodynamic characteristics, Reynolds number equals 13.1 million per meter.	71
9	Effect of nose shape for two Reynolds numbers at various angles of attack, zero control surface deflections.	83

Notes:

1. Positive directions of force coefficients, moment coefficients, and angles are indicated by arrows
2. For clarity, origins of wind and stability axes have been displaced from the center of gravity

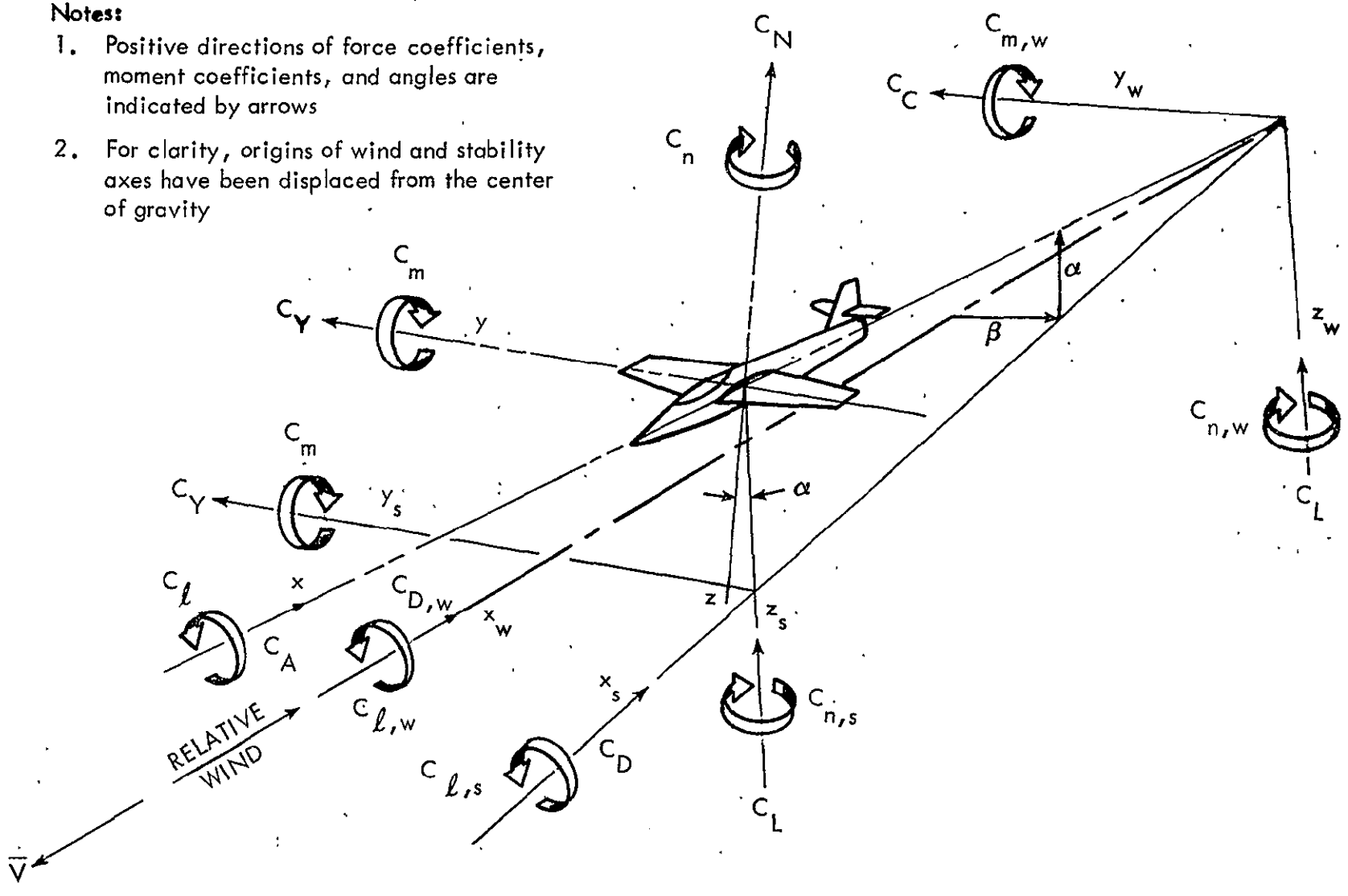

Figure 1. - Axis systems.

ORIGINAL PAGE IS
OF POOR QUALITY

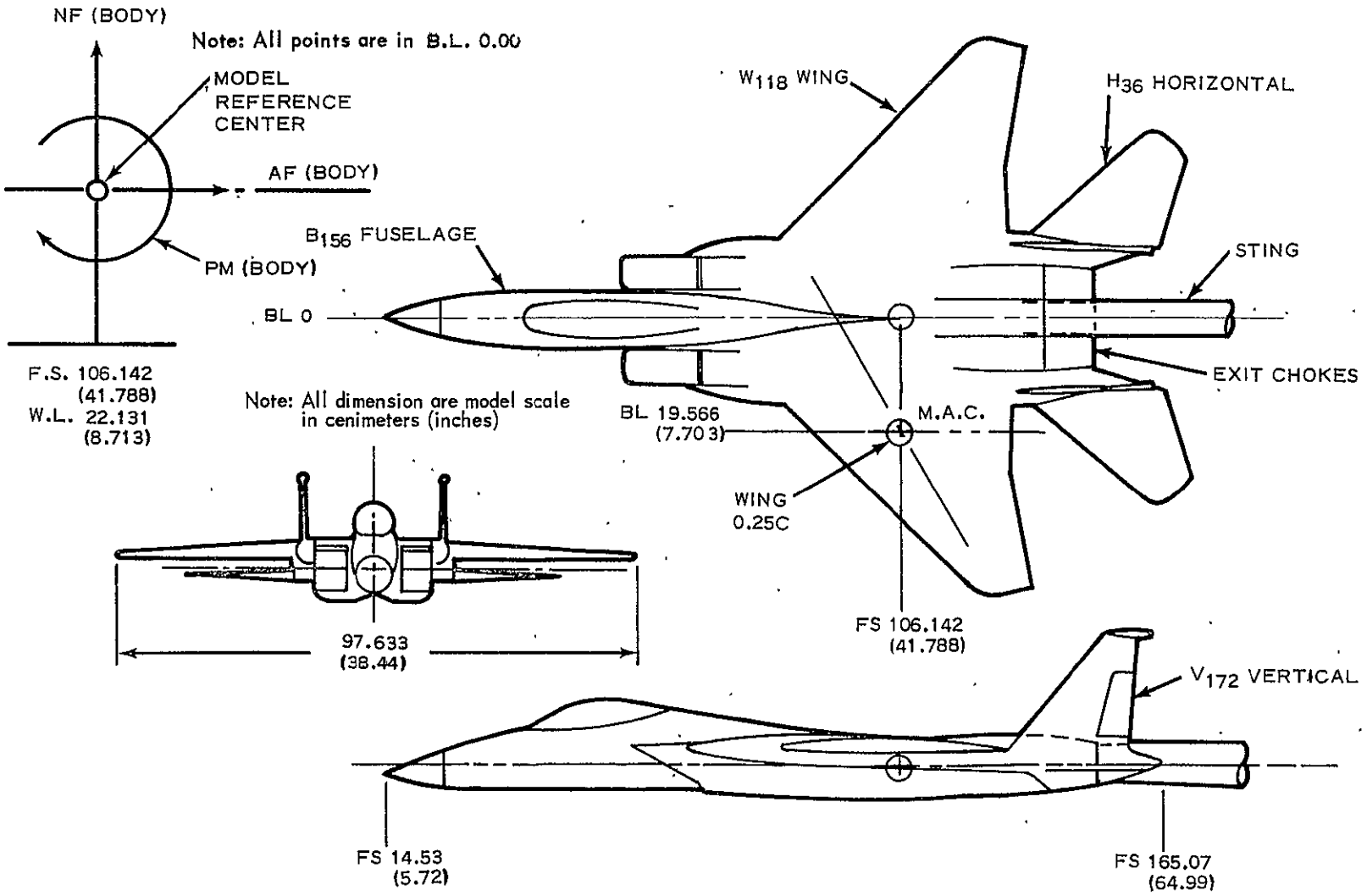

(a) General arrangement of the F-15 model

Figure 2.—Model drawings.

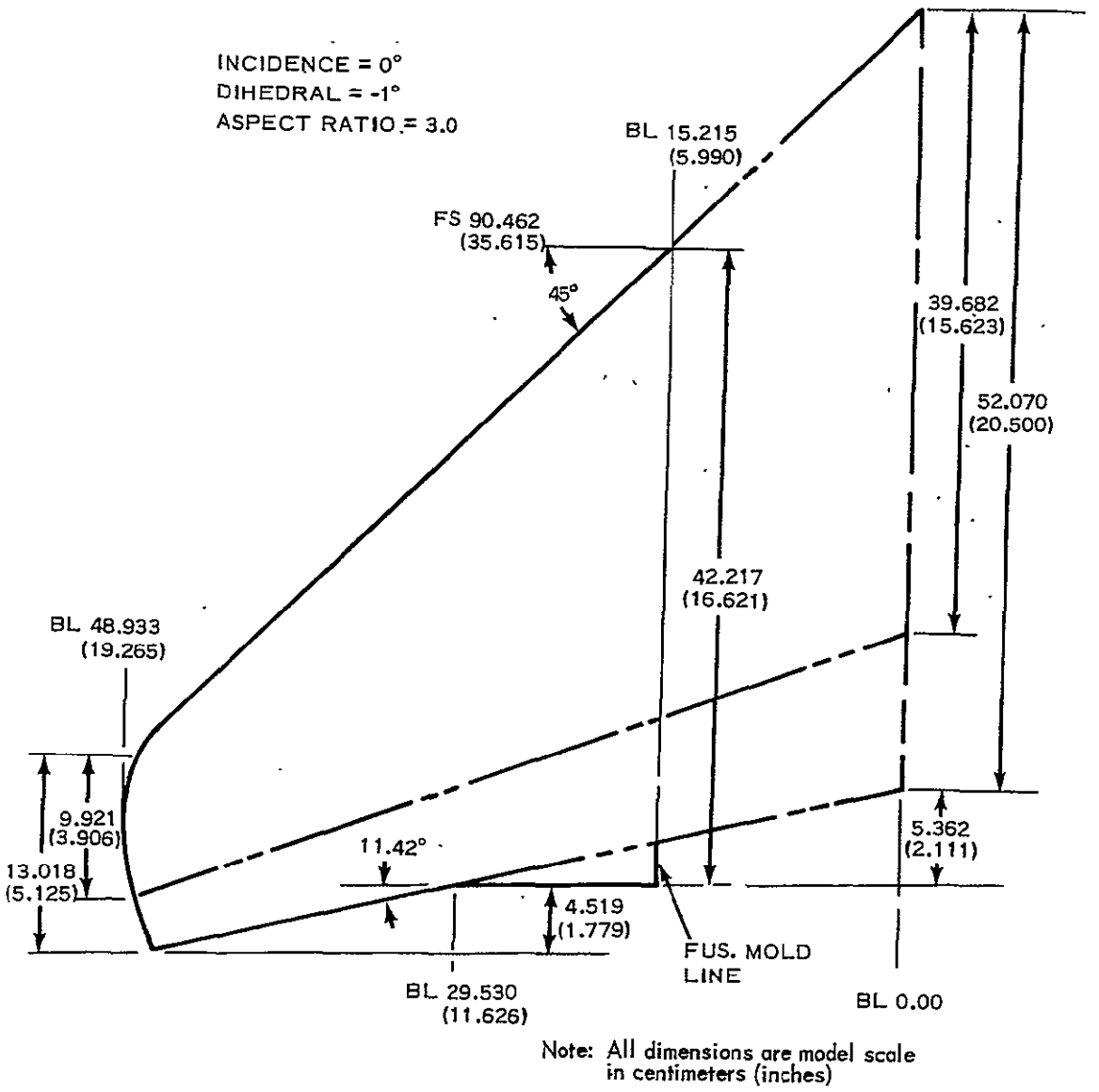

(b) Wing (W_{118})

Figure 2.–Continued.

ORIGINAL PAGE IS
OF POOR QUALITY

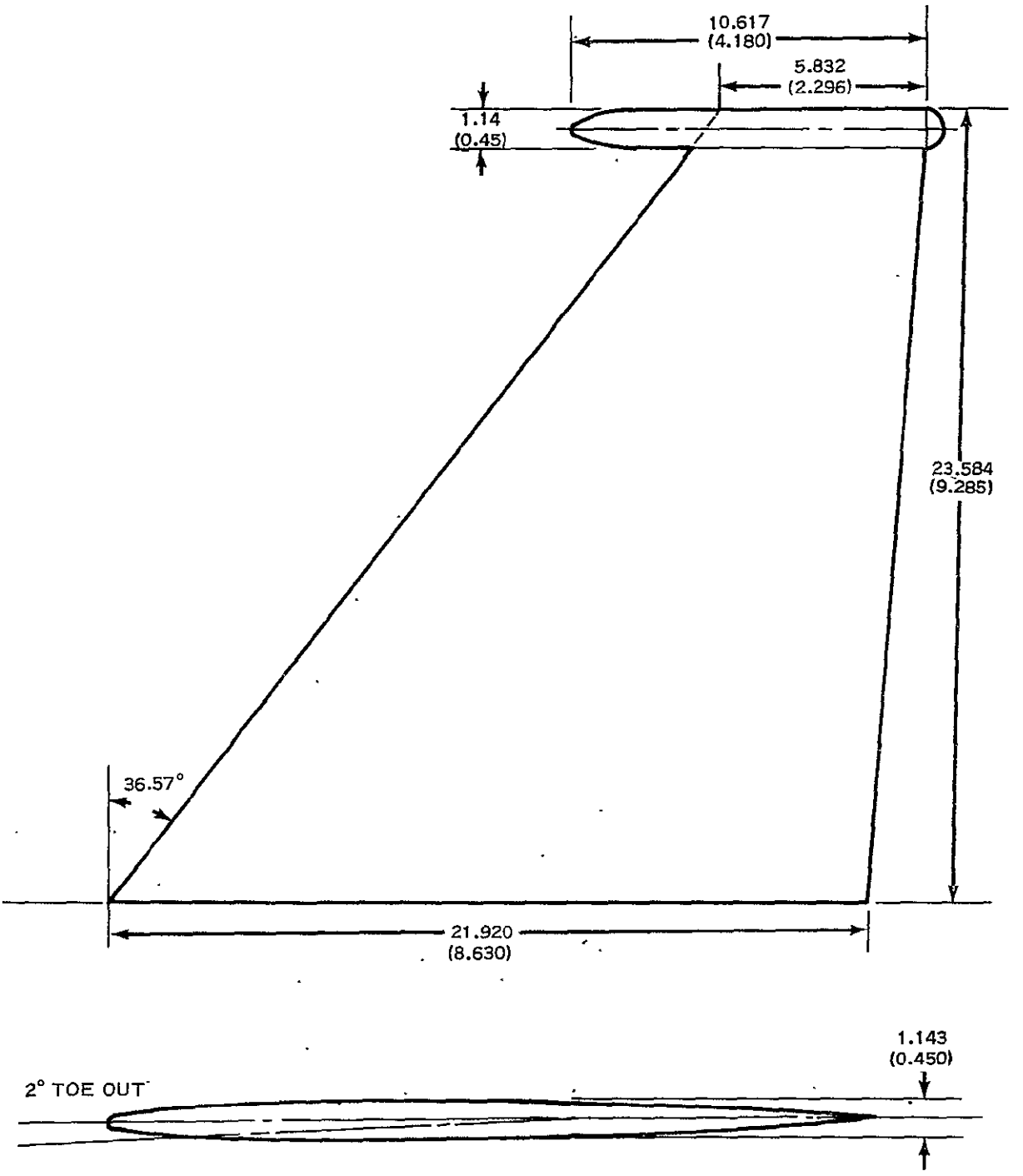

Note: All dimensions are model scale in centimeters (inches)

(c) Vertical stabilizer (V_{172})

Figure 2.—Continued.

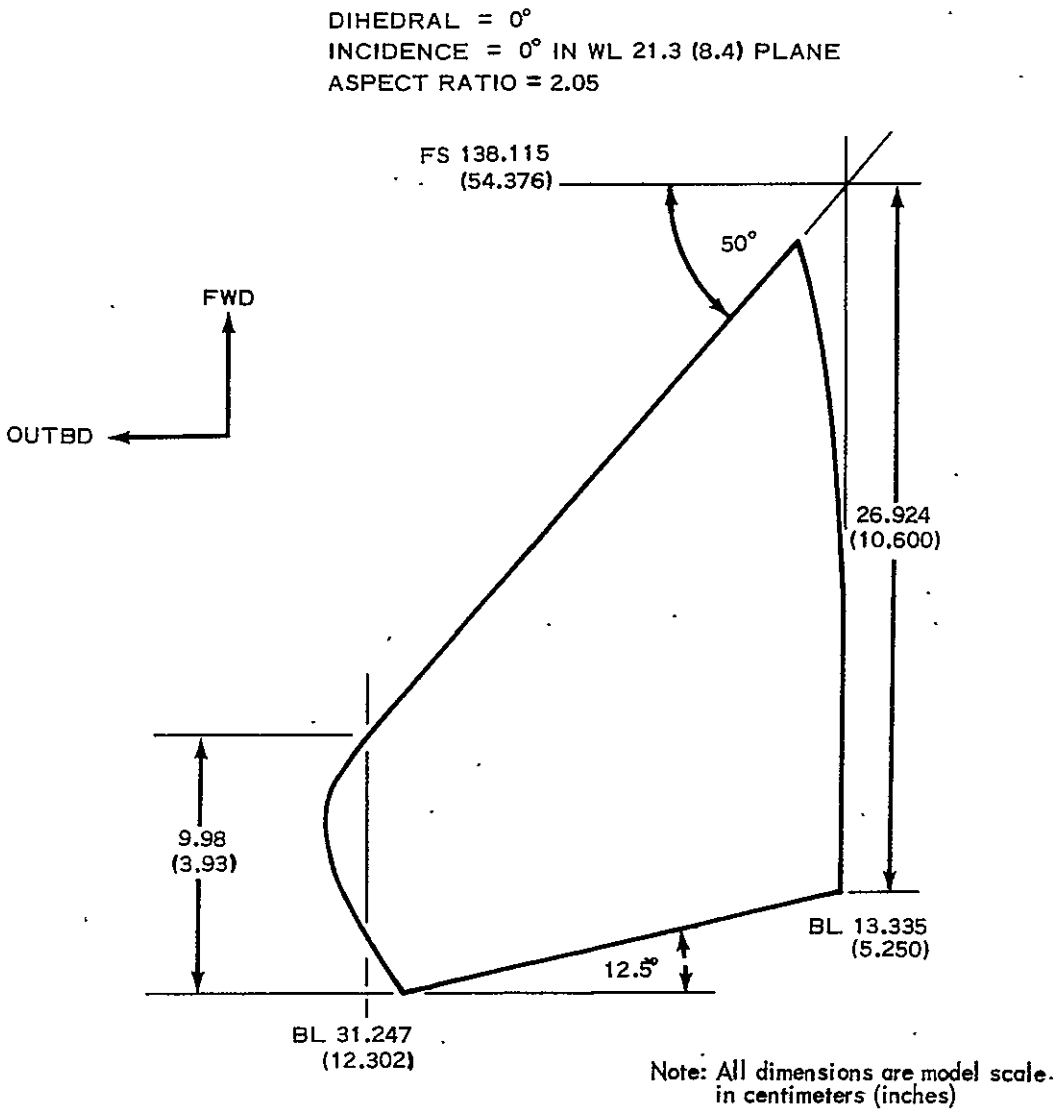

(d) Horizontal stabilator (H_{36})

Figure 2.—Continued.

ORIGINAL PAGE IS
OF POOR QUALITY

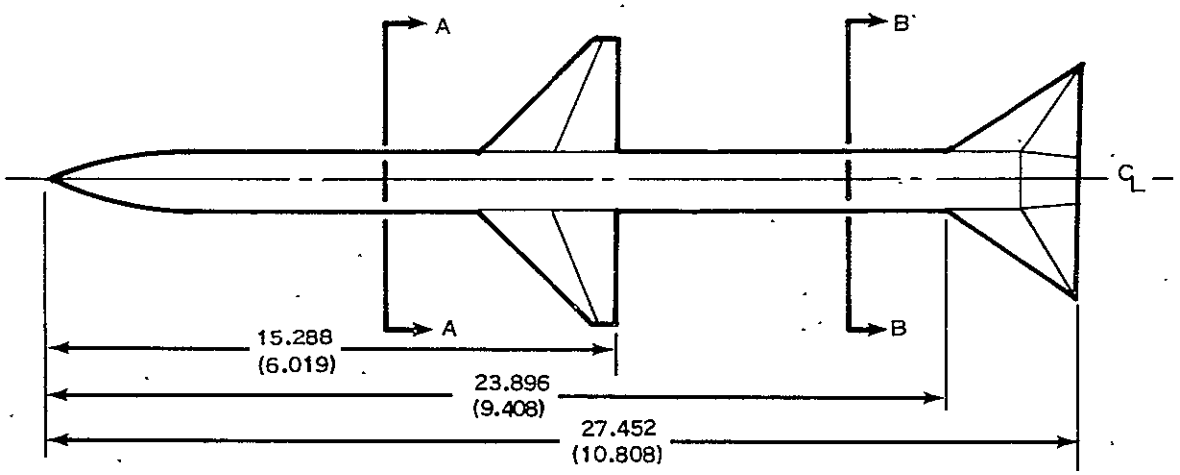

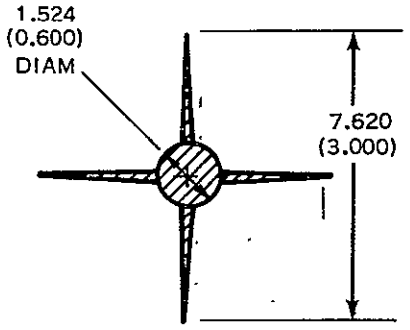

SECTION A-A

VIEW LOOKING AFT

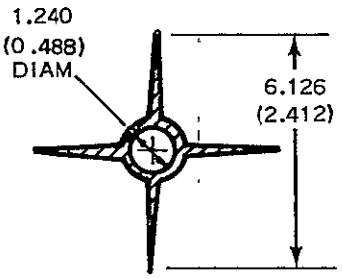

SECTION B-B

VIEW LOOKING FORWARD

Note: All dimensions are model scale in centimeters (inches)

(e) Sparrows (T_{25})

Figure 2.–Continued.

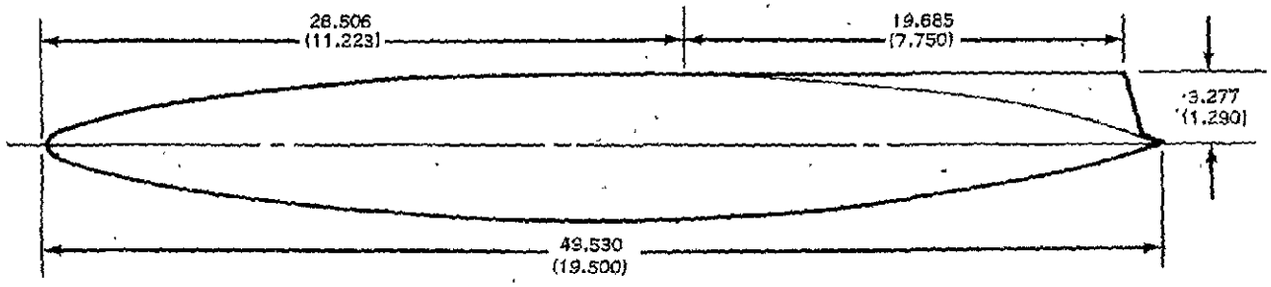

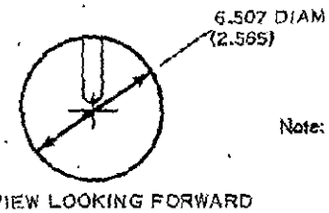

END VIEW LOOKING FORWARD

Note: All dimensions are model scale in centimeters (inches)

(f) 600-gal fuel tank (T_{25})

Figure 2.—Continued.

ORIGINAL PAGE IS
OF POOR QUALITY

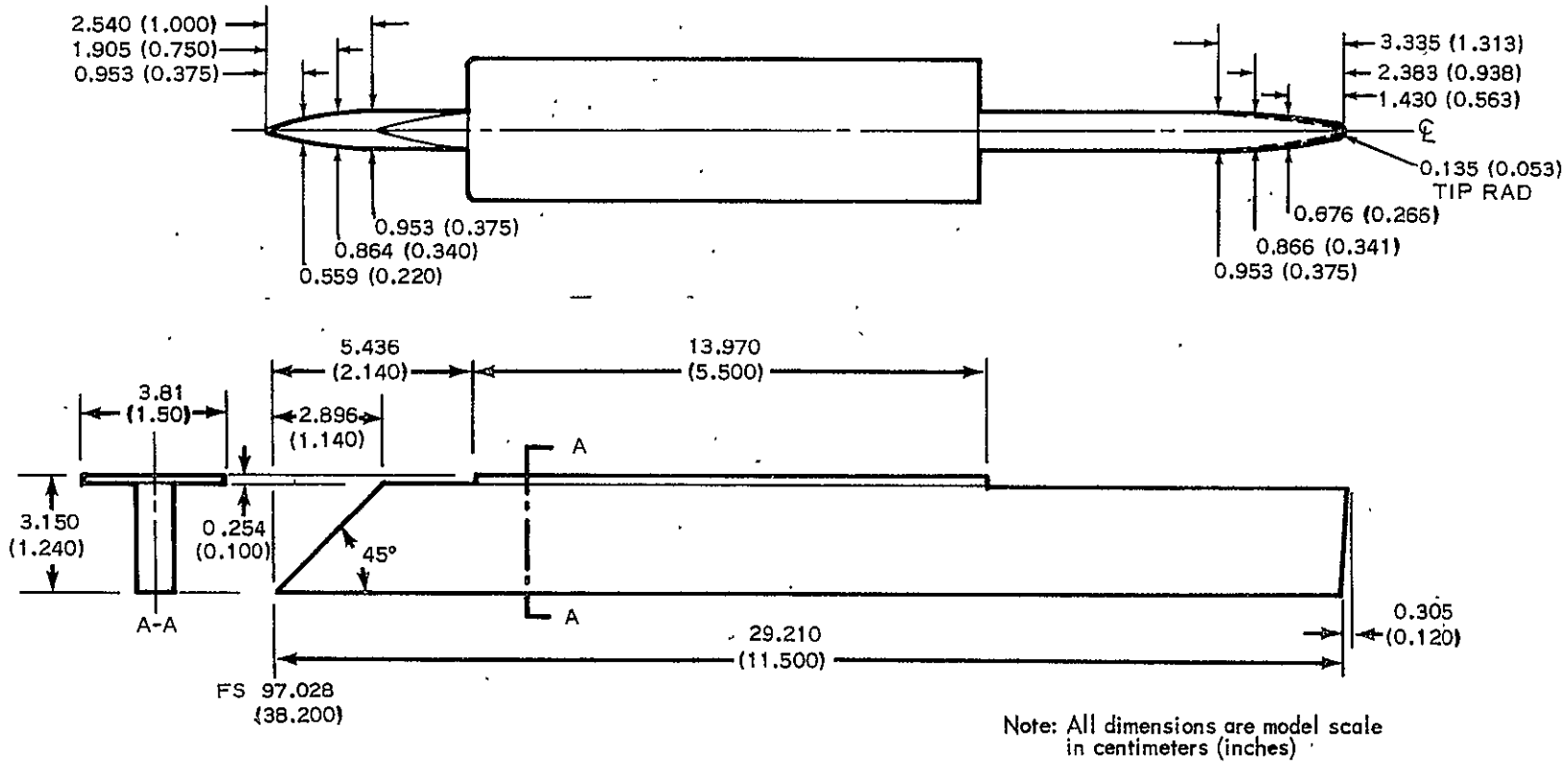

(g) Inboard wing pylon (Y_{22})

Figure 2.—Continued.

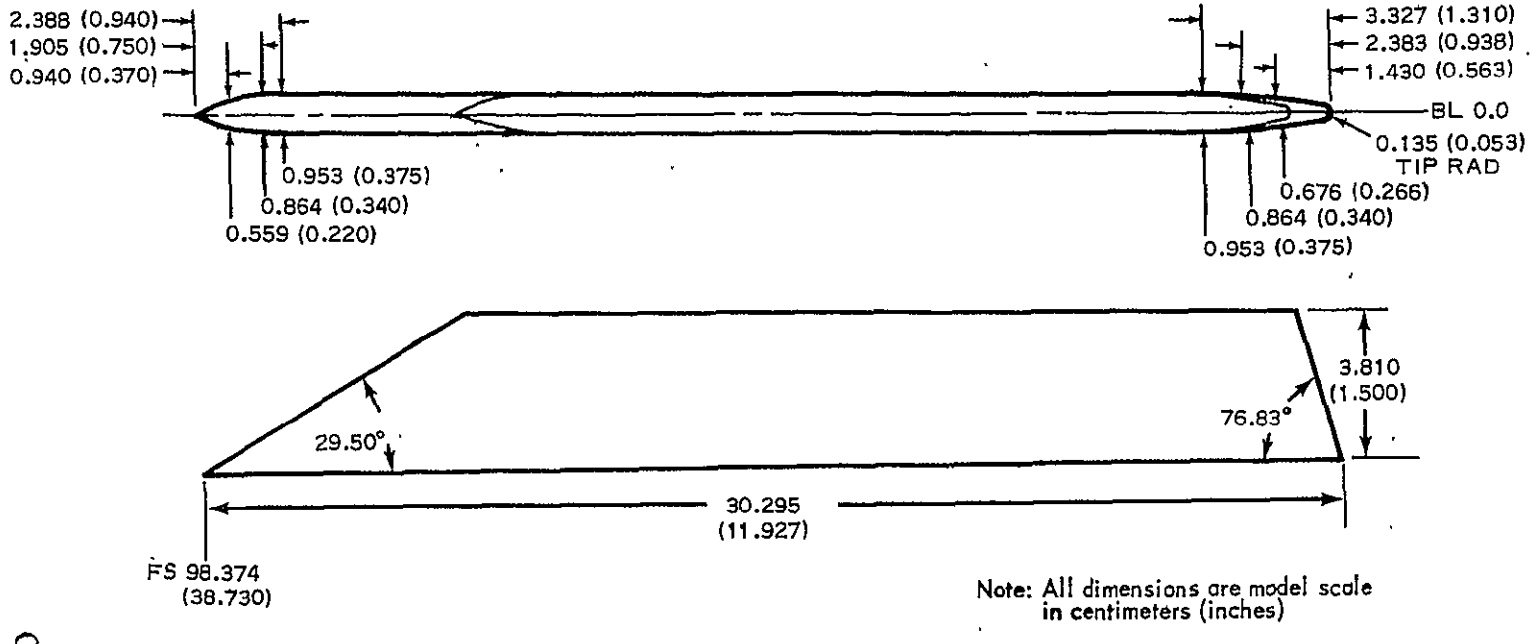

(h) Center pylon (Y_{24})

Figure 2.–Continued.

ORIGINAL PAGE IS
OF POOR QUALITY

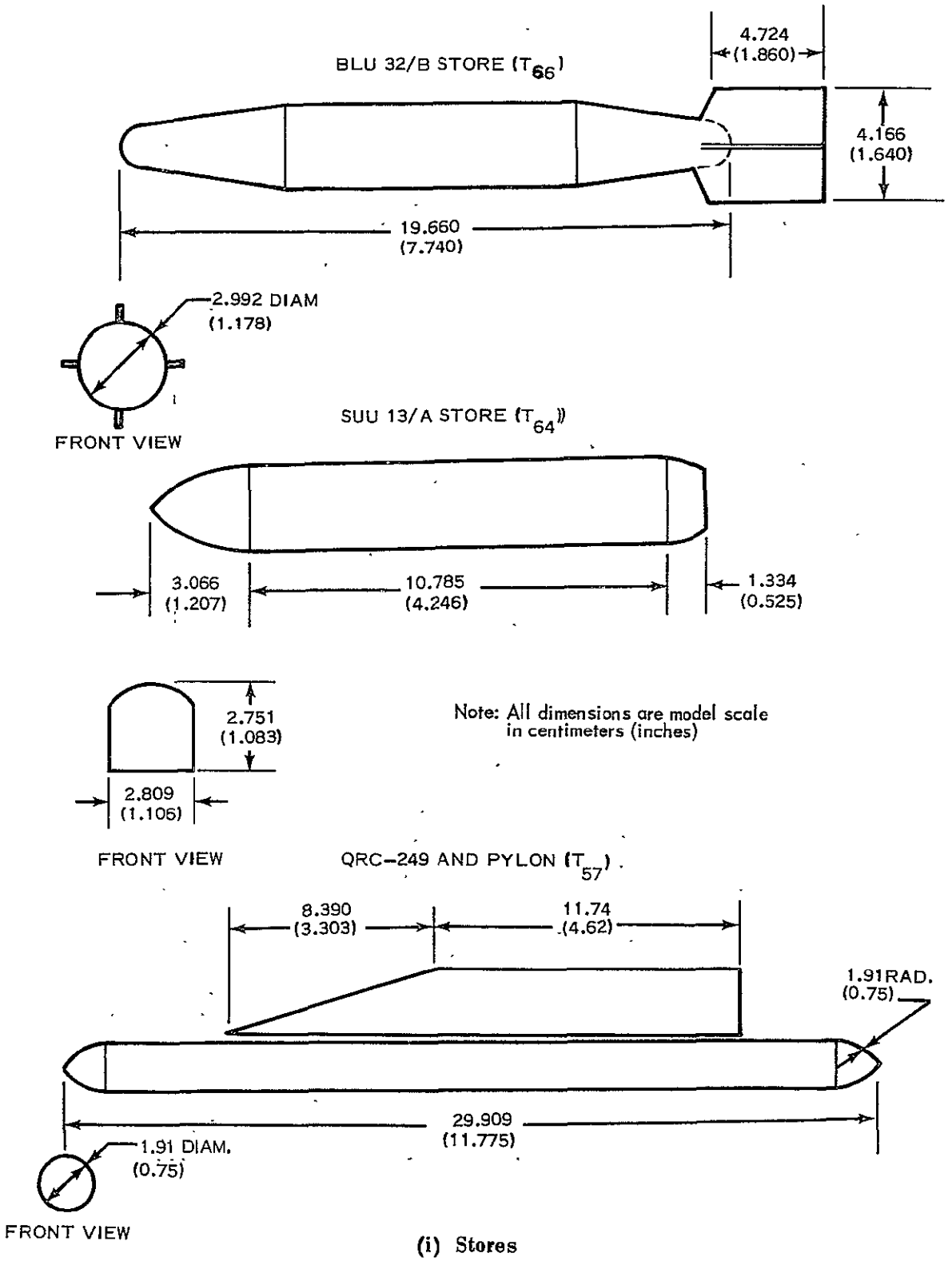

(i) Stores

Figure 2.—Continued.

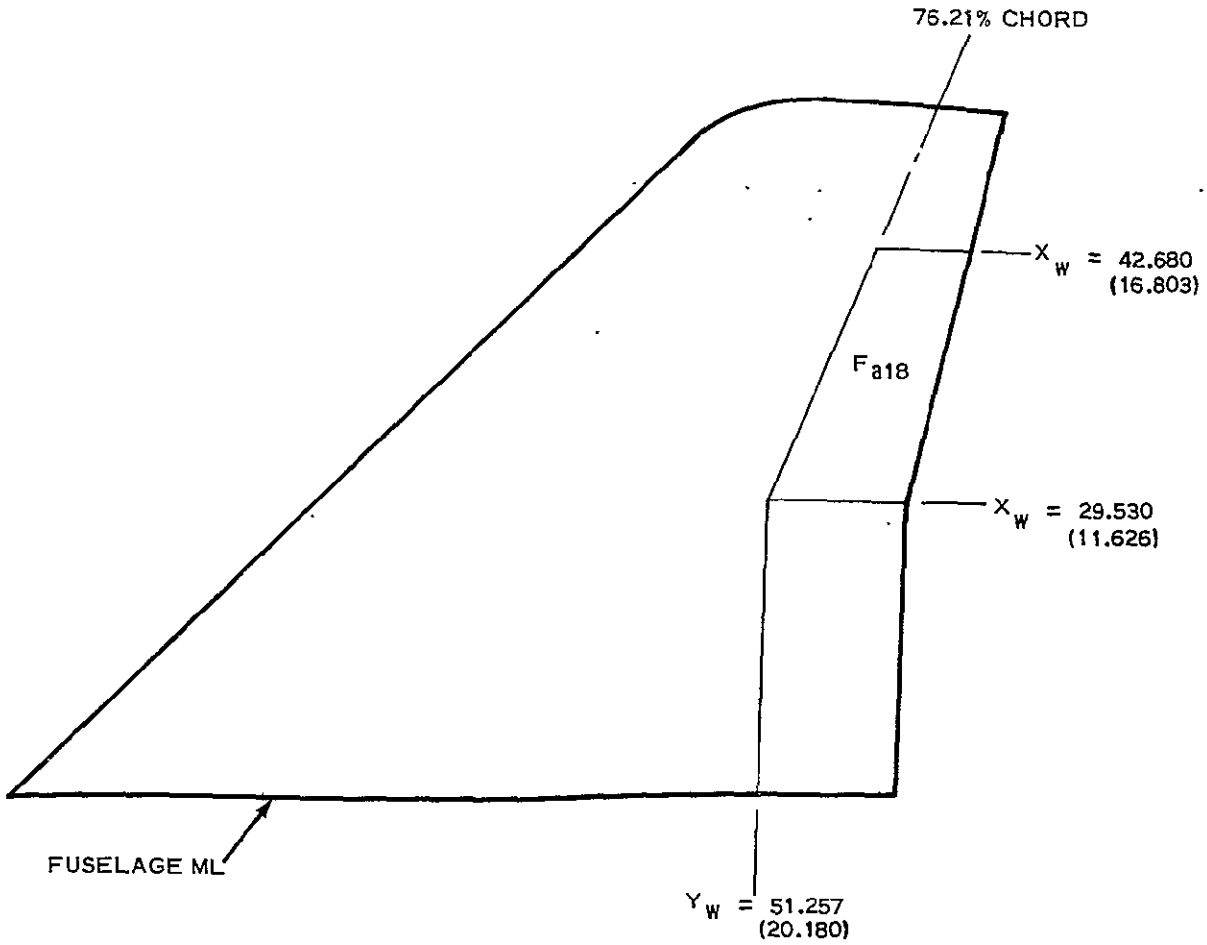

Note: All dimensions are model scale in centimeters (inches)

(j) Aileron (F_{a18})

Figure 2.—Continued.

ORIGINAL PAGE IS
OF POOR QUALITY

PLAN VIEW

SIDE VIEW

Note: All dimensions are model scale in centimeters (inches)

(k) B_{156} fuselage with M_{12} radome

Figure 2.—Continued.

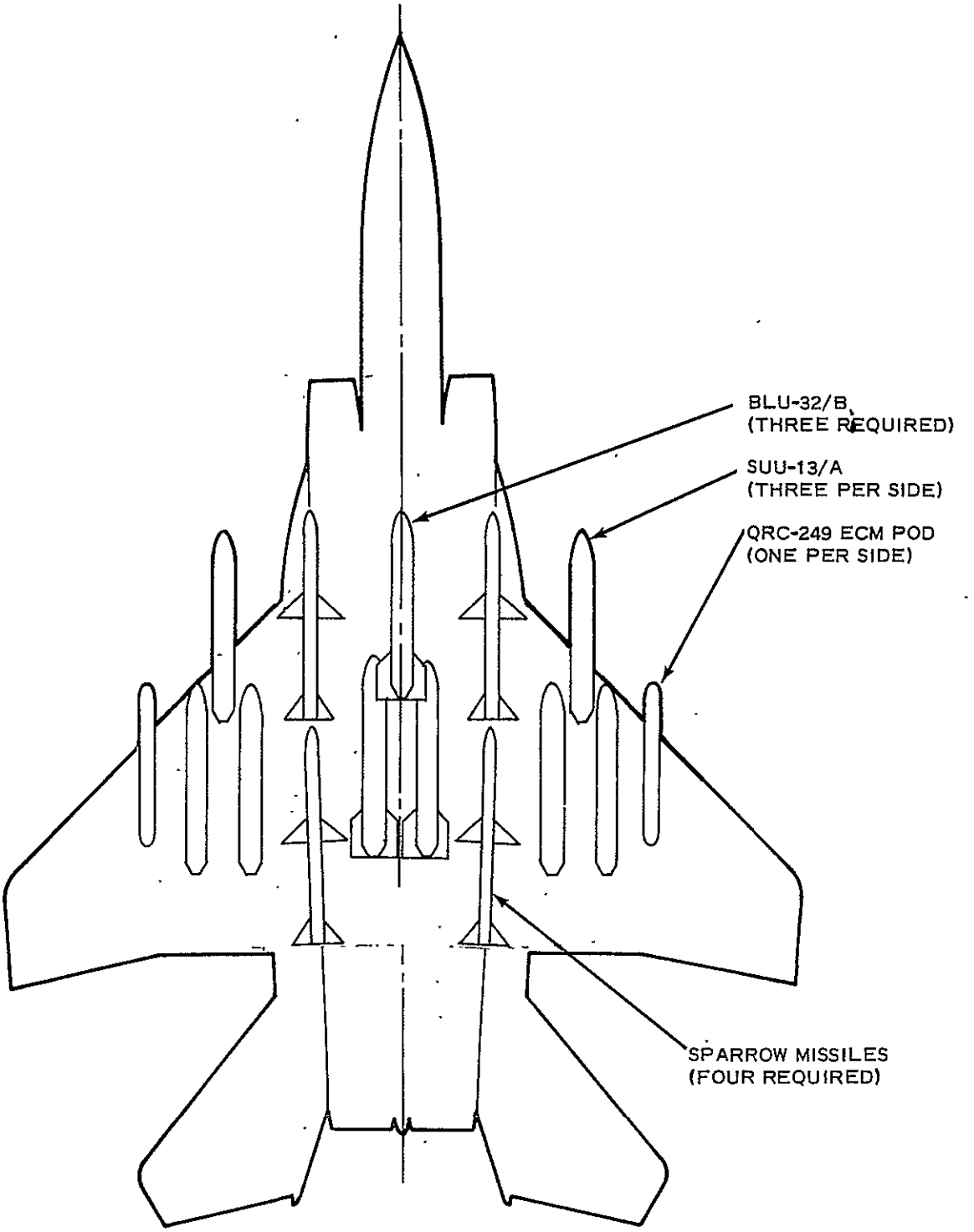

(l) External store loadings

Figure 2.–Continued.

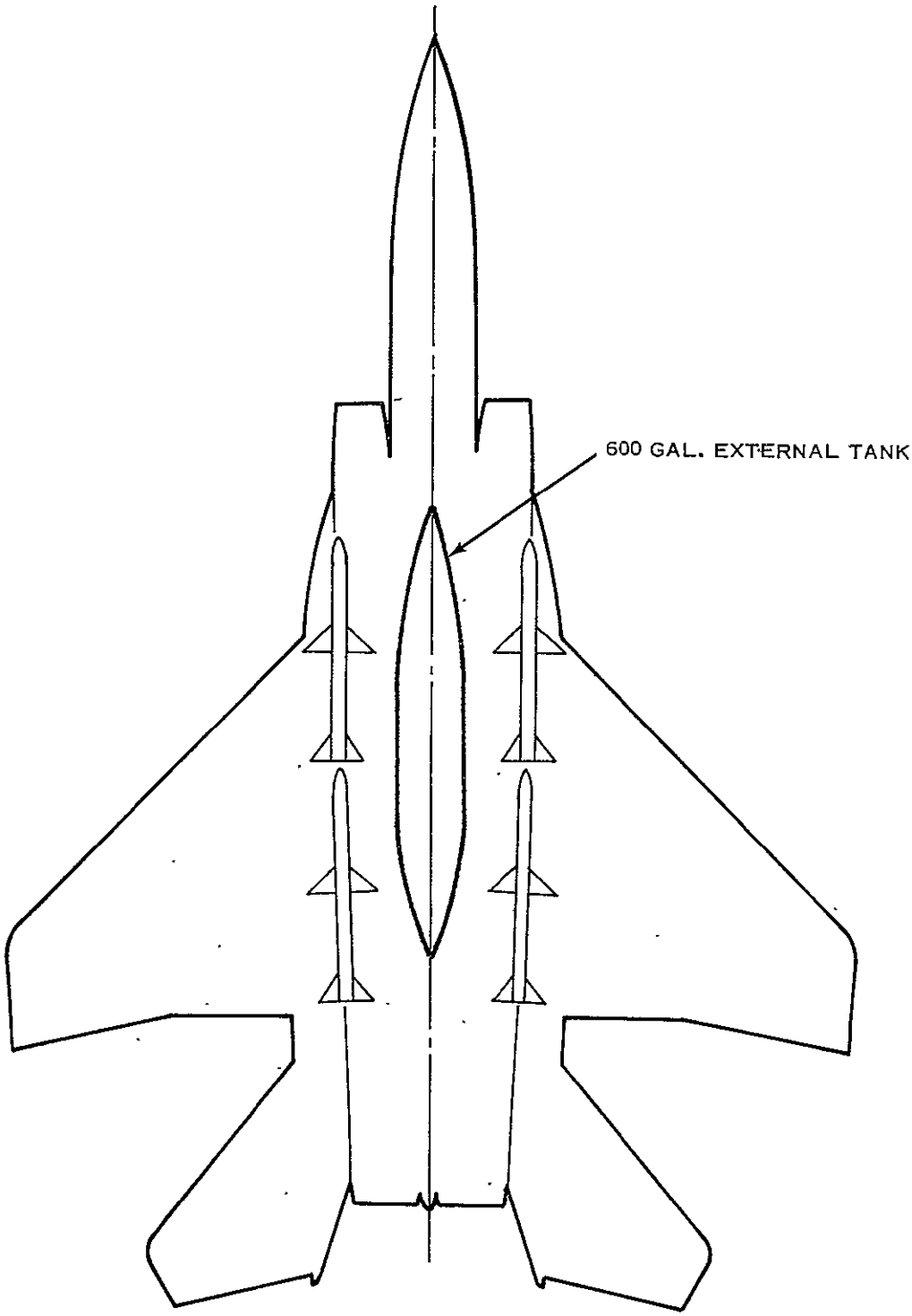

(m) External store loadings

Figure 2.–Continued.

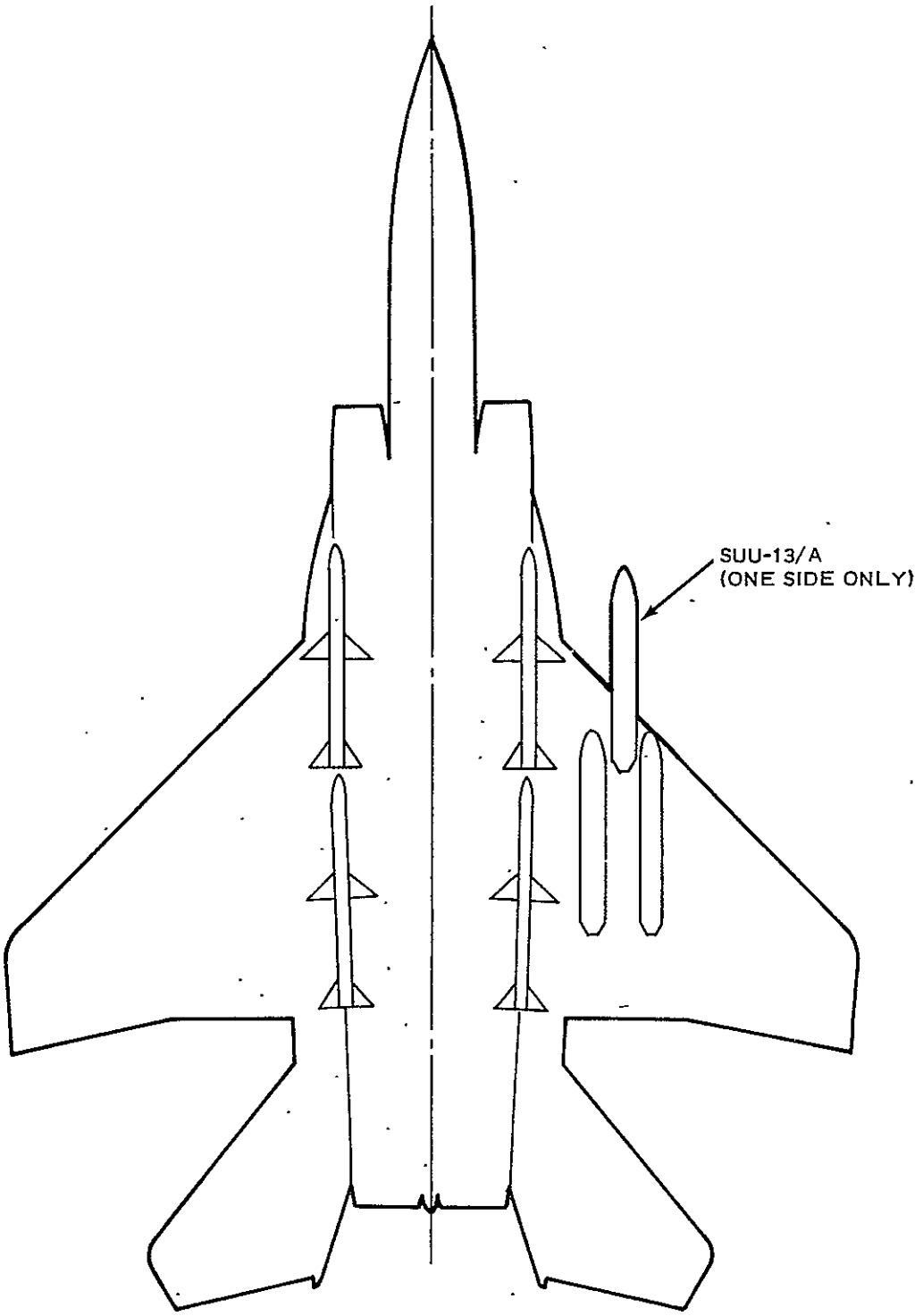

(n) External store loadings

Figure 2.– Concluded.

ORIGINAL PAGE IS
OF POOR QUALITY

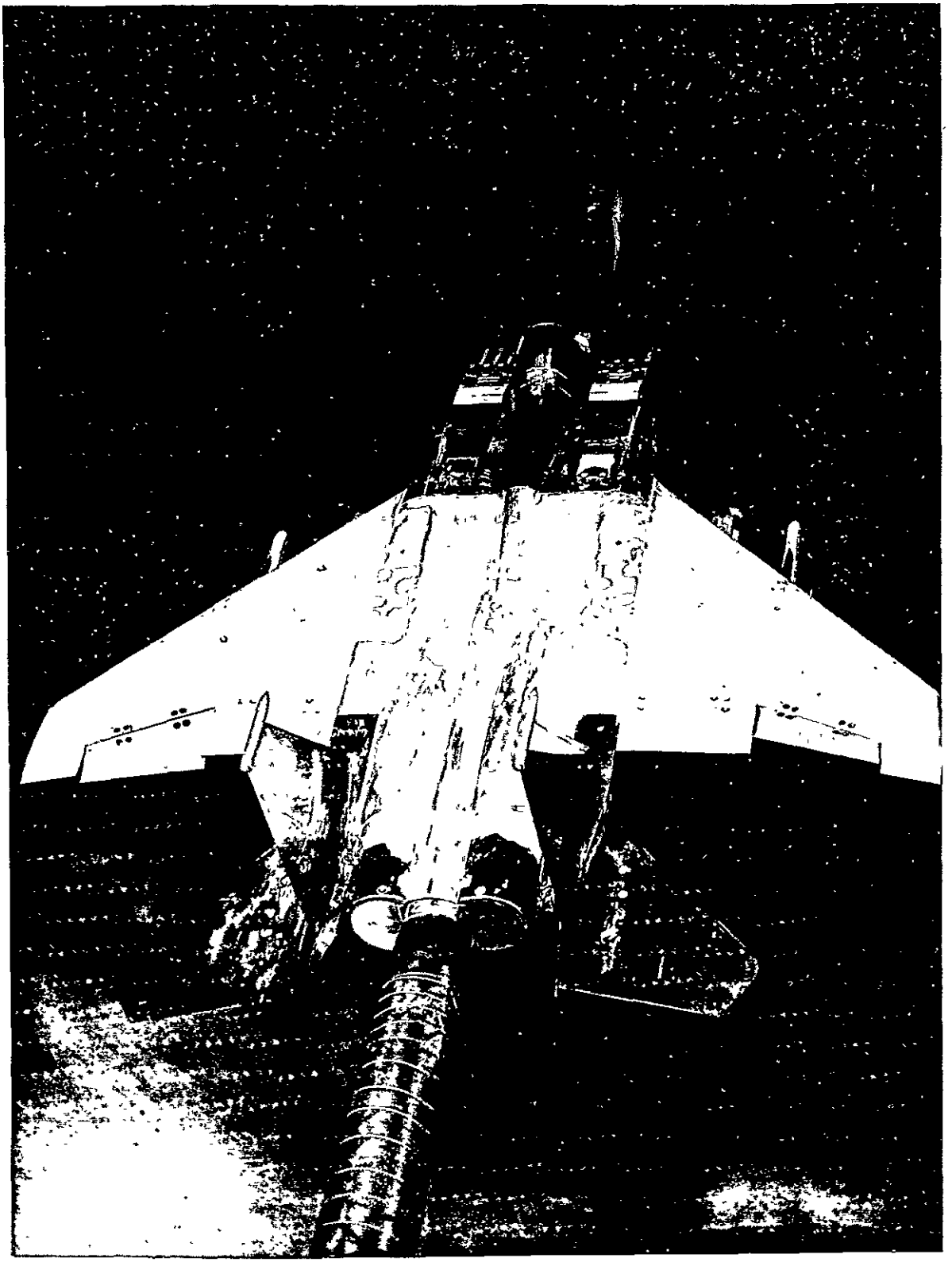

(a) Top view

Figure 3. - Model installation photographs.

ORIGINAL PAGE IS
OF POOR QUALITY

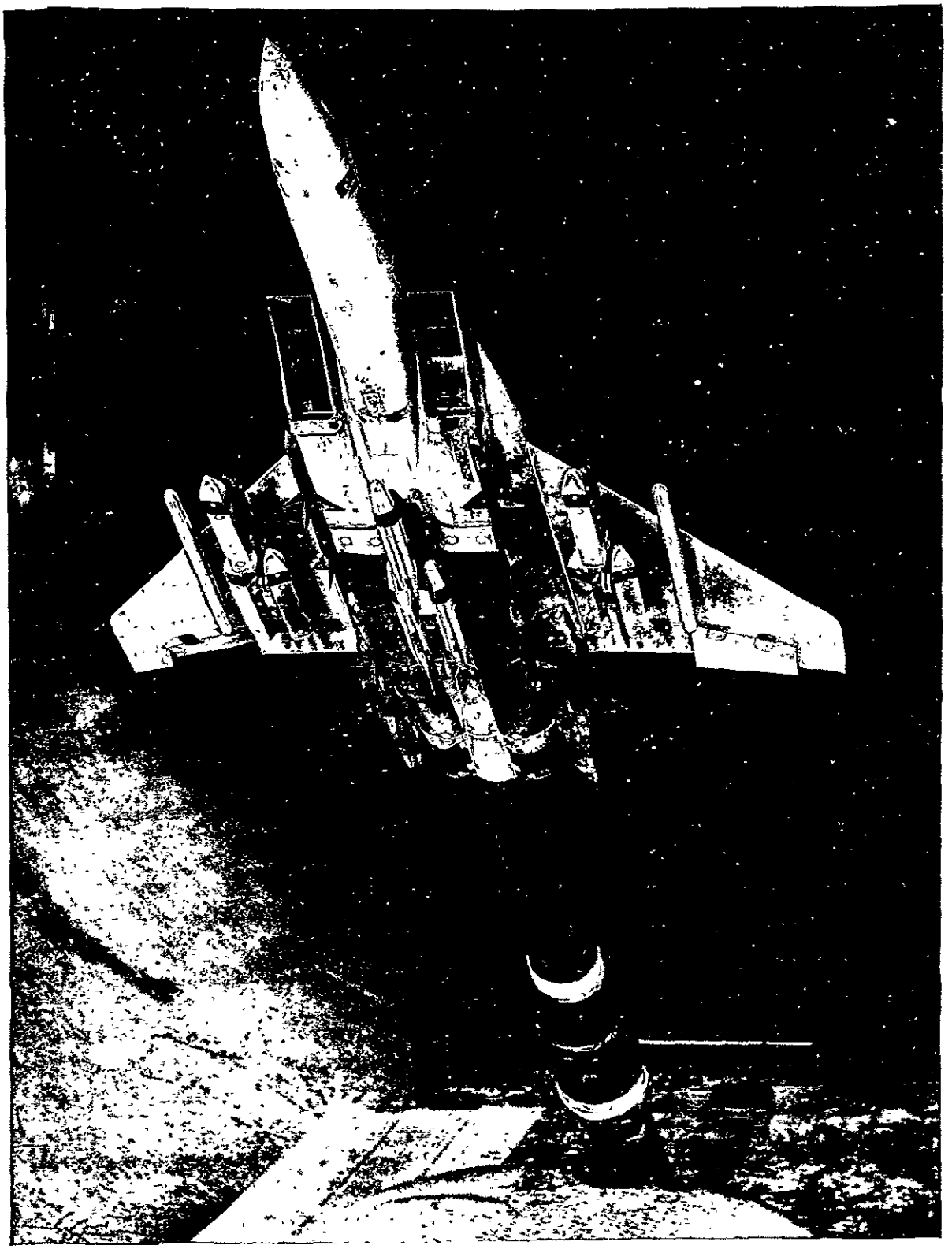

(b) Bottom view

Figure 3. - Concluded.

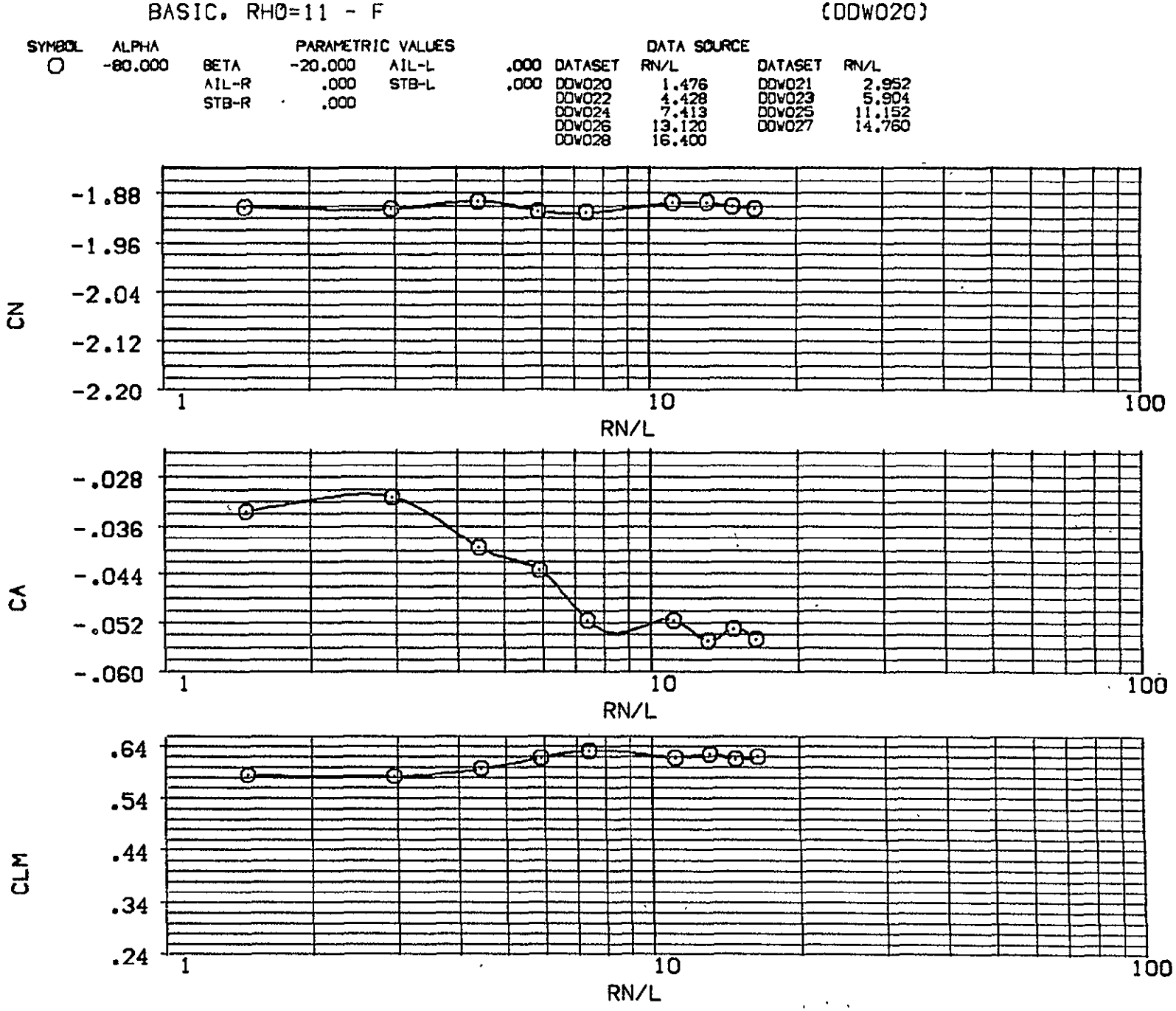

FIG. 4 VARIATION OF AERO. CHAR. WITH REYNOLDS NO. AT VARIOUS ANGLES OF ATTACK.

ORIGINAL PAGE IS
OF POOR QUALITY

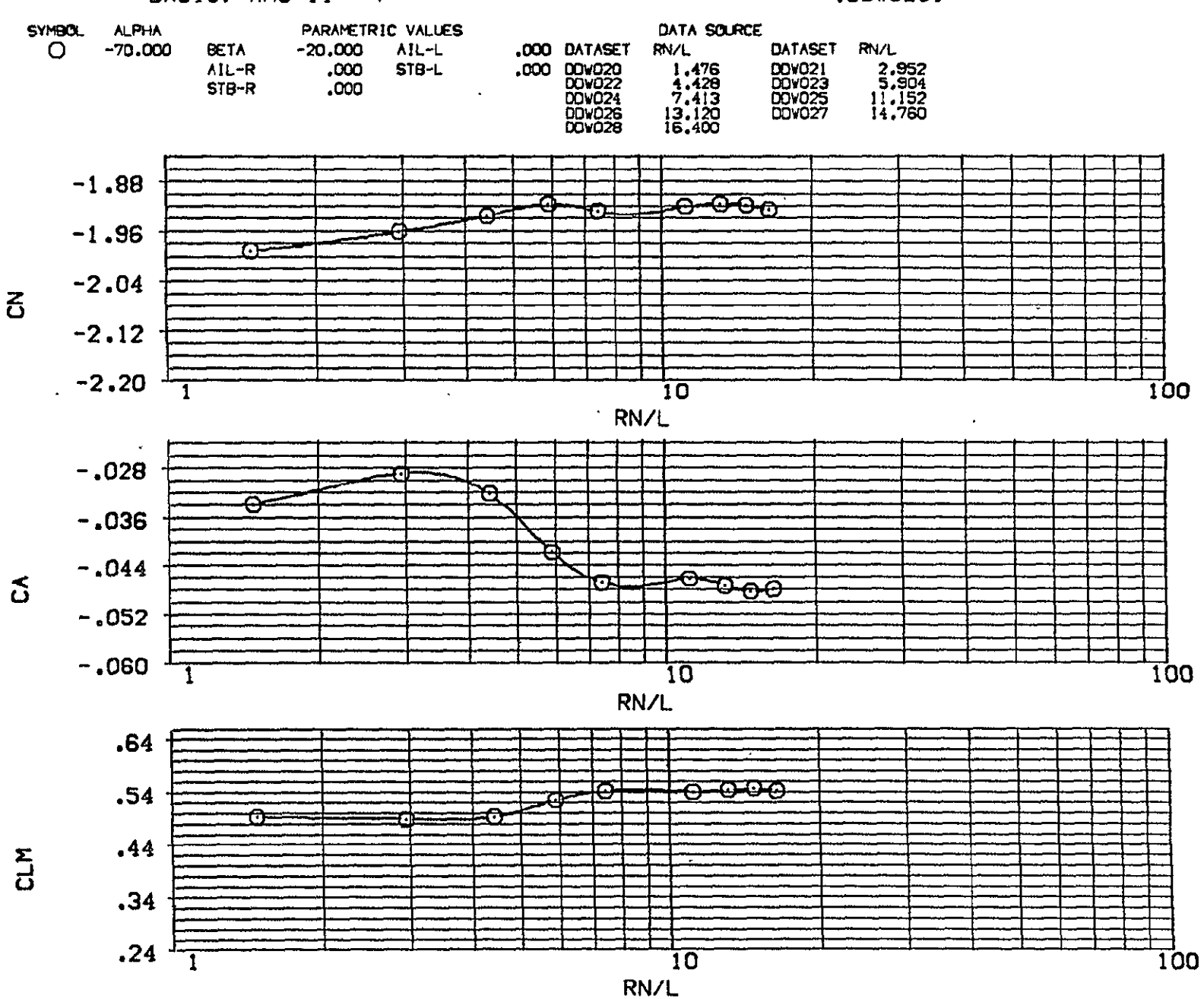

FIG. 4 VARIATION OF AERO. CHAR. WITH REYNOLDS NO. AT VARIOUS ANGLES OF ATTACK.

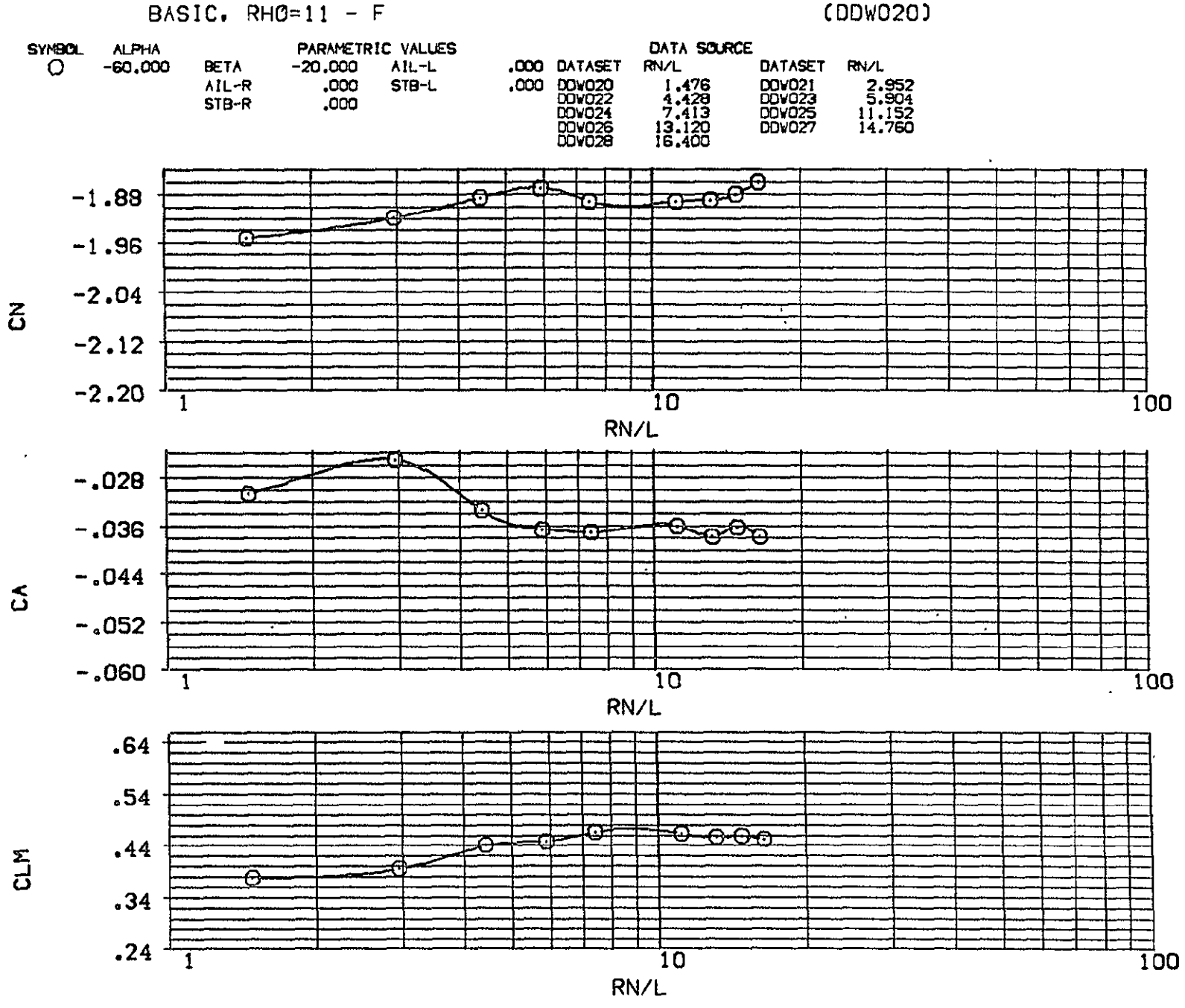

FIG. 4 VARIATION OF AERO. CHAR. WITH REYNOLDS NO. AT VARIOUS ANGLES OF ATTACK.

ORIGINAL PAGE IS
OF POOR QUALITY

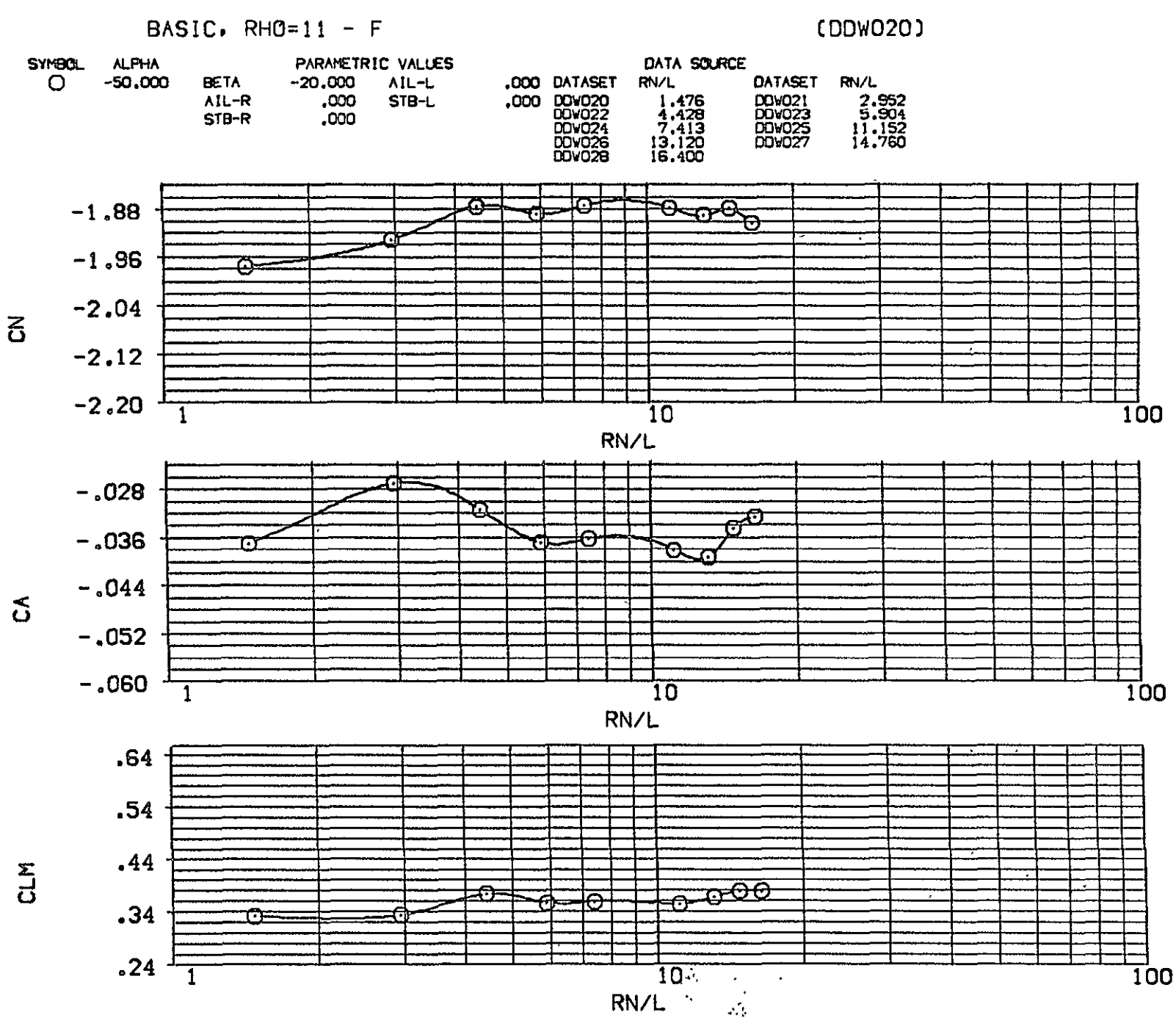

FIG. 4 VARIATION OF AERO. CHAR. WITH REYNOLDS NO. AT VARIOUS ANGLES OF ATTACK.

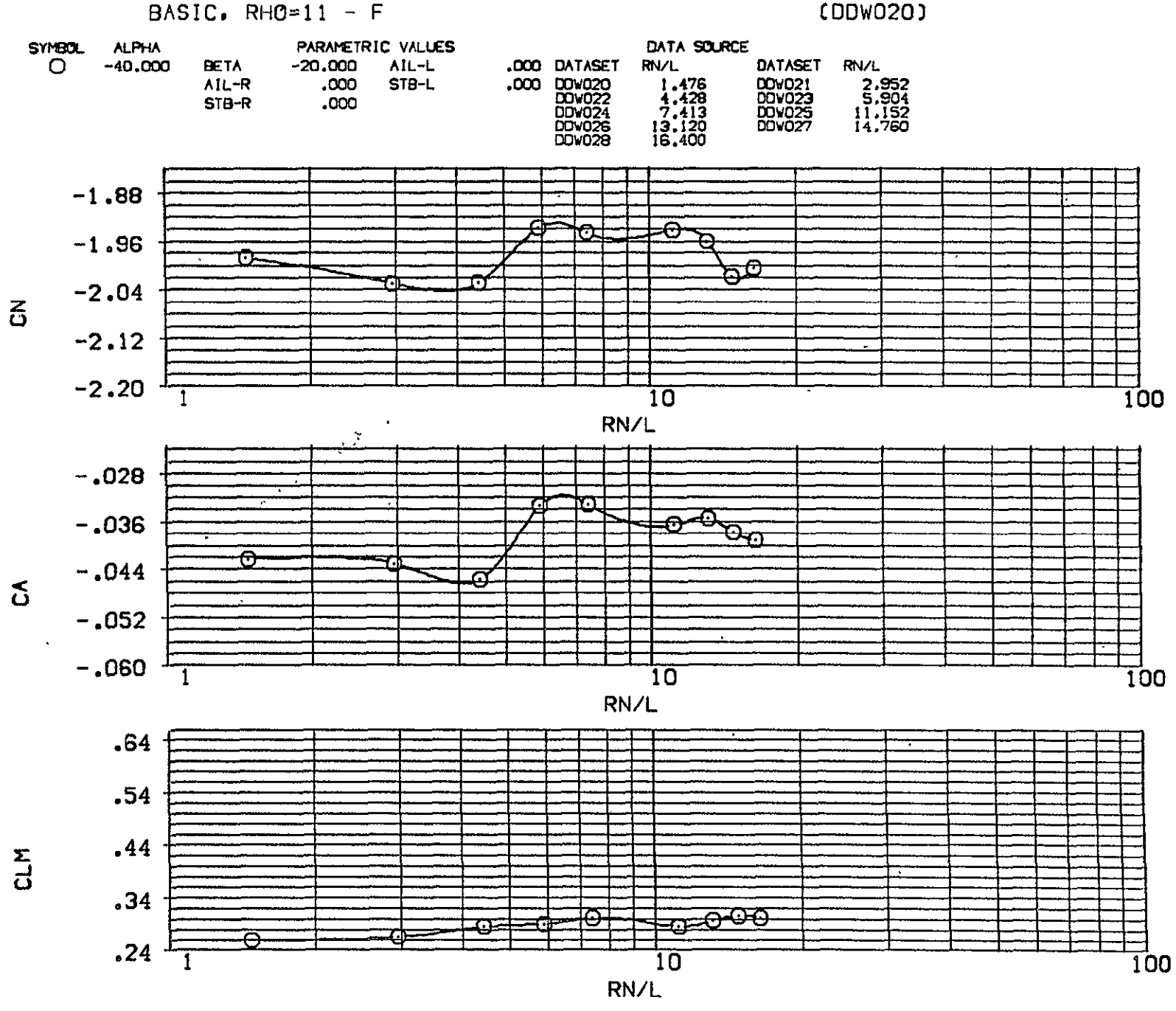

FIG. 4 VARIATION OF AERO. CHAR. WITH REYNOLDS NO. AT VARIOUS ANGLES OF ATTACK.

ORIGINAL PAGE IS
OF POOR QUALITY

BASIC. RHO=11 - F (DDW020)

SYMBOL	ALPHA	PARAMETRIC VALUES			
O	-80.000	BETA	-10.000	AIL-L	.000
		AIL-R	.000	STB-L	.000
		STB-R	.000		

DATA SOURCE

DATASET	RN/L	DATASET	RN/L
DDW020	1.476	DDW021	2.952
DDW022	4.428	DDW023	5.904
DDW024	7.413	DDW025	11.152
DDW026	13.120	DDW027	14.760
DDW028	16.400		

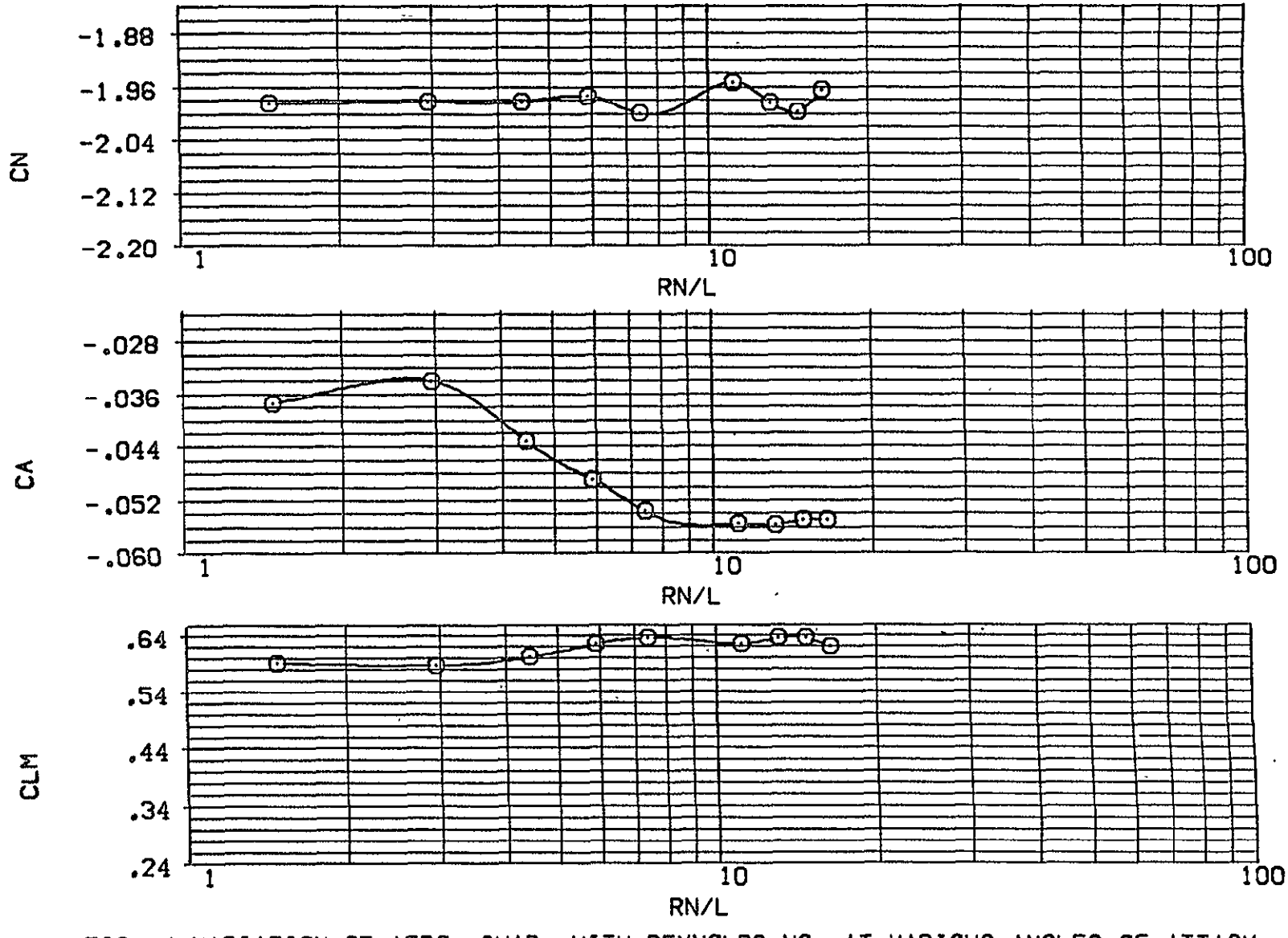

FIG. 4 VARIATION OF AERO. CHAR. WITH REYNOLDS NO. AT VARIOUS ANGLES OF ATTACK.

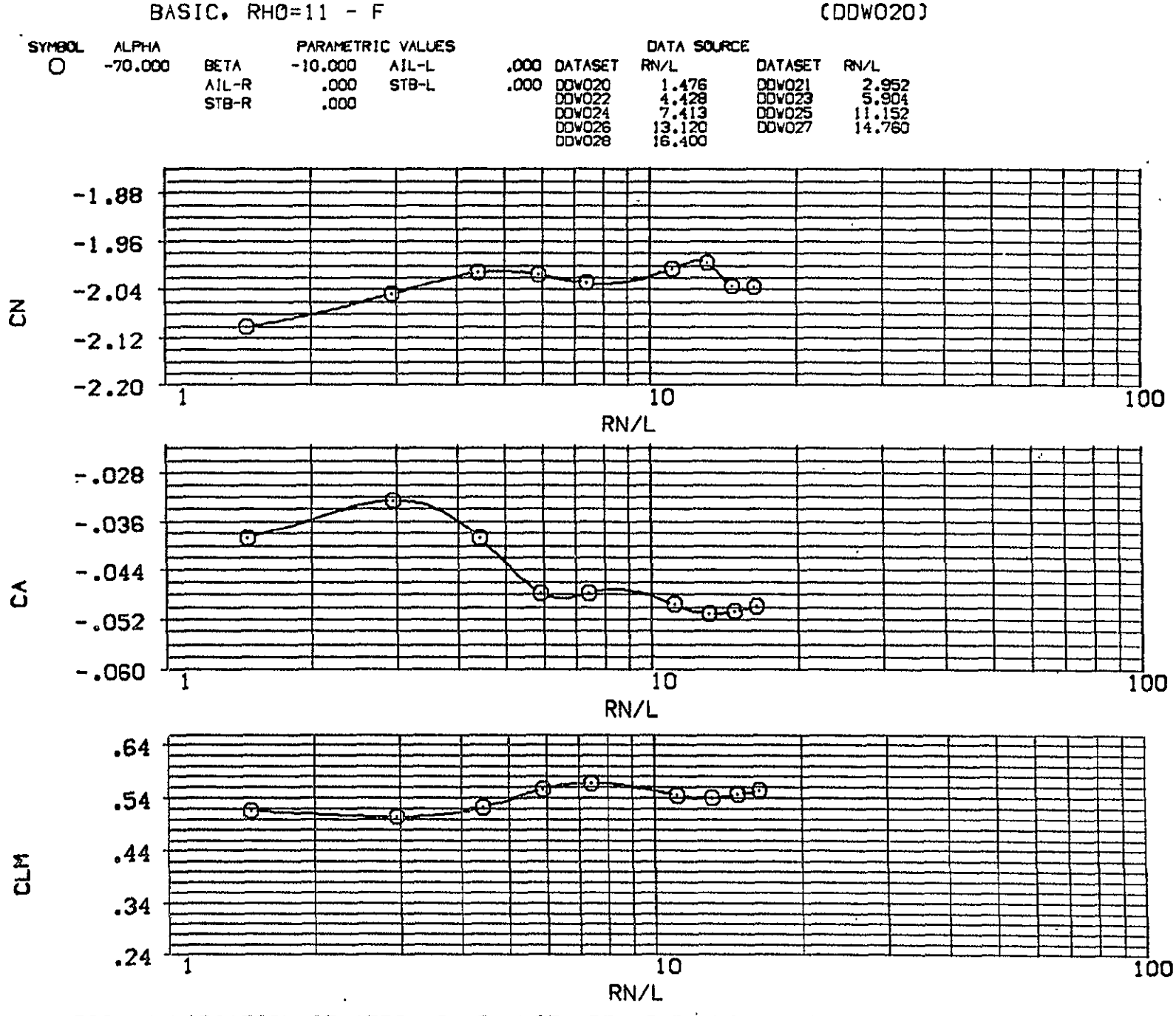

FIG. 4 VARIATION OF AERO. CHAR. WITH REYNOLDS NO. AT VARIOUS ANGLES OF ATTACK.

ORIGINAL PAGE IS
OF POOR QUALITY

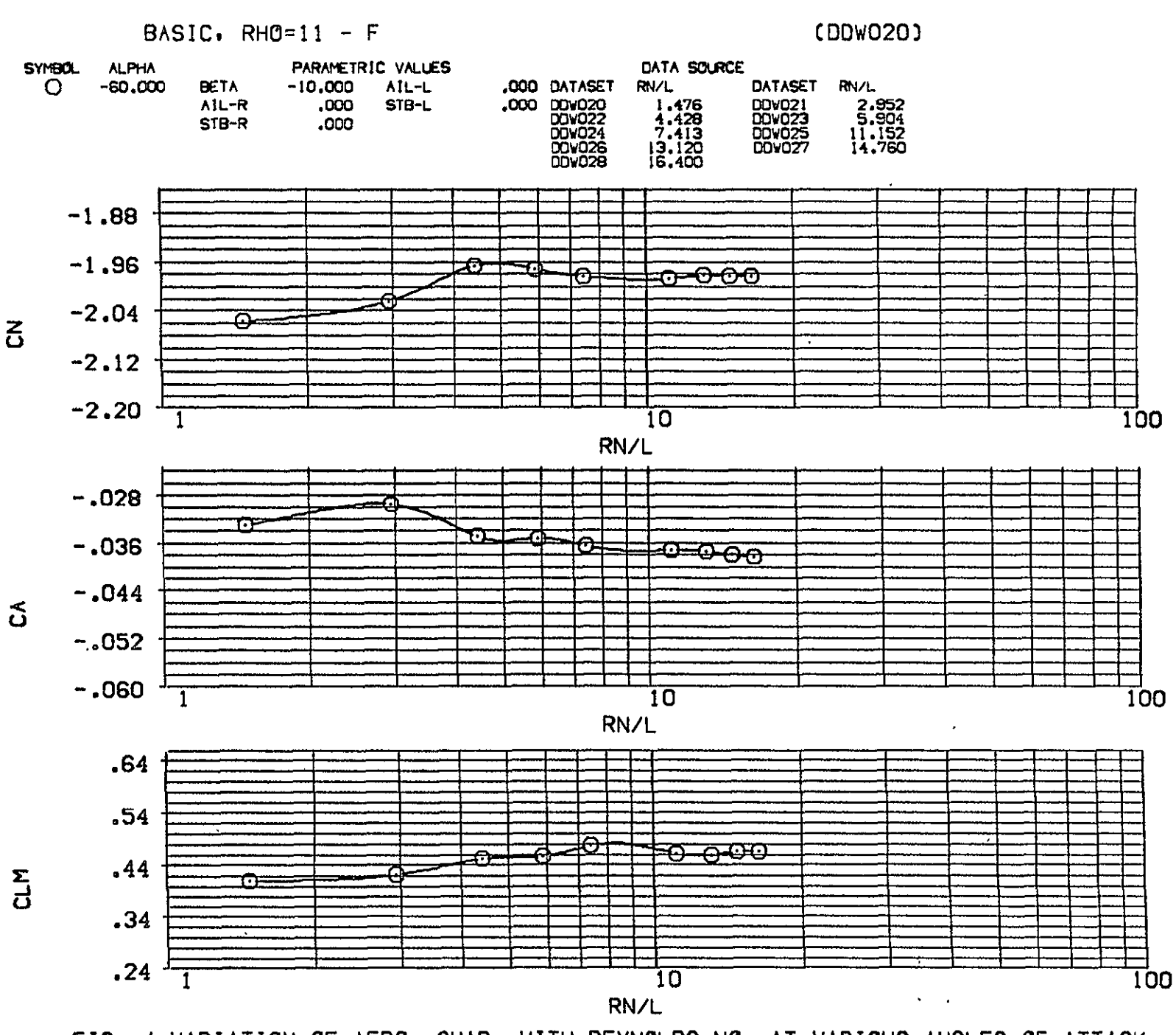

FIG. 4 VARIATION OF AERO. CHAR. WITH REYNOLDS NO. AT VARIOUS ANGLES OF ATTACK.

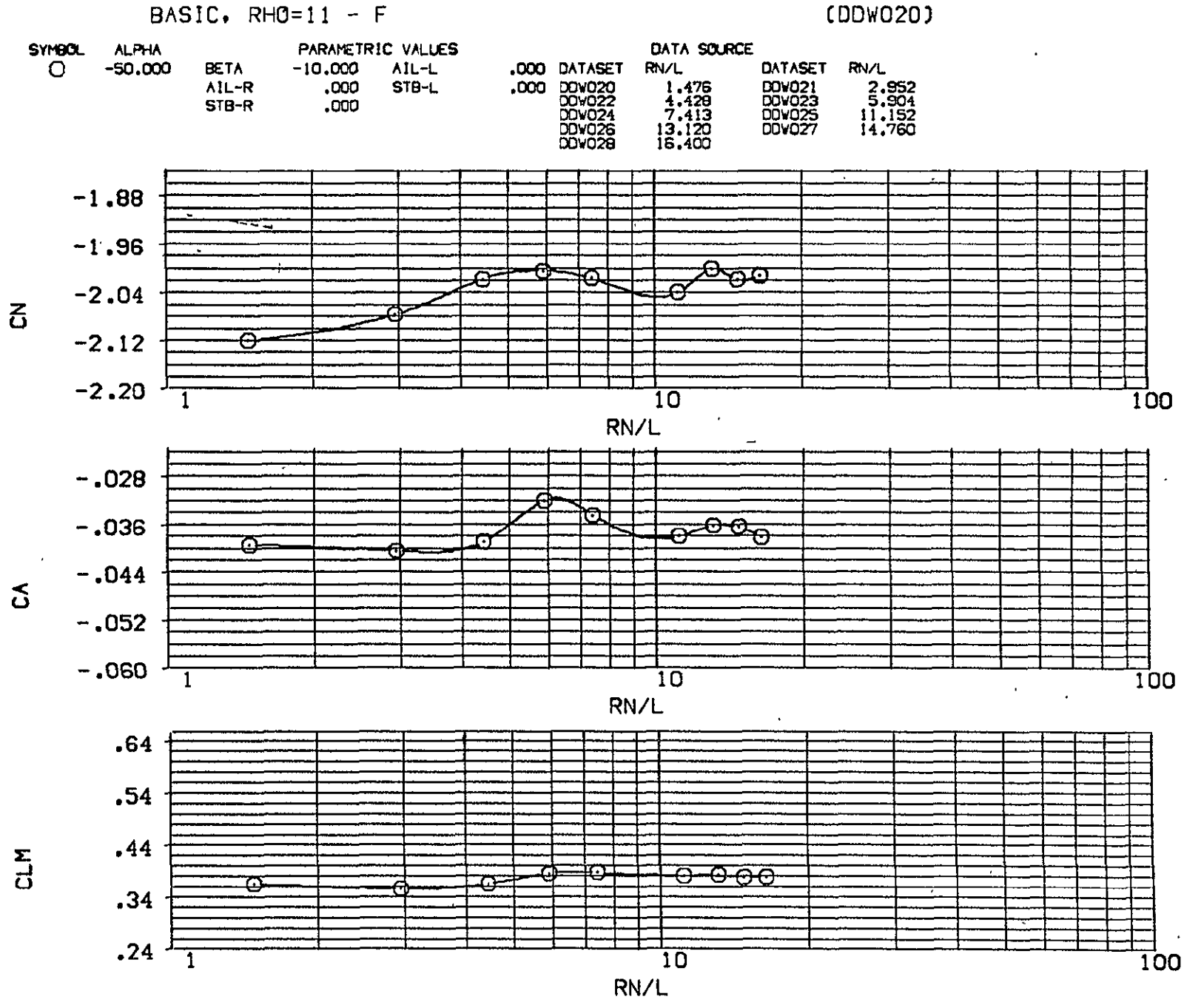

FIG. 4 VARIATION OF AERO. CHAR. WITH REYNOLDS NO. AT VARIOUS ANGLES OF ATTACK.

40

ORIGINAL PAGE IS
OF POOR QUALITY

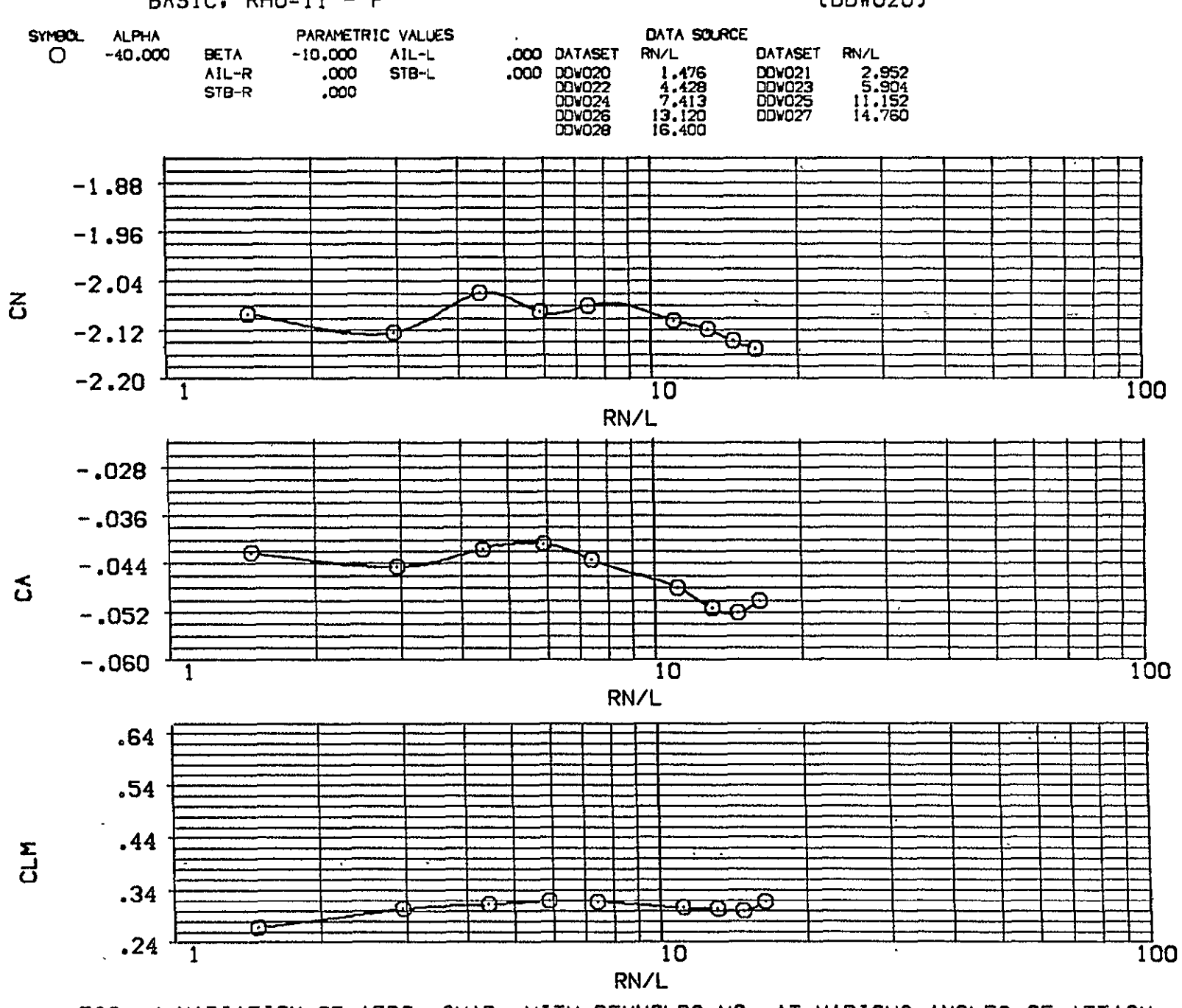

FIG. 4 VARIATION OF AERO. CHAR. WITH REYNOLDS NO. AT VARIOUS ANGLES OF ATTACK.

ORIGINAL PAGE IS
OF POOR QUALITY

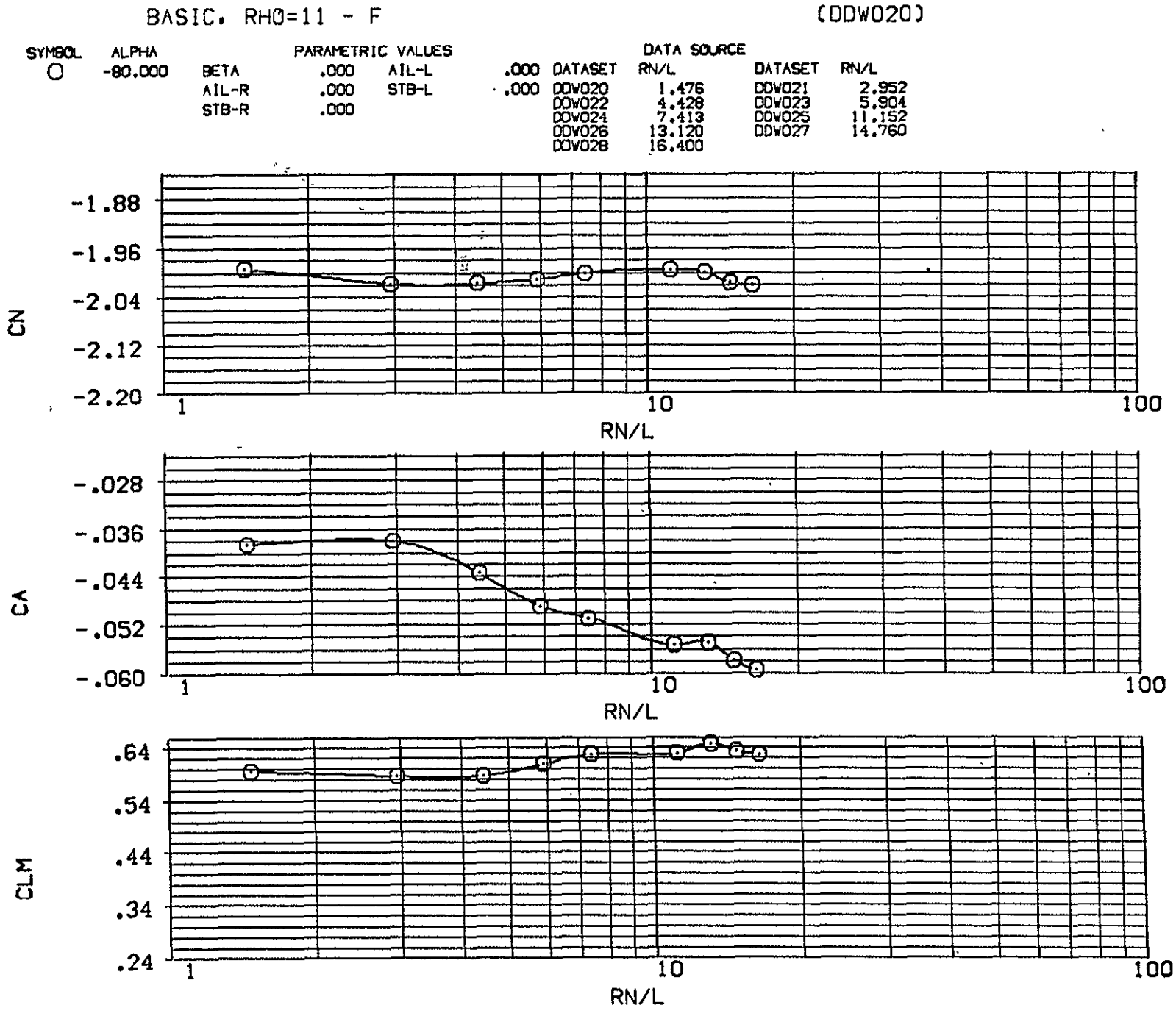

FIG. 4 VARIATION OF AERO. CHAR. WITH REYNOLDS NO. AT VARIOUS ANGLES OF ATTACK.

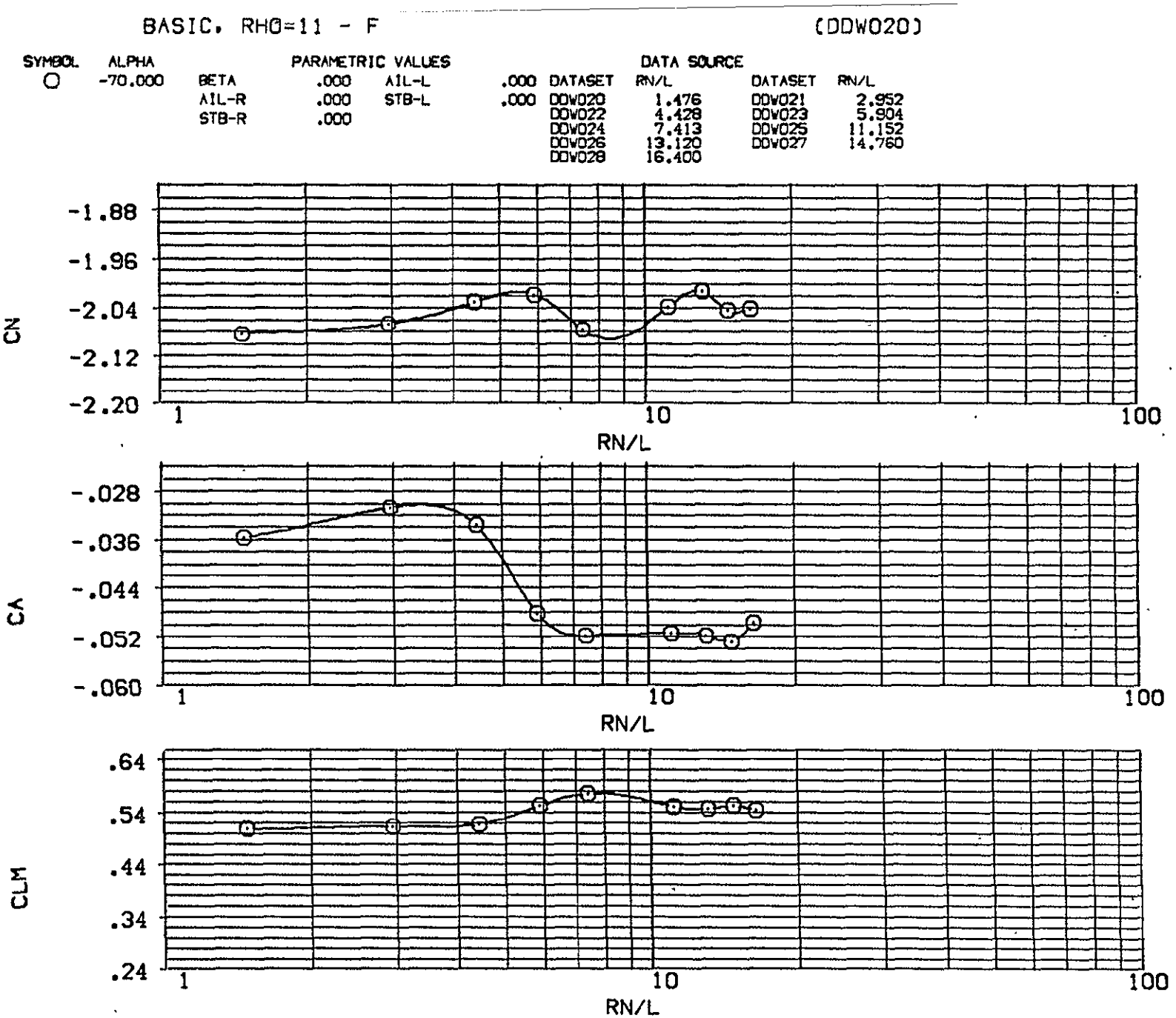

FIG. 4 VARIATION OF AERO. CHAR. WITH REYNOLDS NO. AT VARIOUS ANGLES OF ATTACK.

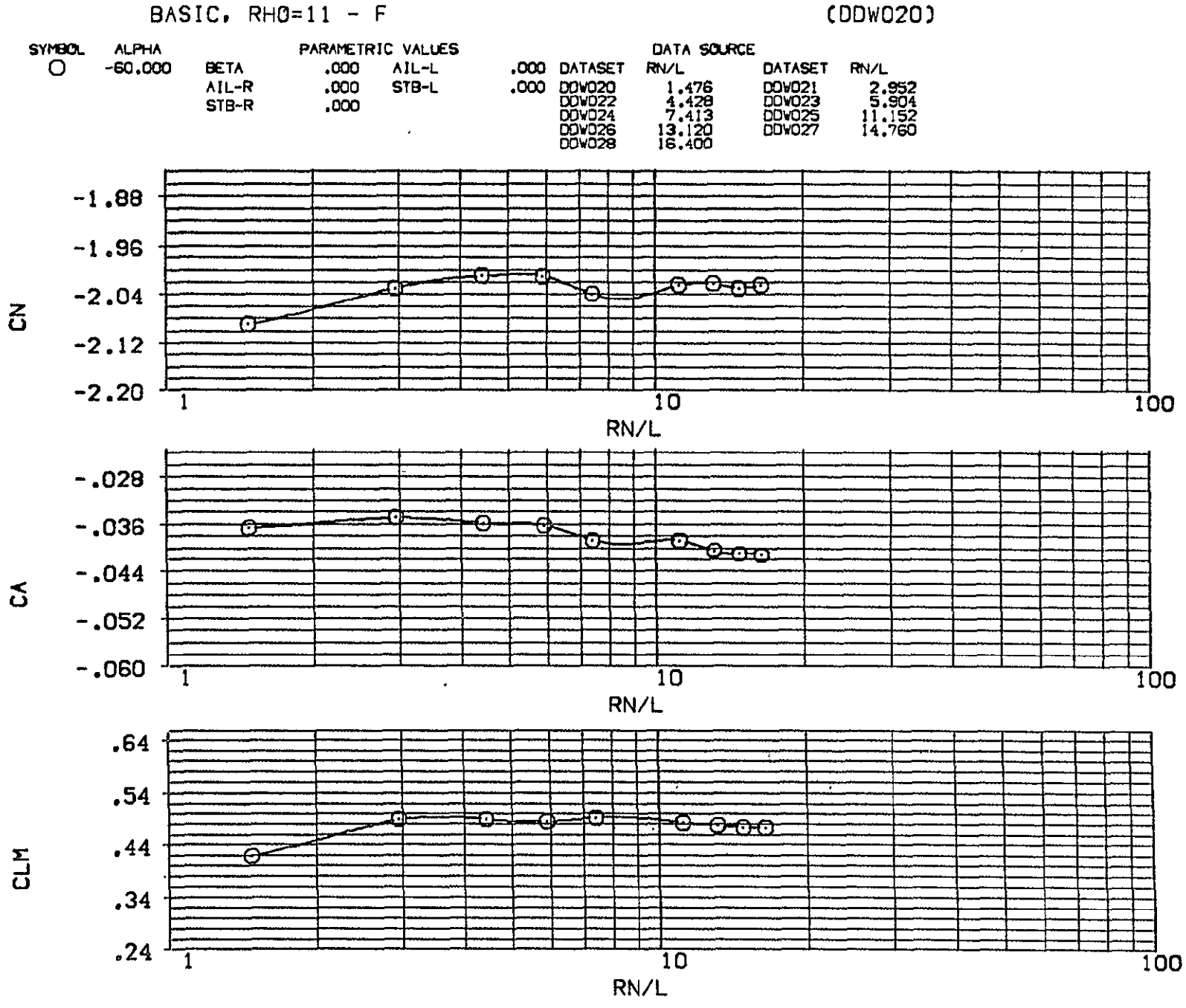

FIG. 4 VARIATION OF AERO. CHAR. WITH REYNOLDS NO. AT VARIOUS ANGLES OF ATTACK.

ORIGINAL PAGE IS
OF POOR QUALITY

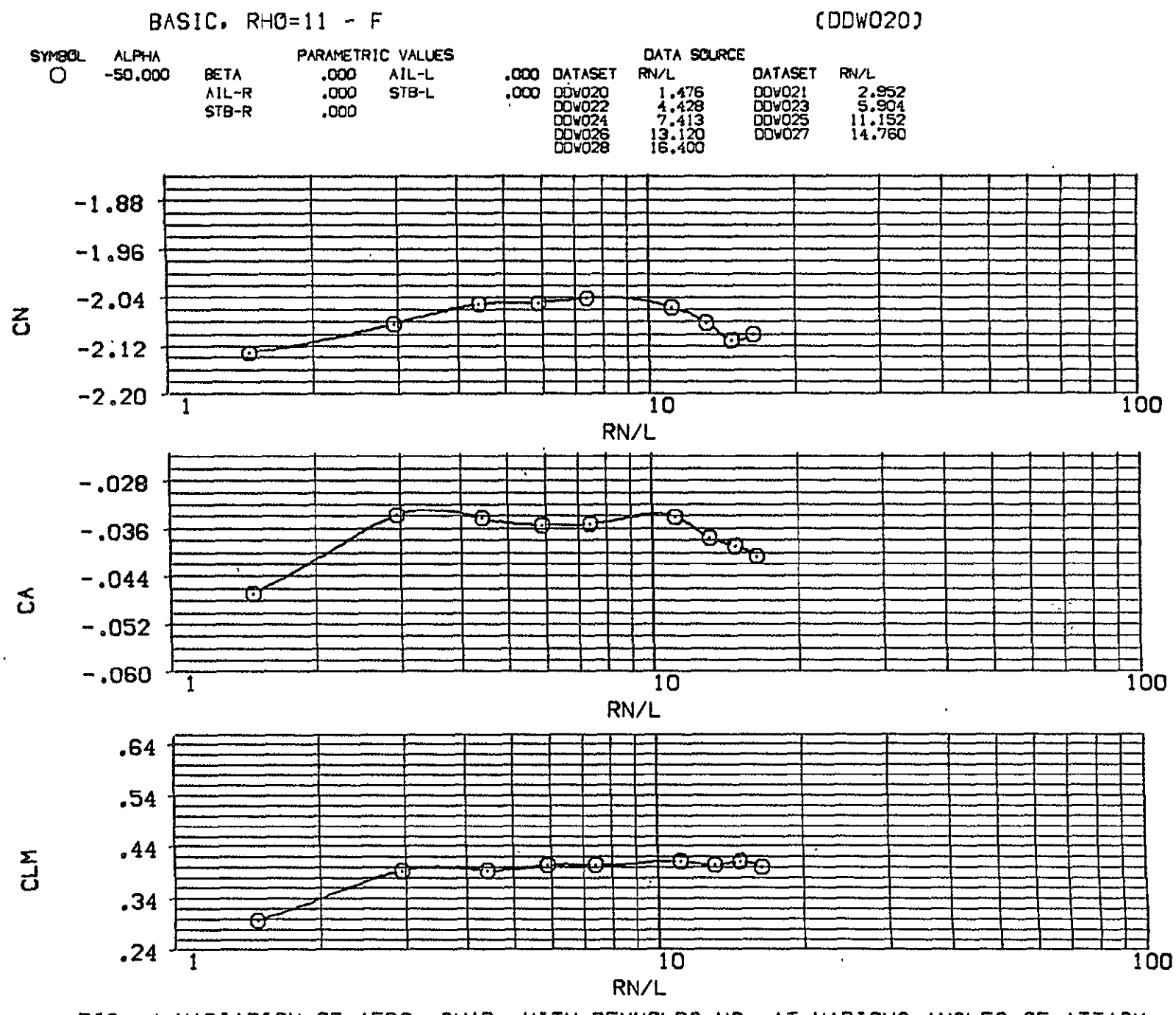

FIG. 4 VARIATION OF AERO. CHAR. WITH REYNOLDS NO. AT VARIOUS ANGLES OF ATTACK.

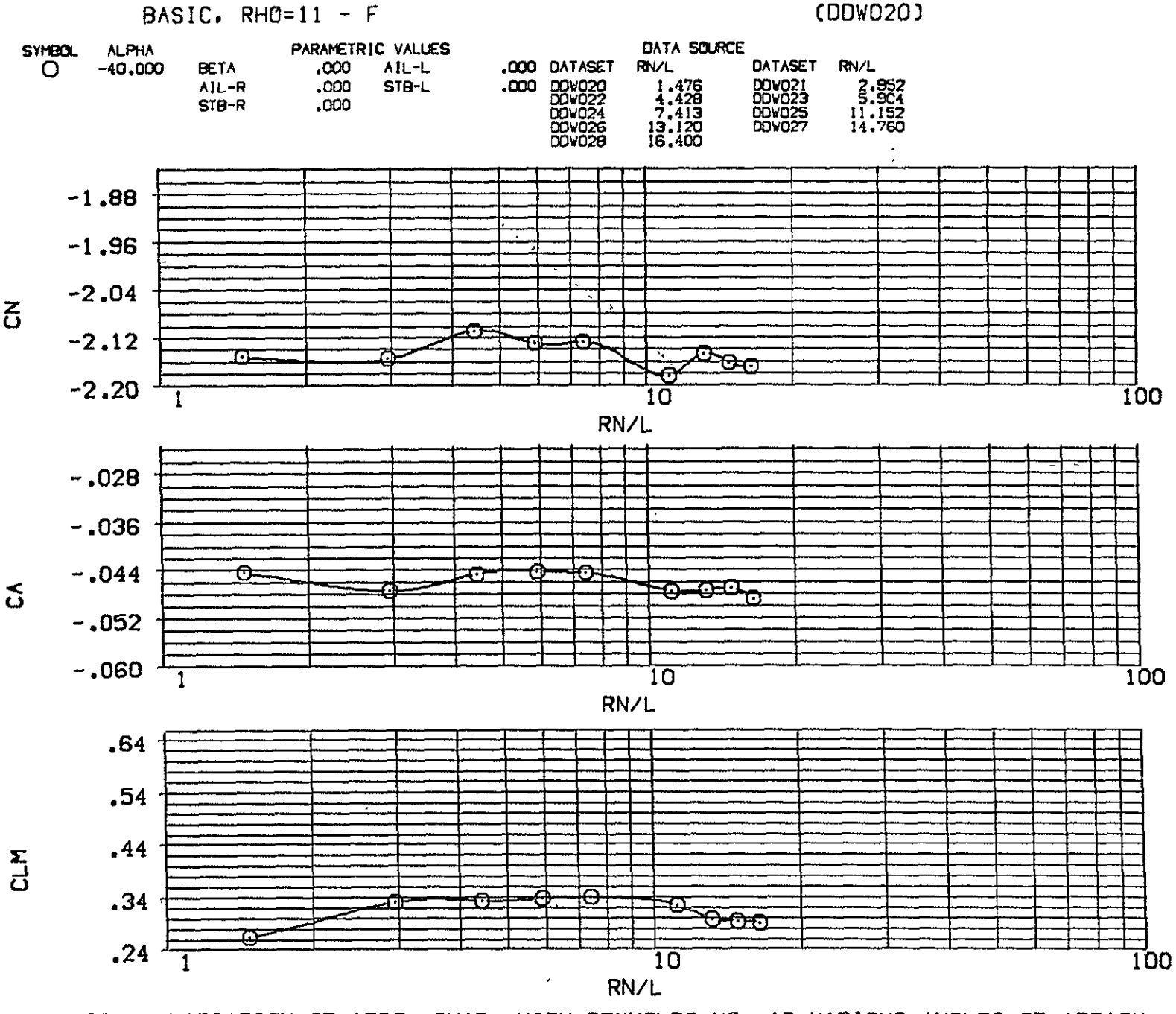

FIG. 4 VARIATION OF AERO. CHAR. WITH REYNOLDS NO. AT VARIOUS ANGLES OF ATTACK.

ORIGINAL PAGE IS OF POOR QUALITY

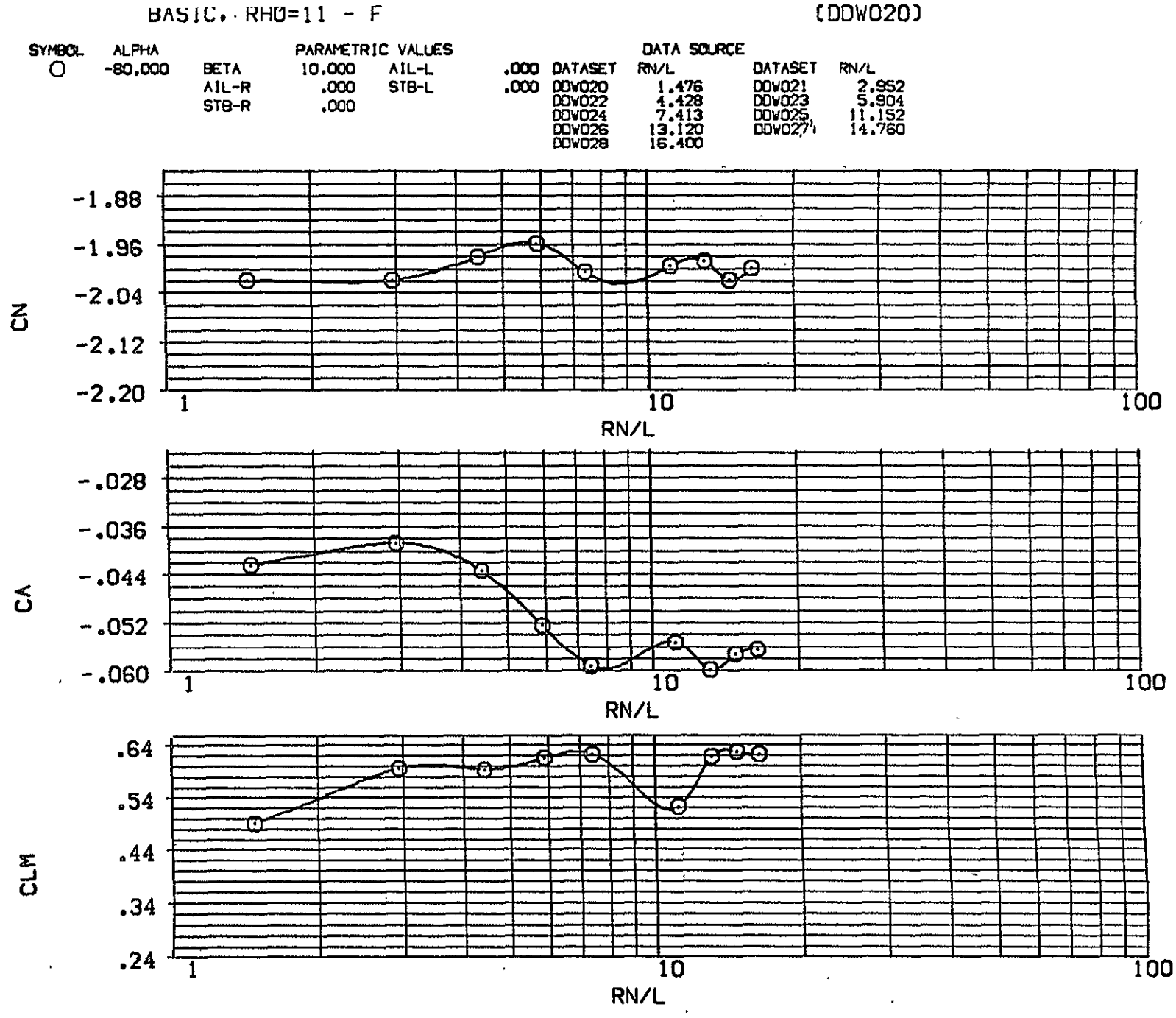

FIG. 4 VARIATION OF AERO. CHAR. WITH REYNOLDS NO. AT VARIOUS ANGLES OF ATTACK.

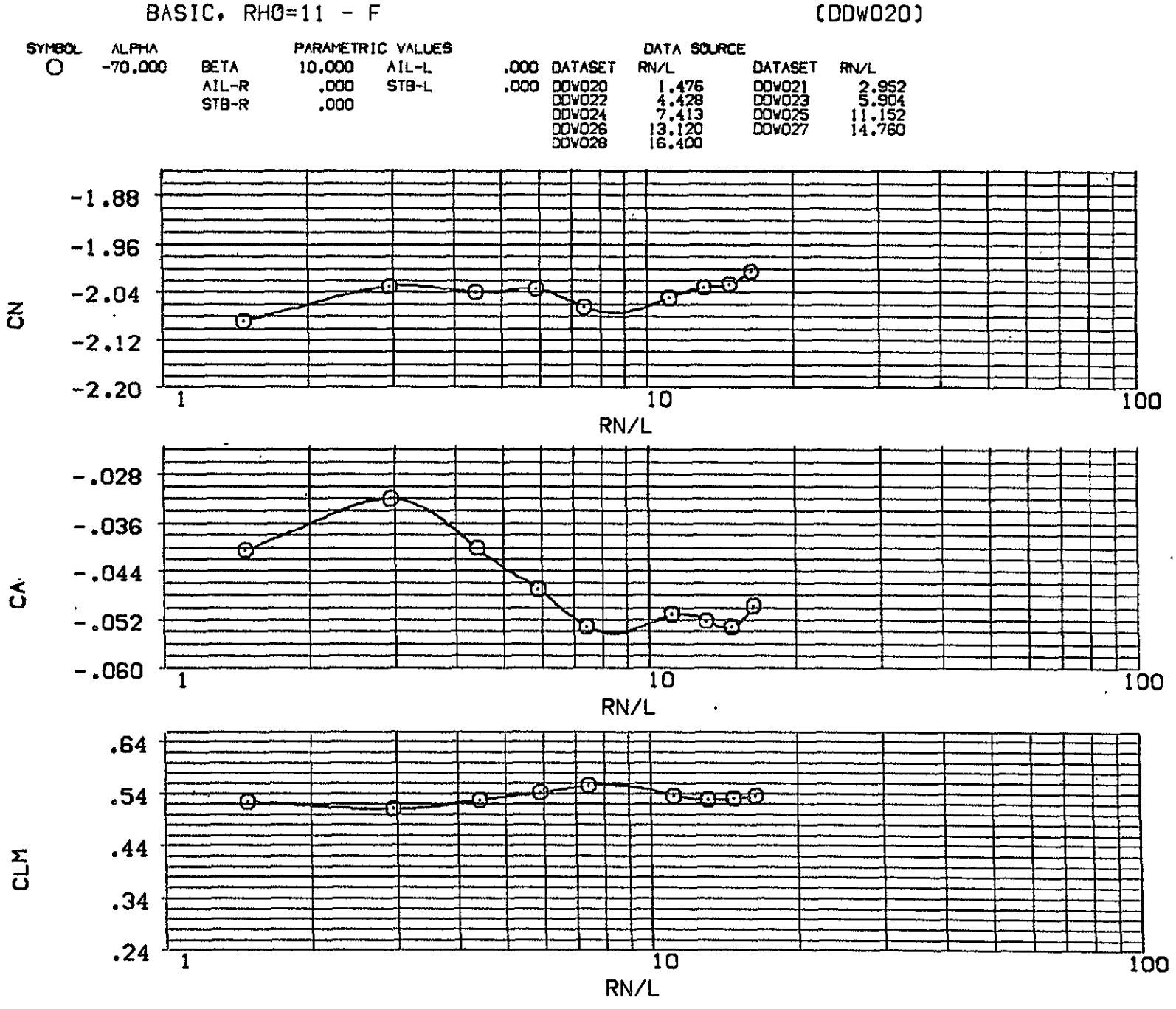

FIG. 4 VARIATION OF AERO. CHAR. WITH REYNOLDS NO. AT VARIOUS ANGLES OF ATTACK.

ORIGINAL PAGE IS
OF POOR QUALITY

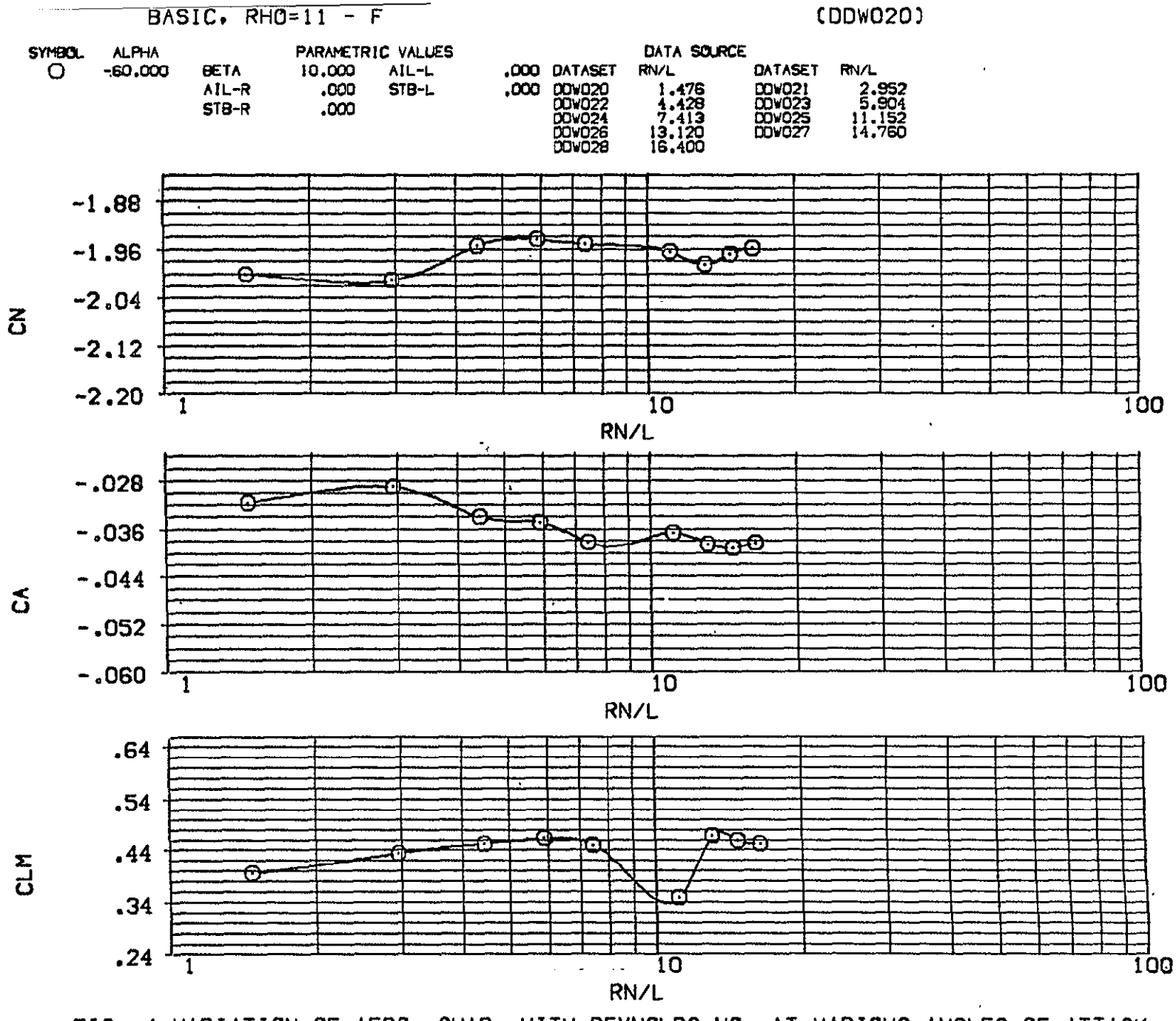

FIG. 4 VARIATION OF AERO. CHAR. WITH REYNOLDS NO. AT VARIOUS ANGLES OF ATTACK.

ORIGINAL PAGE IS
OF POOR QUALITY

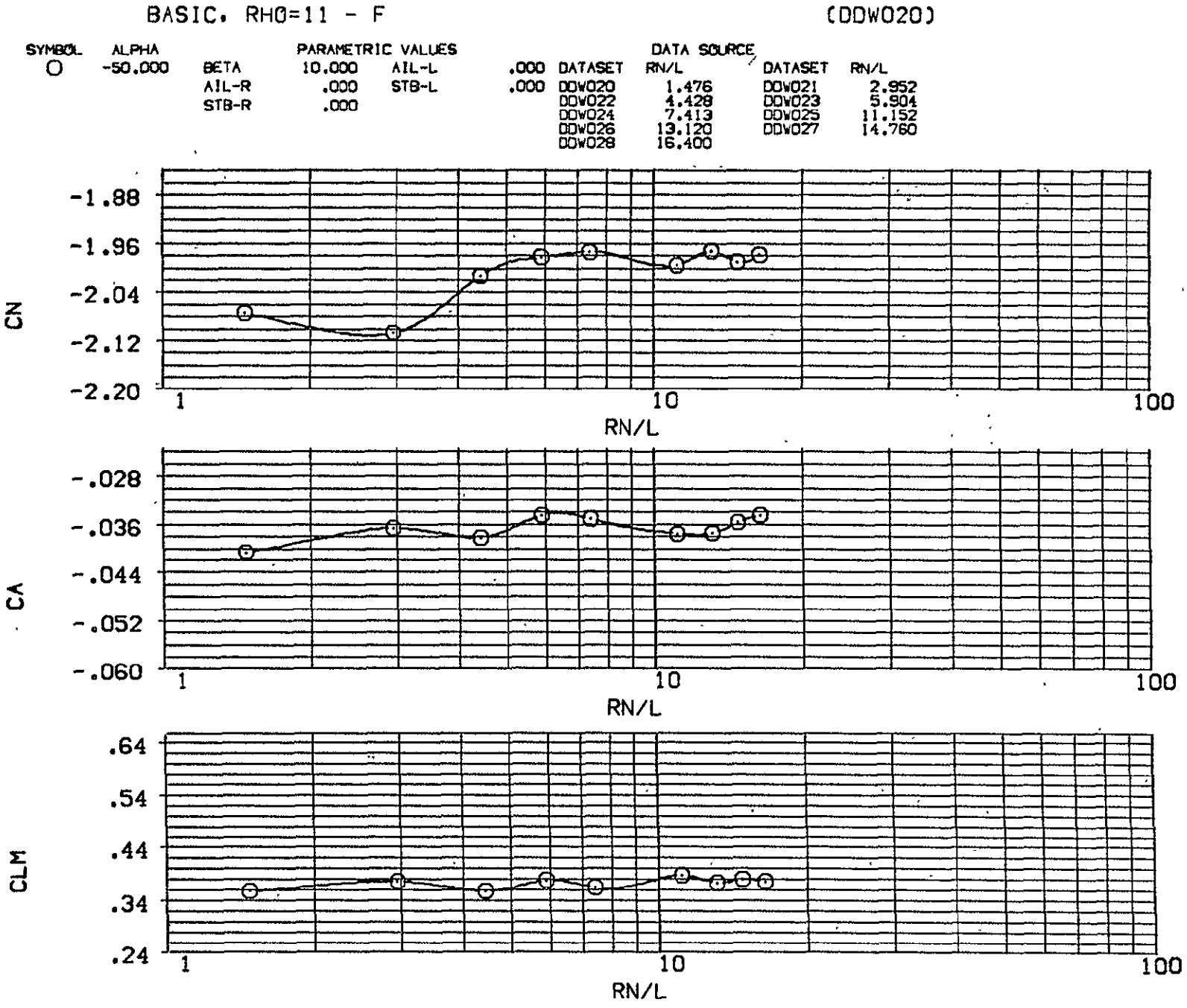

FIG. 4 VARIATION OF AERO. CHAR. WITH REYNOLDS NO. AT VARIOUS ANGLES OF ATTACK.

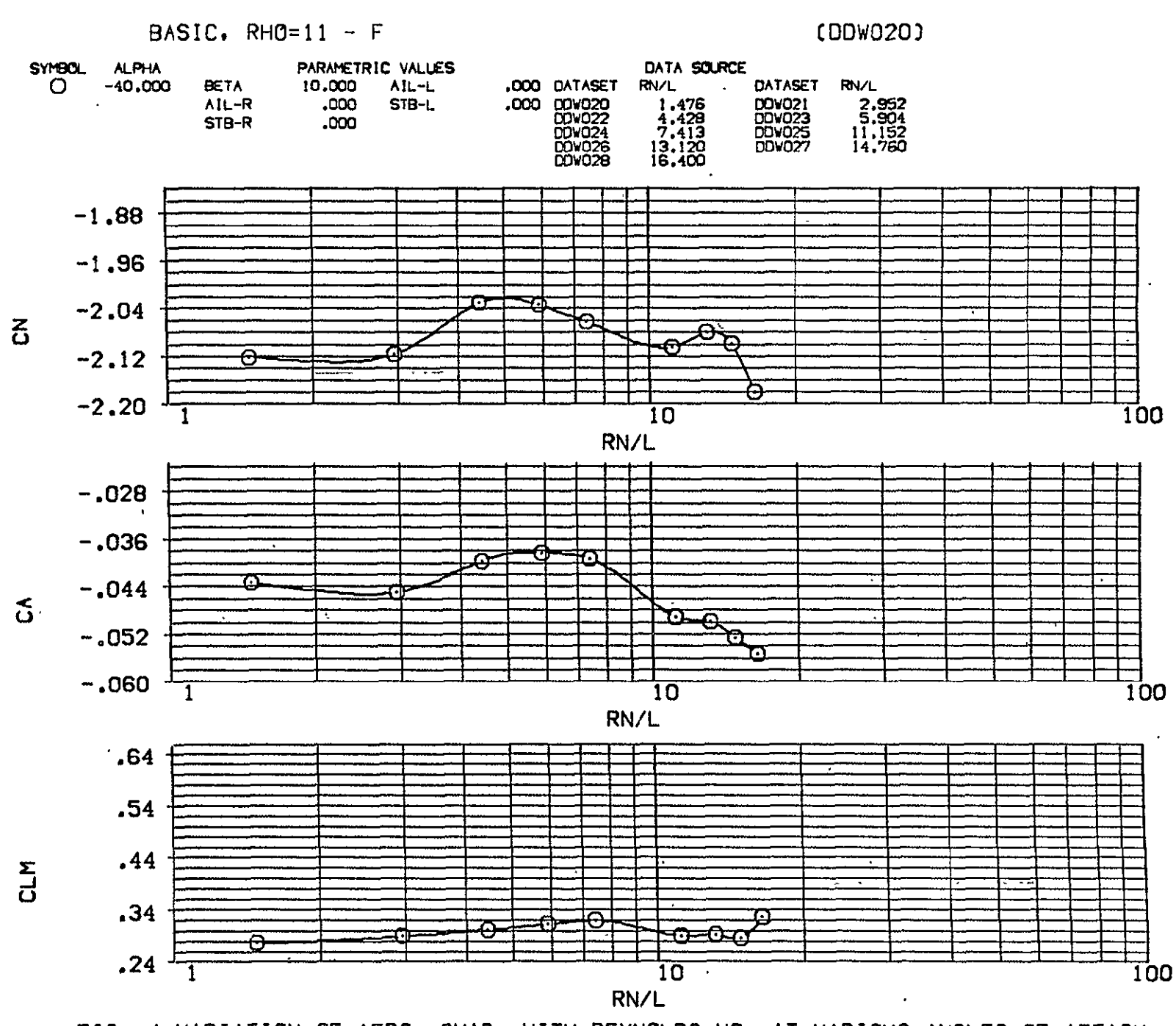

FIG. 4 VARIATION OF AERO. CHAR. WITH REYNOLDS NO. AT VARIOUS ANGLES OF ATTACK.

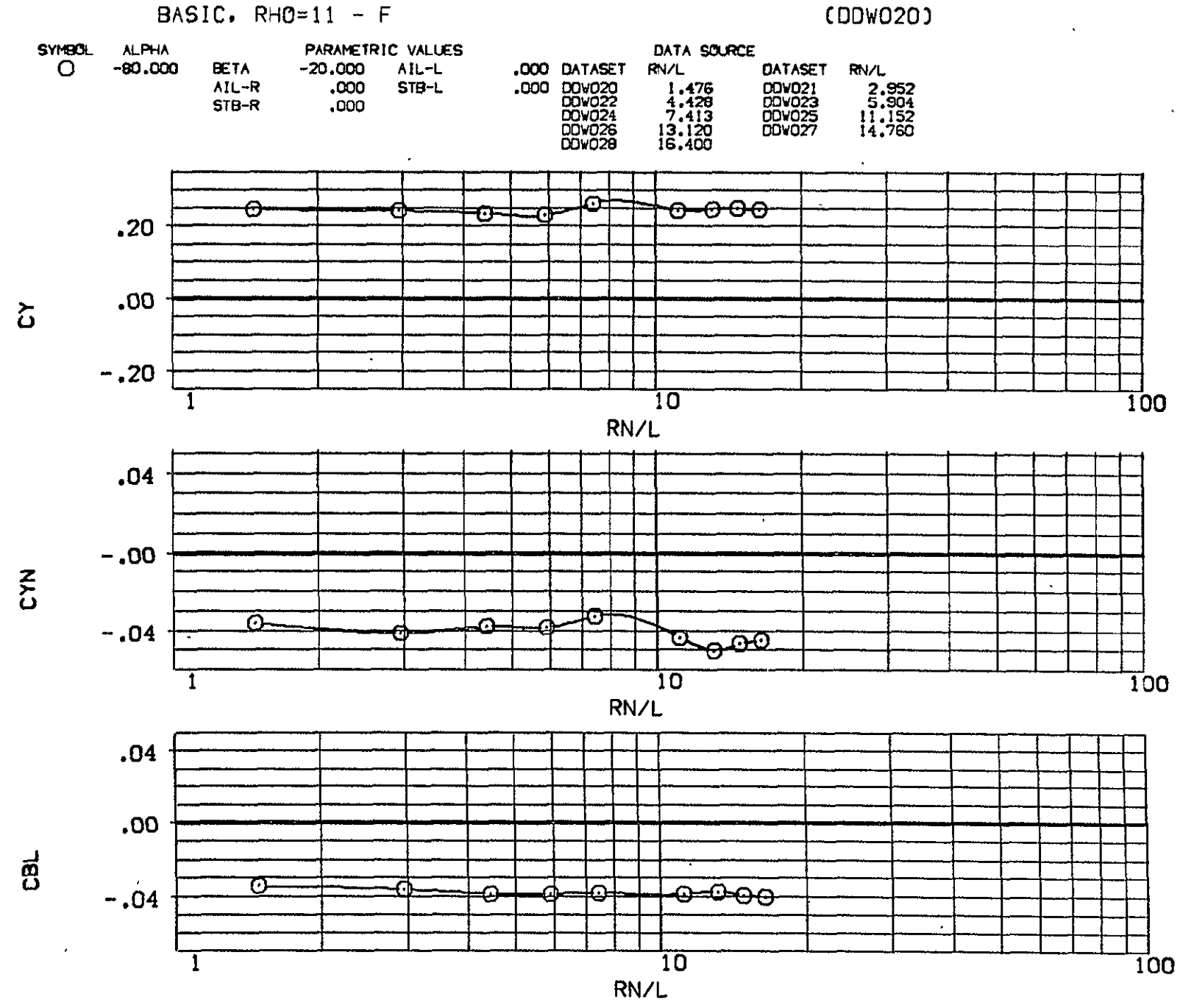

FIG. 4 VARIATION OF AERO. CHAR. WITH REYNOLDS NO. AT VARIOUS ANGLES OF ATTACK.

ORIGINAL PAGE IS
OF POOR QUALITY

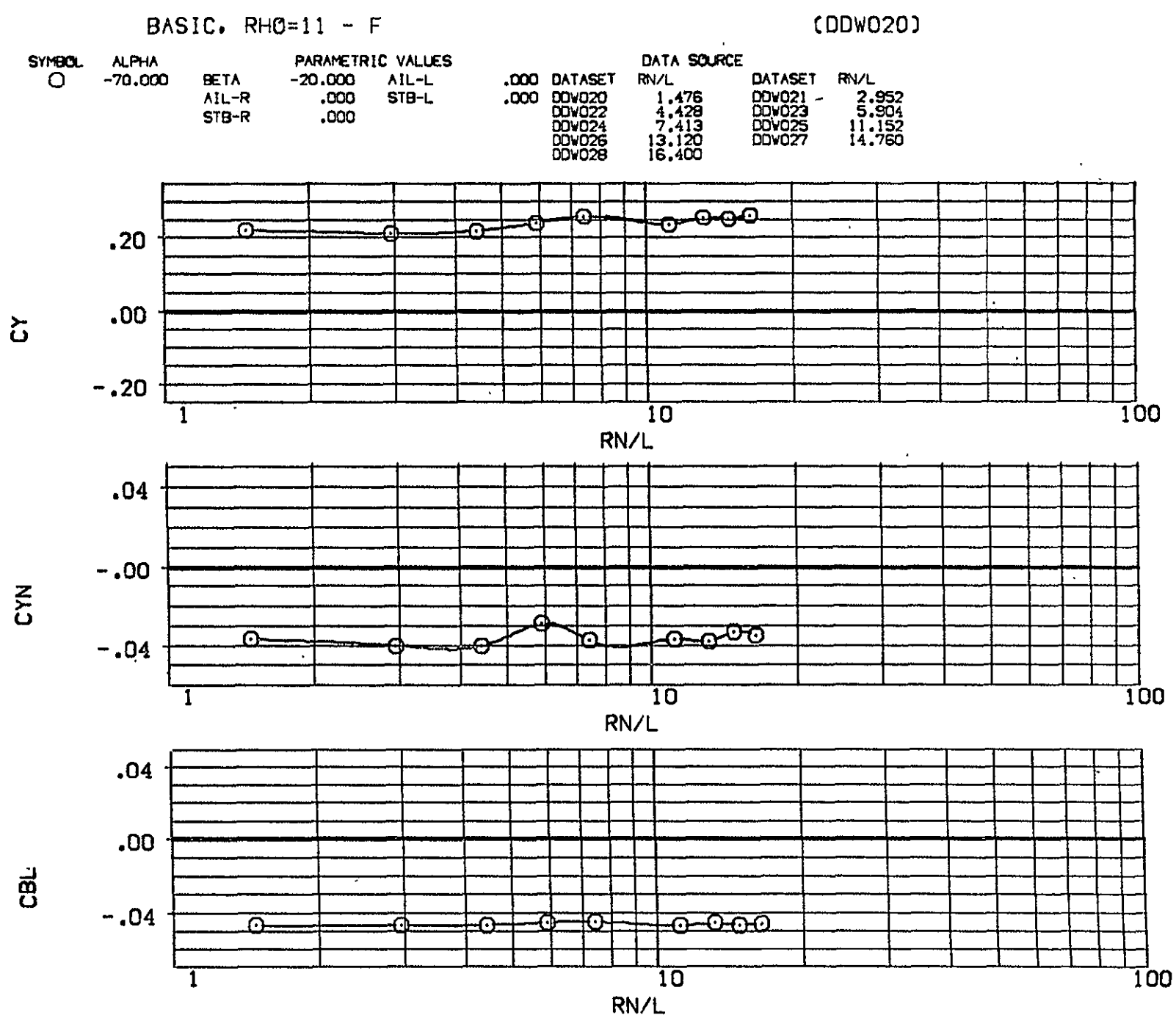

FIG. 4 VARIATION OF AERO. CHAR. WITH REYNOLDS NO. AT VARIOUS ANGLES OF ATTACK.

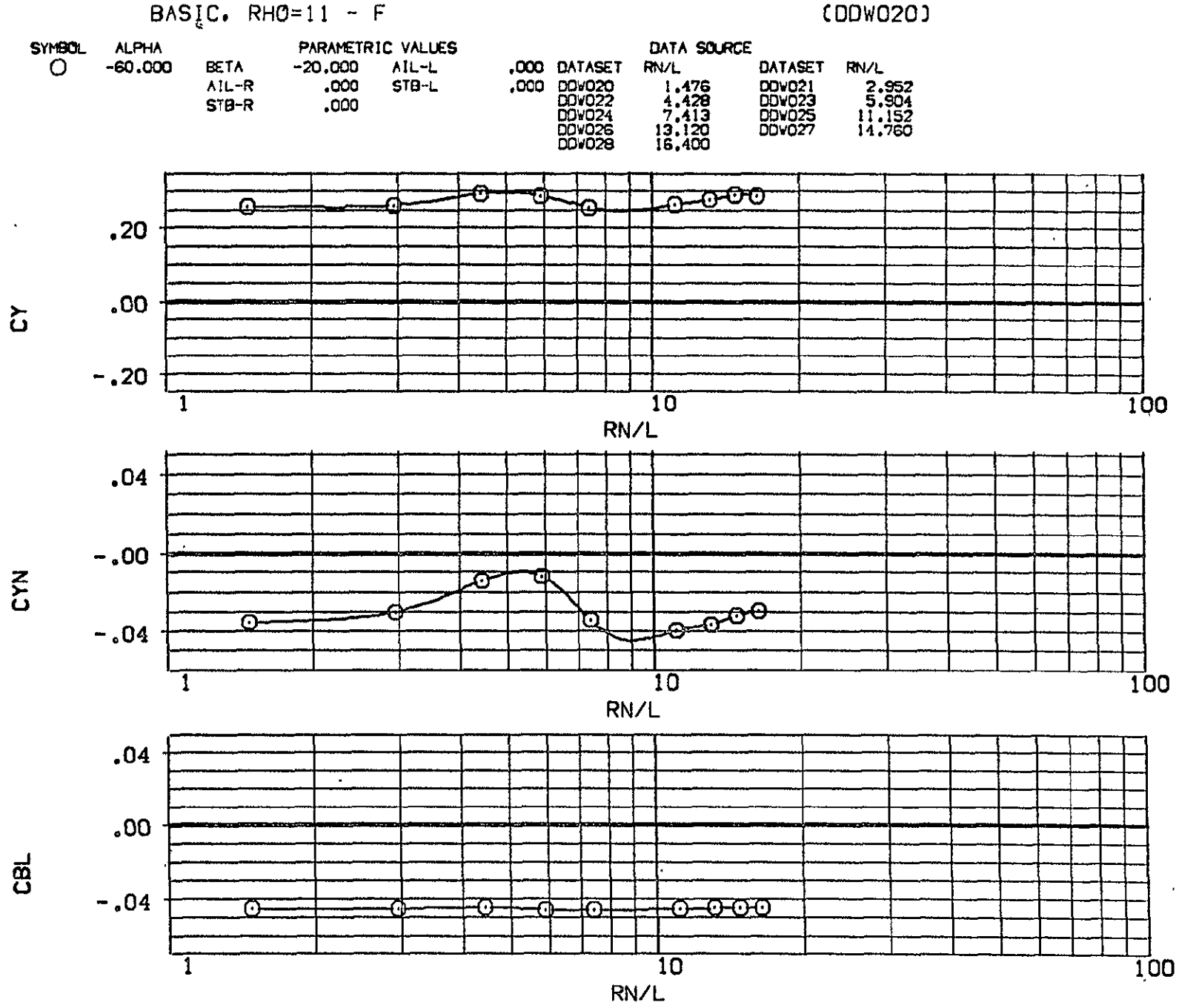

FIG. 4 VARIATION OF AERO. CHAR. WITH REYNOLDS NO. AT VARIOUS ANGLES OF ATTACK.

34

ORIGINAL PAGE IS
OF POOR QUALITY

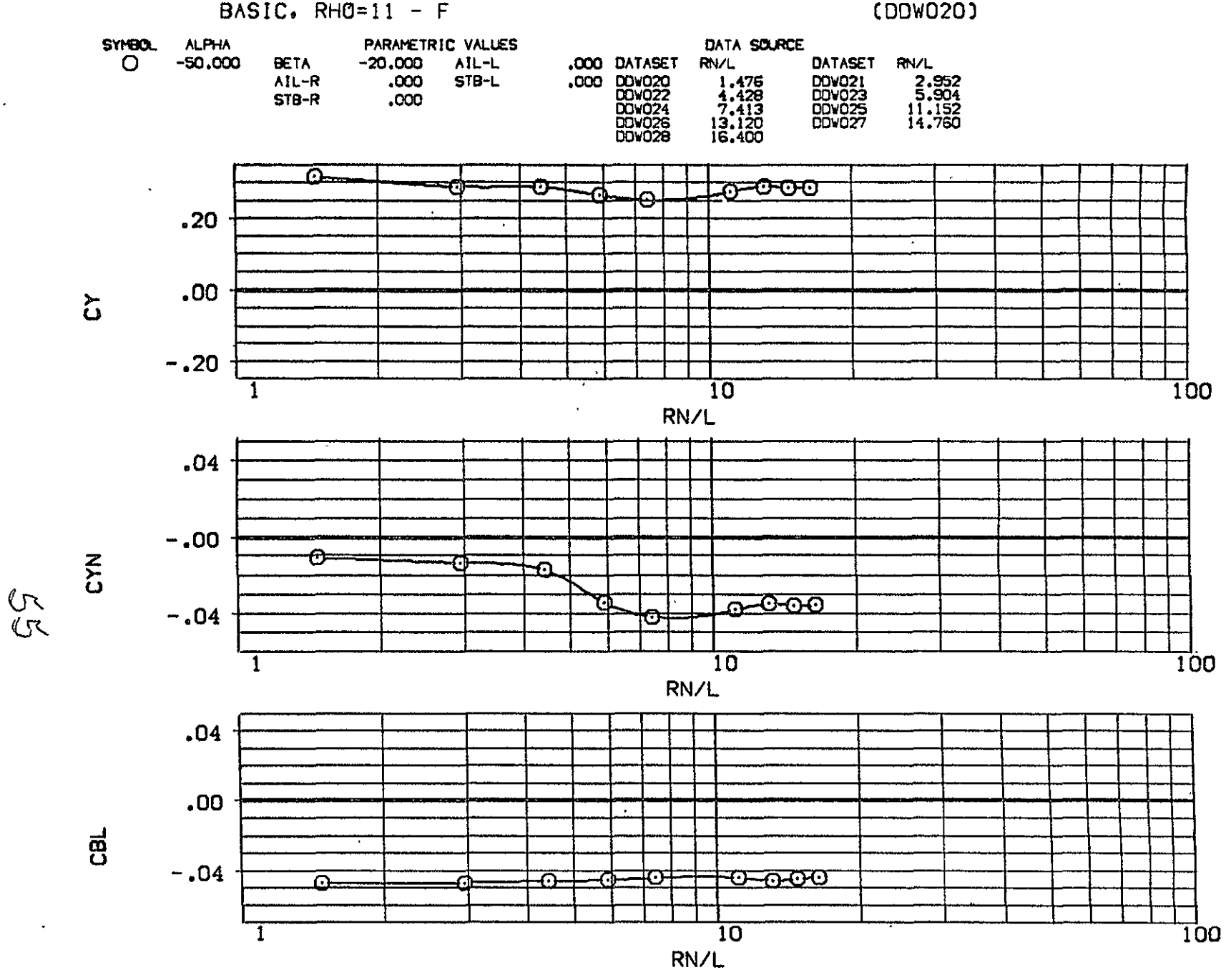

FIG. 4 VARIATION OF AERO. CHAR. WITH REYNOLDS NO. AT VARIOUS ANGLES OF ATTACK.

ORIGINAL PAGE IS
OF POOR QUALITY

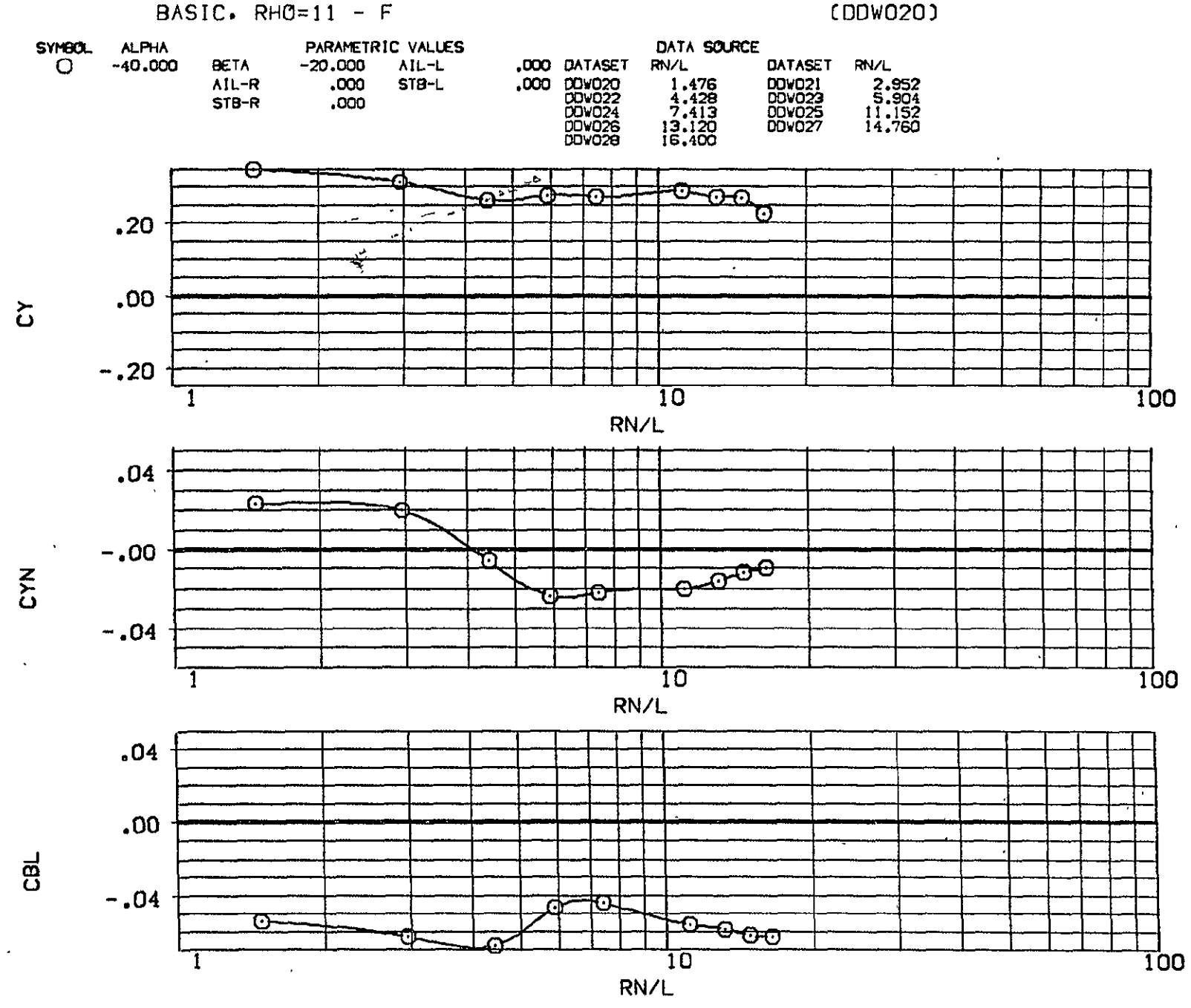

FIG. 4 VARIATION OF AERO. CHAR. WITH REYNOLDS NO. AT VARIOUS ANGLES OF ATTACK.

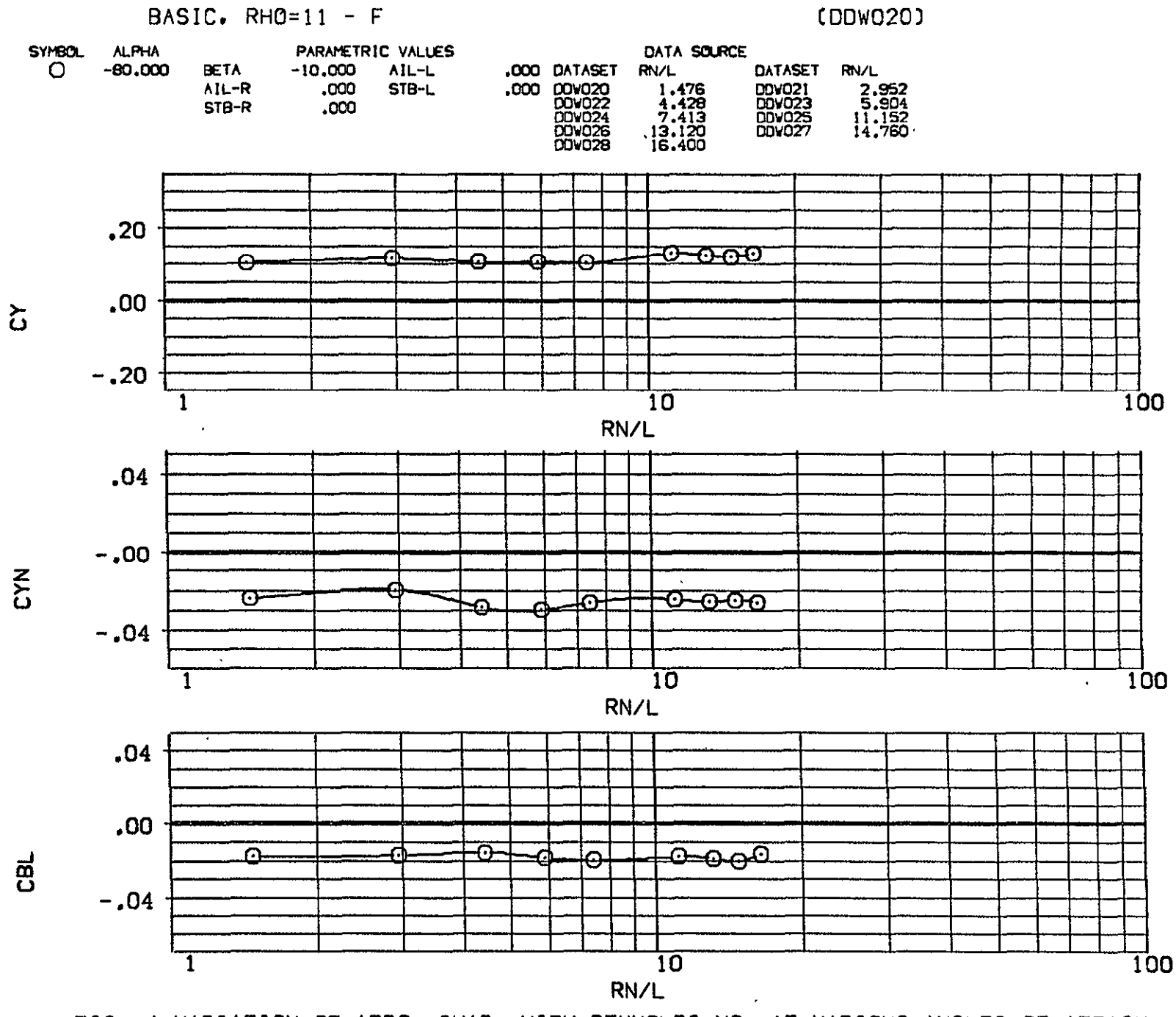

FIG. 4 VARIATION OF AERO. CHAR. WITH REYNOLDS NO. AT VARIOUS ANGLES OF ATTACK.

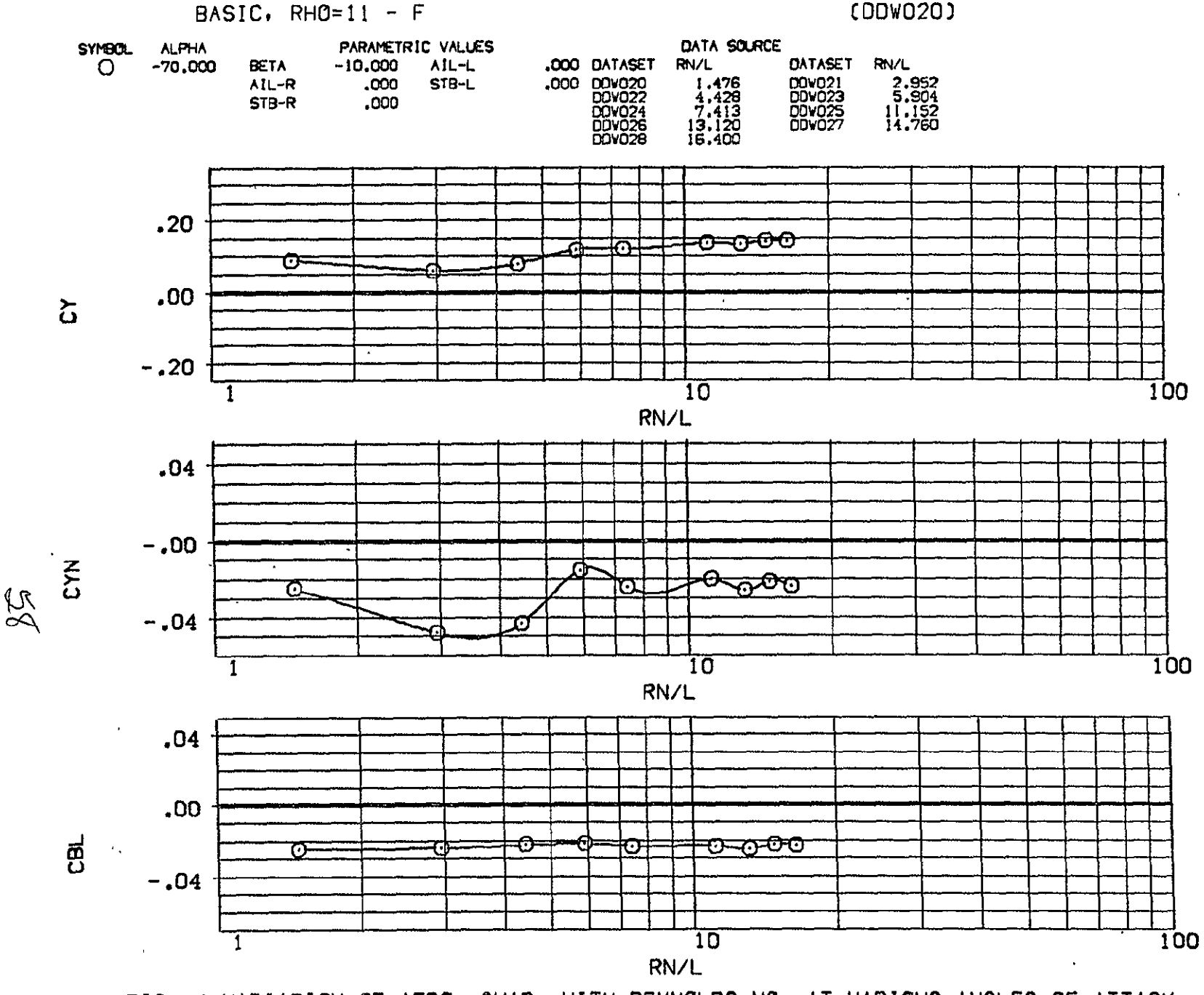

FIG. 4 VARIATION OF AERO. CHAR. WITH REYNOLDS NO. AT VARIOUS ANGLES OF ATTACK.

ORIGINAL PAGE IS
OF POOR QUALITY.

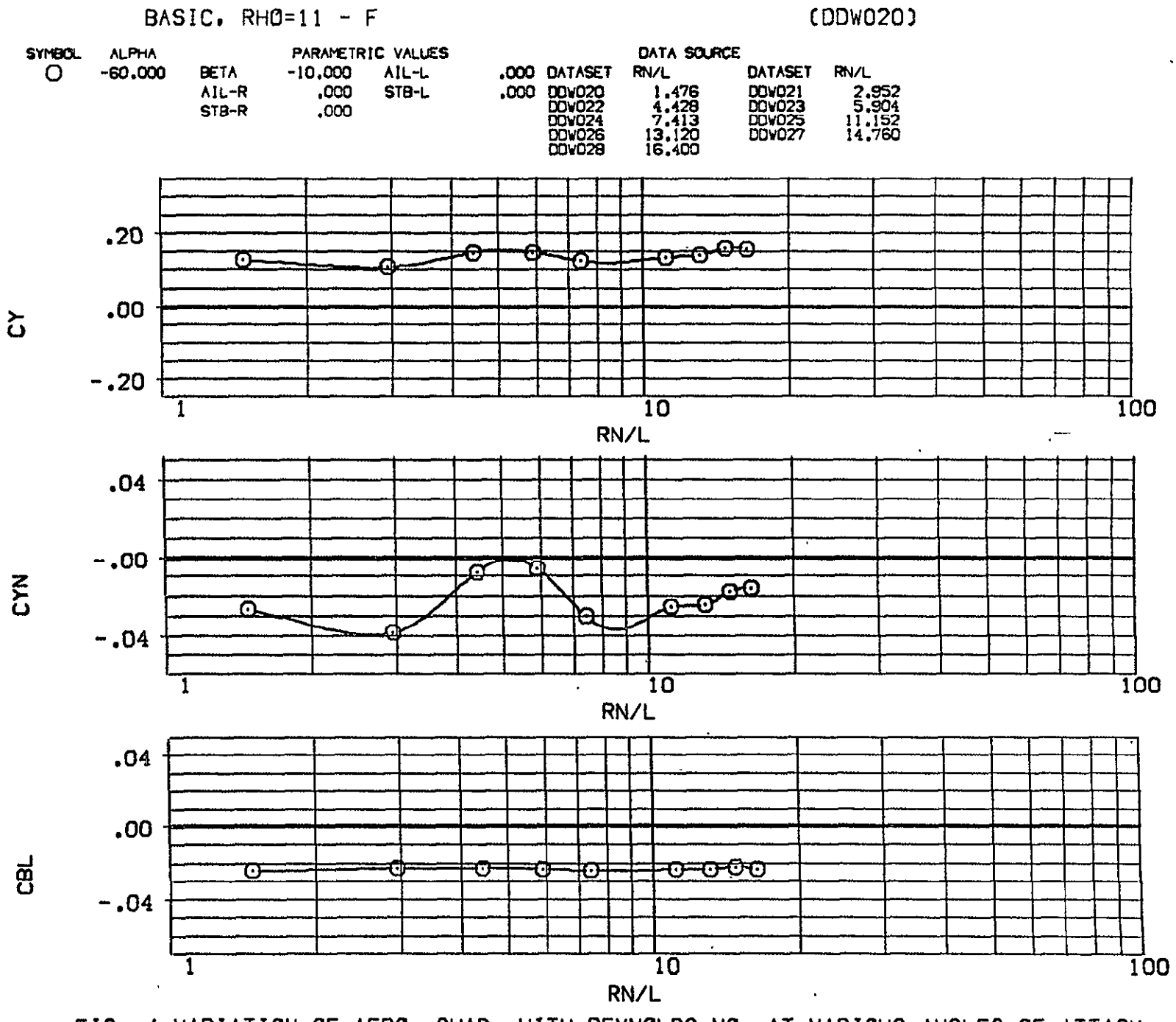

FIG. 4 VARIATION OF AERO. CHAR. WITH REYNOLDS NO. AT VARIOUS ANGLES OF ATTACK.

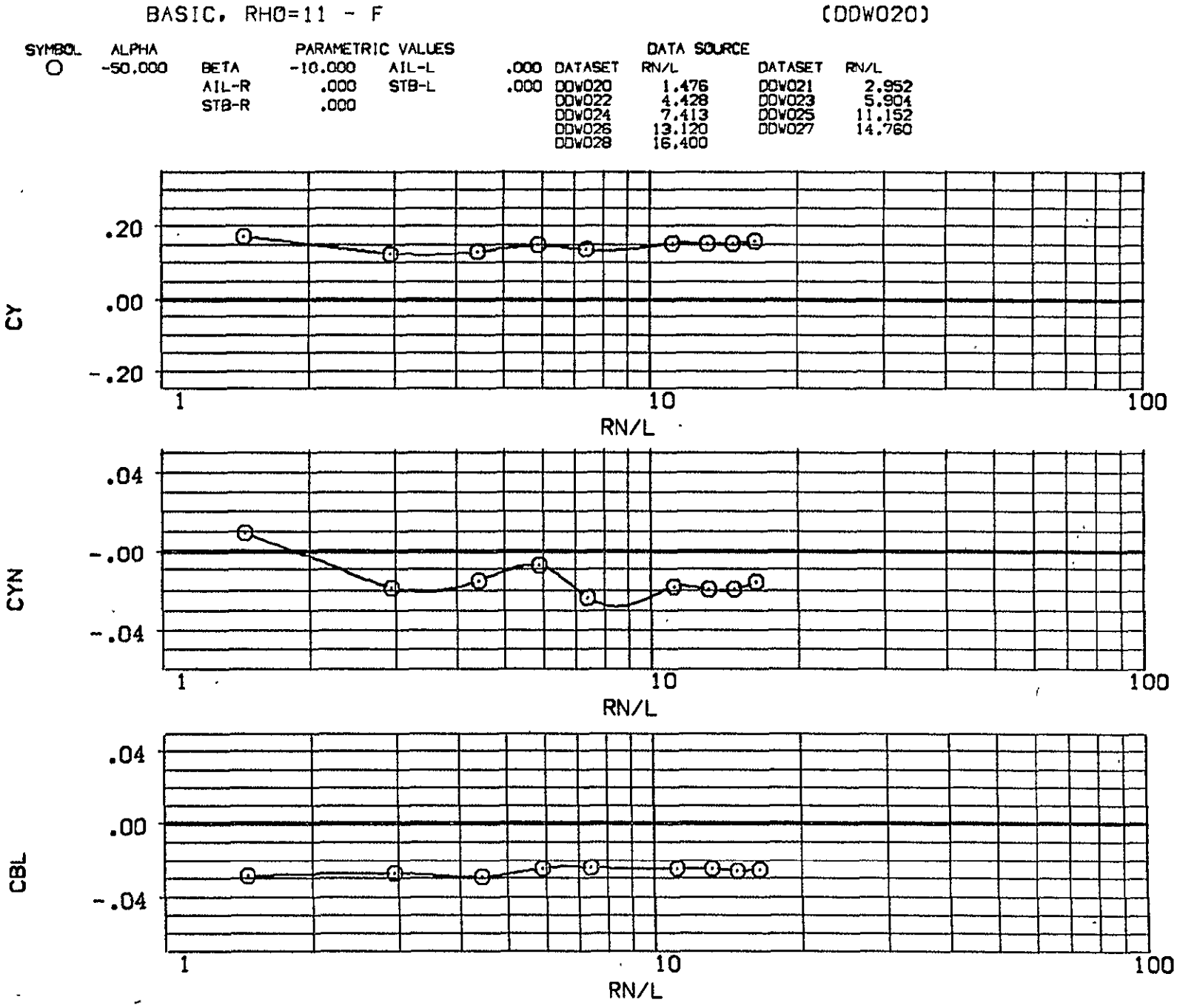

FIG. 4 VARIATION OF AERO. CHAR. WITH REYNOLDS NO. AT VARIOUS ANGLES OF ATTACK.

ORIGINAL PAGE IS
OF POOR QUALITY

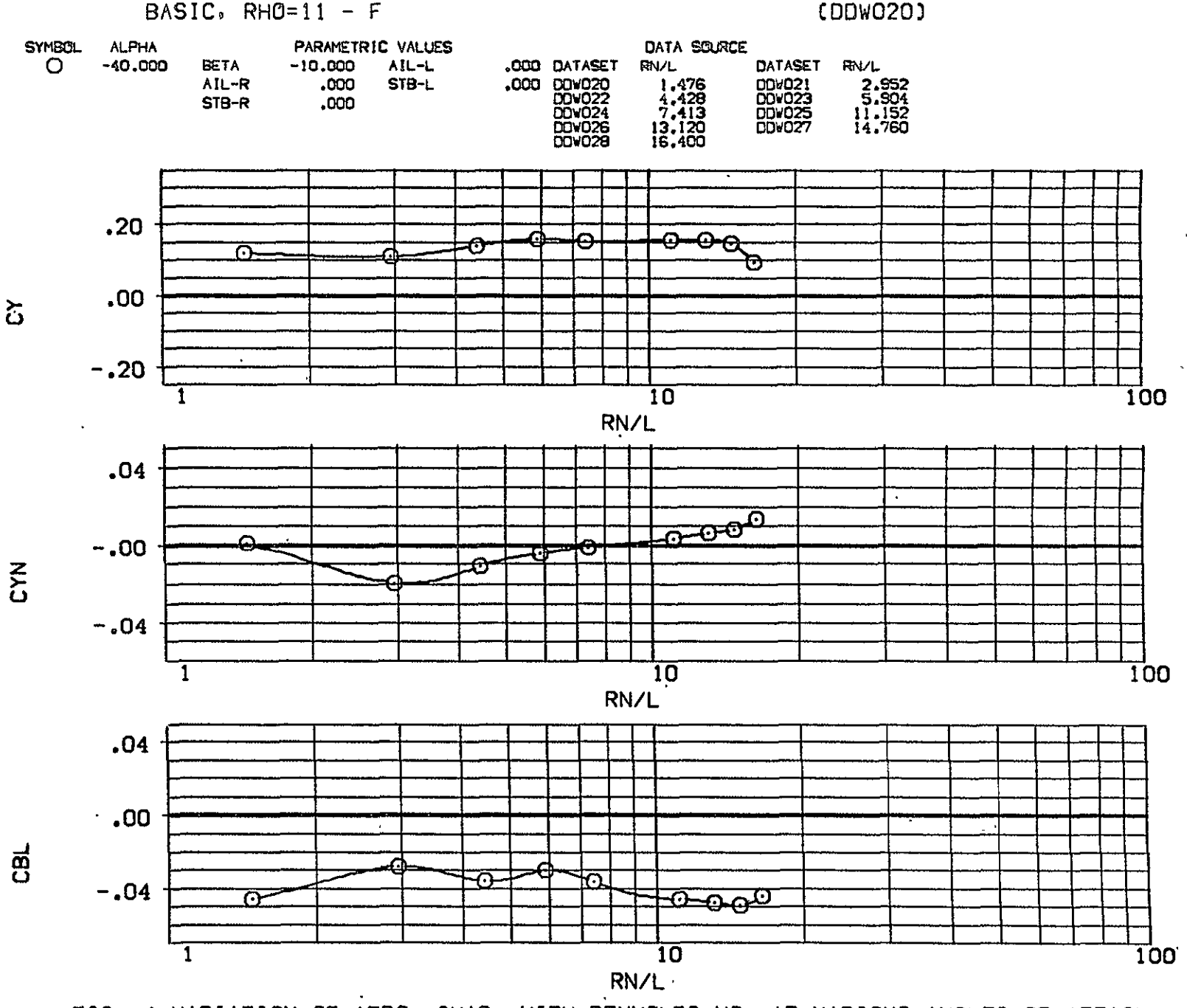

FIG. 4 VARIATION OF AERO. CHAR. WITH REYNOLDS NO. AT VARIOUS ANGLES OF ATTACK.

ORIGINAL PAGE IS
OF POOR QUALITY

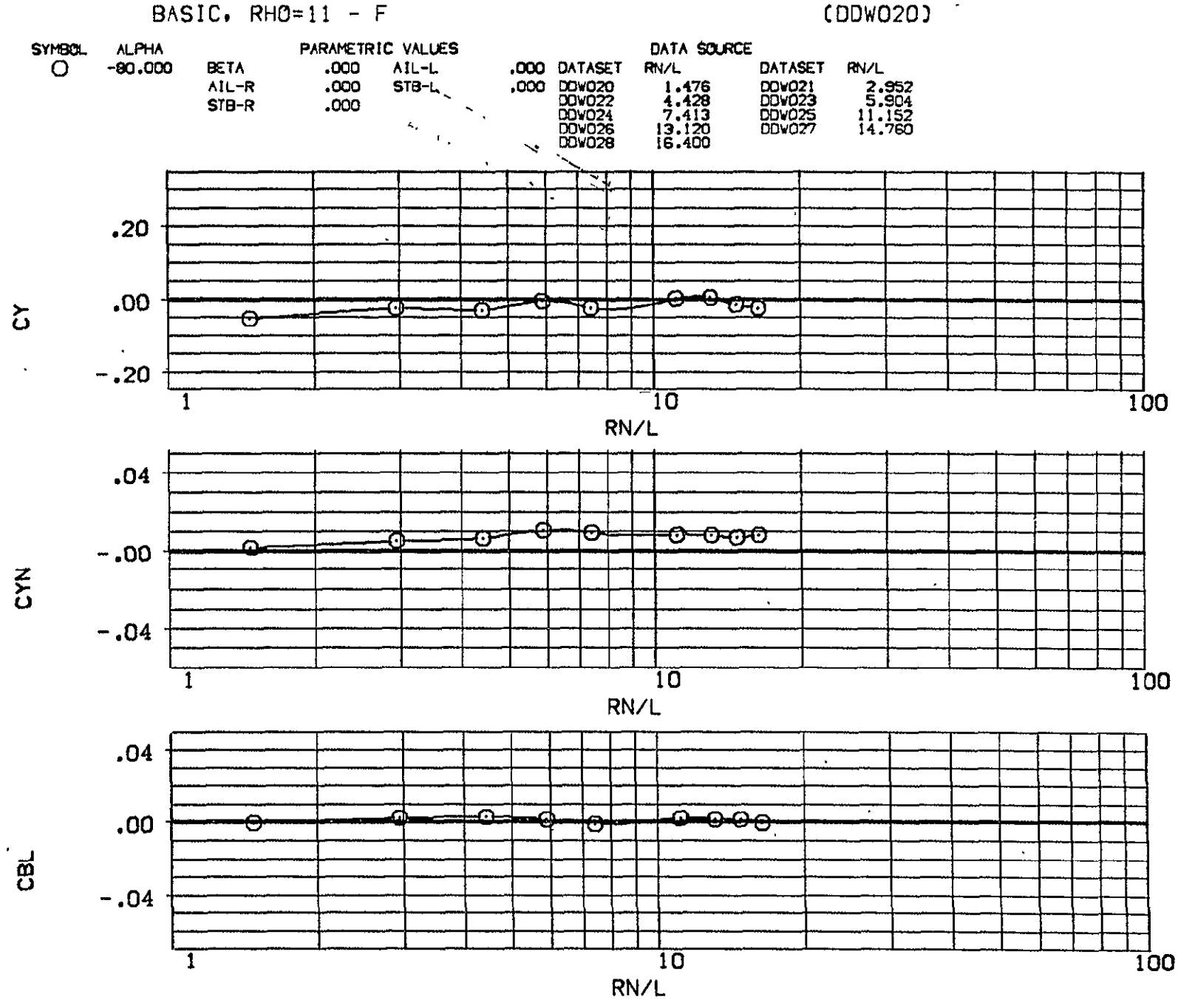

FIG. 4 VARIATION OF AERO. CHAR. WITH REYNOLDS NO. AT VARIOUS ANGLES OF ATTACK.

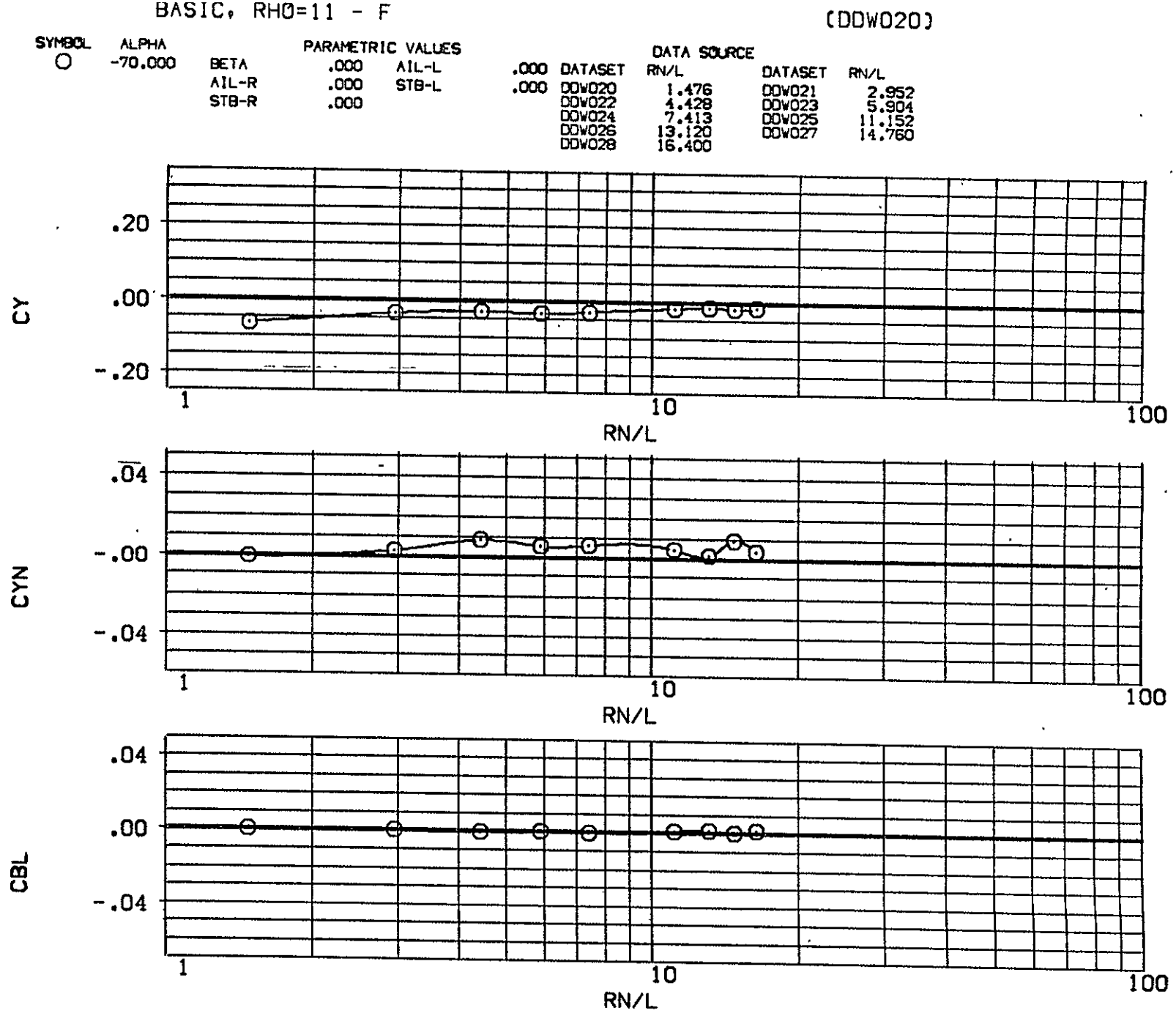

FIG. 4 VARIATION OF AERO. CHAR. WITH REYNOLDS NO. AT VARIOUS ANGLES OF ATTACK.

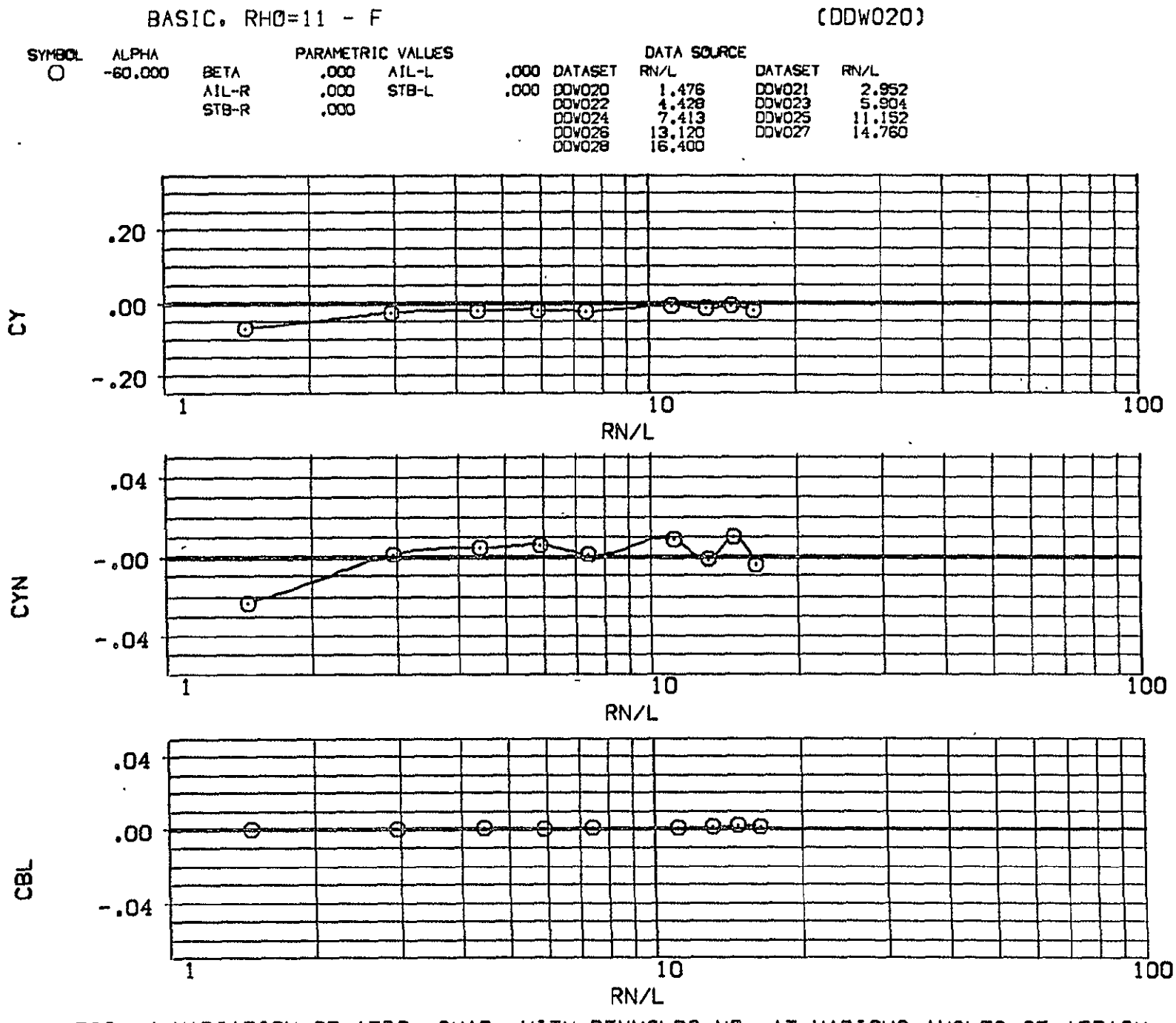

FIG. 4 VARIATION OF AERO. CHAR. WITH REYNOLDS NO. AT VARIOUS ANGLES OF ATTACK.

ORIGINAL PAGE IS
OF POOR QUALITY

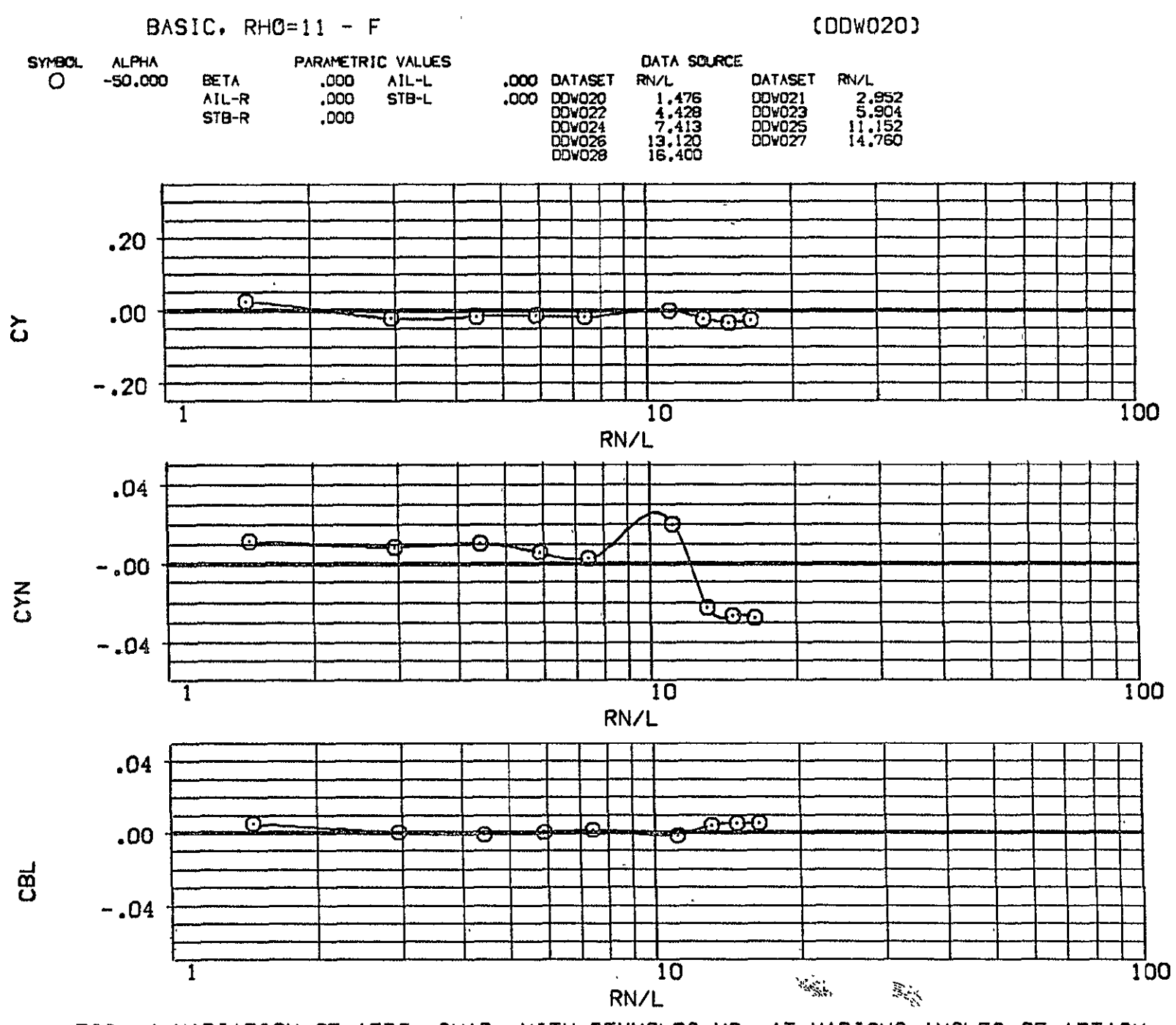

FIG. 4 VARIATION OF AERO. CHAR. WITH REYNOLDS NO. AT VARIOUS ANGLES OF ATTACK.

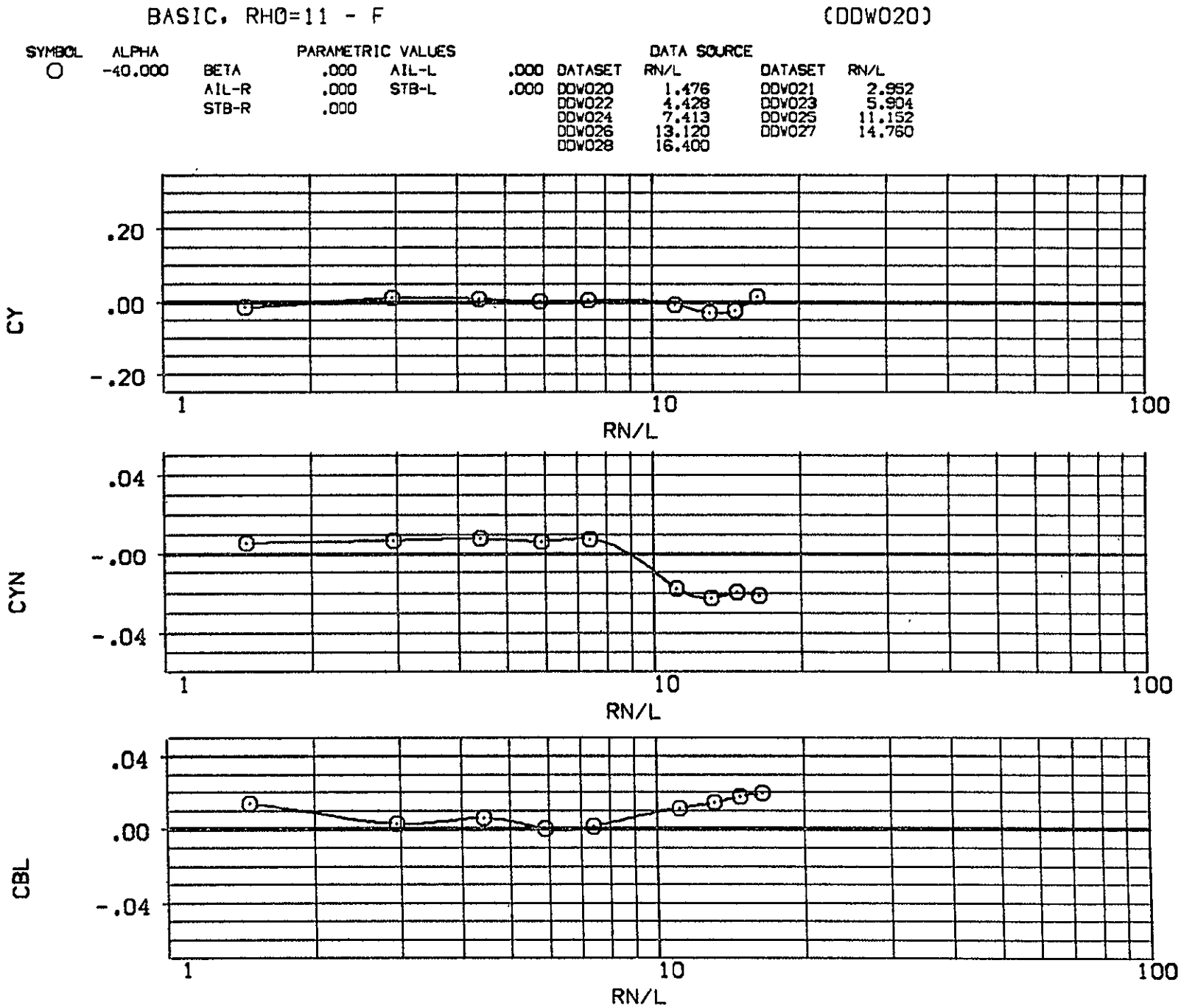

FIG. 4 VARIATION OF AERO. CHAR. WITH REYNOLDS NO. AT VARIOUS ANGLES OF ATTACK.

ORIGINAL PAGE IS
OF POOR QUALITY

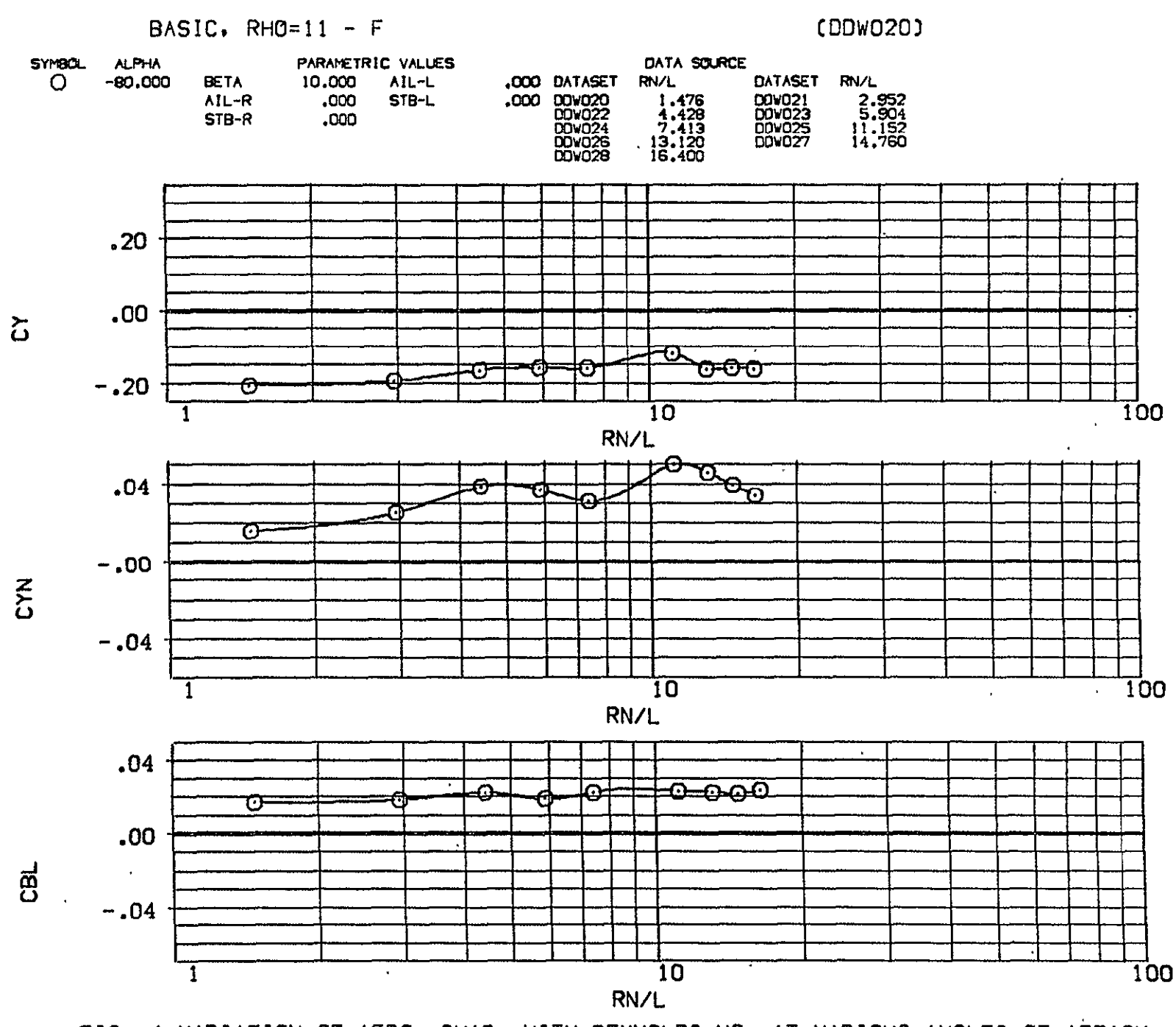

FIG. 4 VARIATION OF AERO. CHAR. WITH REYNOLDS NO. AT VARIOUS ANGLES OF ATTACK.

ORIGINAL PAGE IS
OF POOR QUALITY

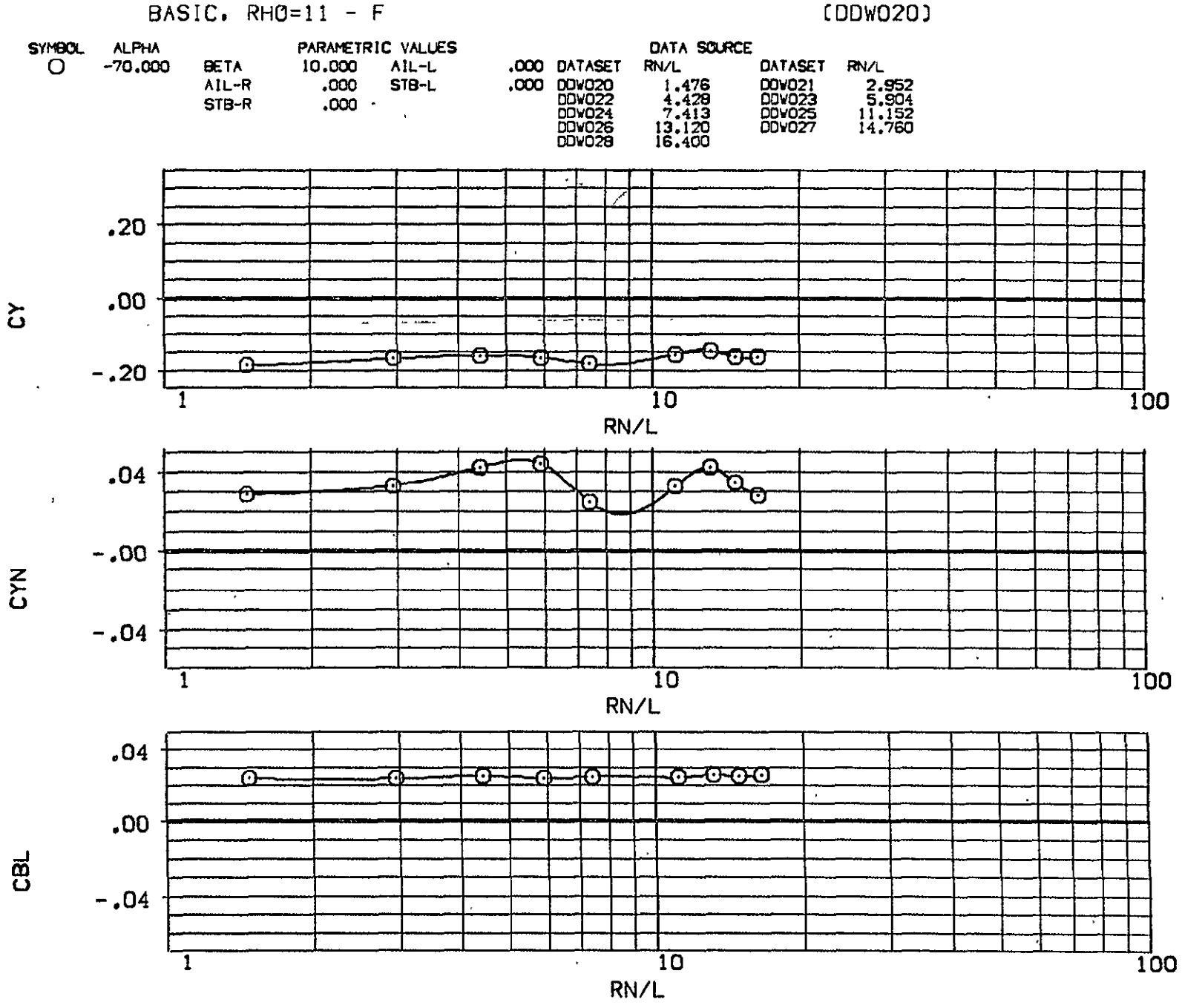

FIG. 4 VARIATION OF AERO. CHAR. WITH REYNOLDS NO. AT VARIOUS ANGLES OF ATTACK.

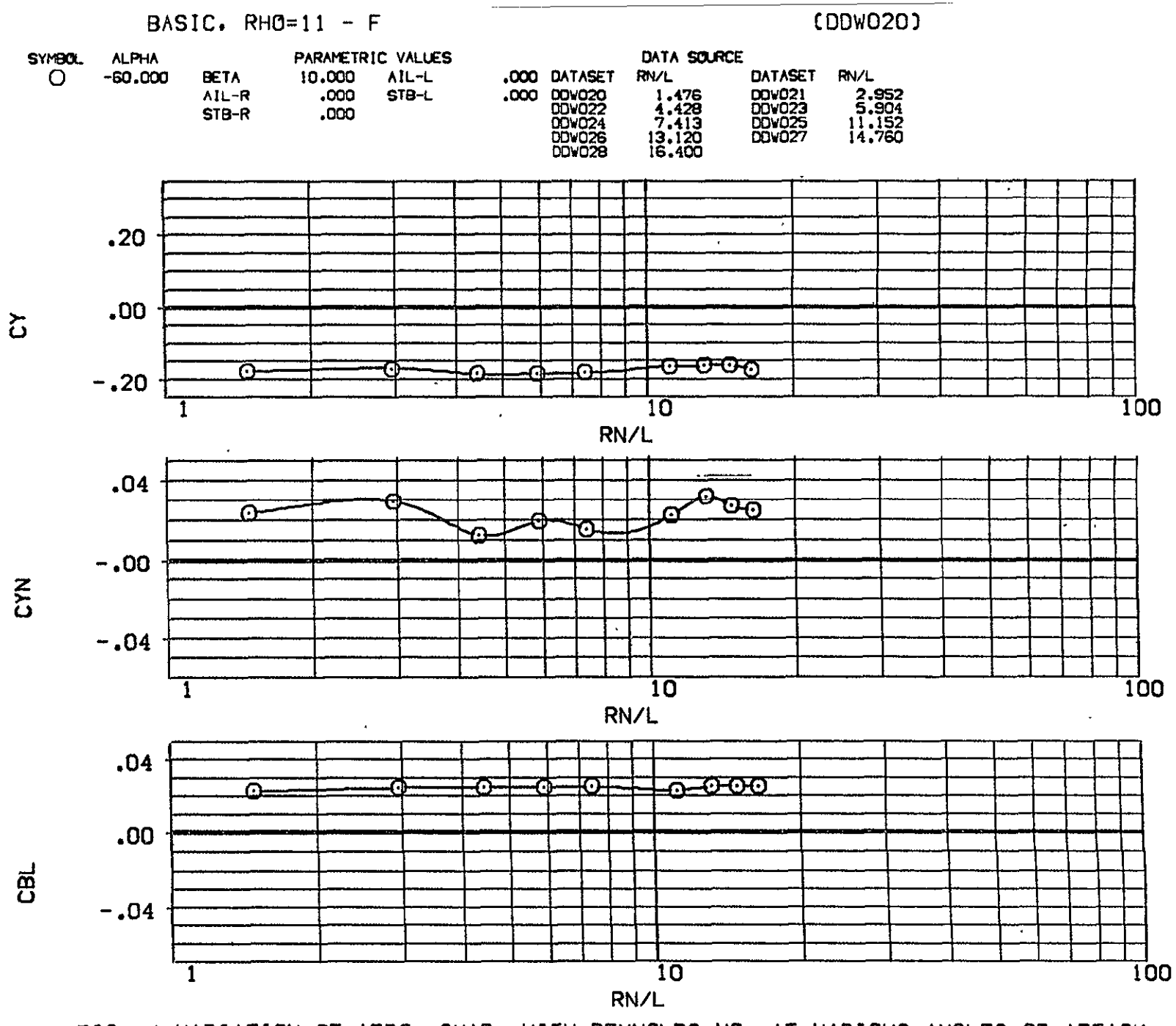

FIG. 4 VARIATION OF AERO. CHAR. WITH REYNOLDS NO. AT VARIOUS ANGLES OF ATTACK.

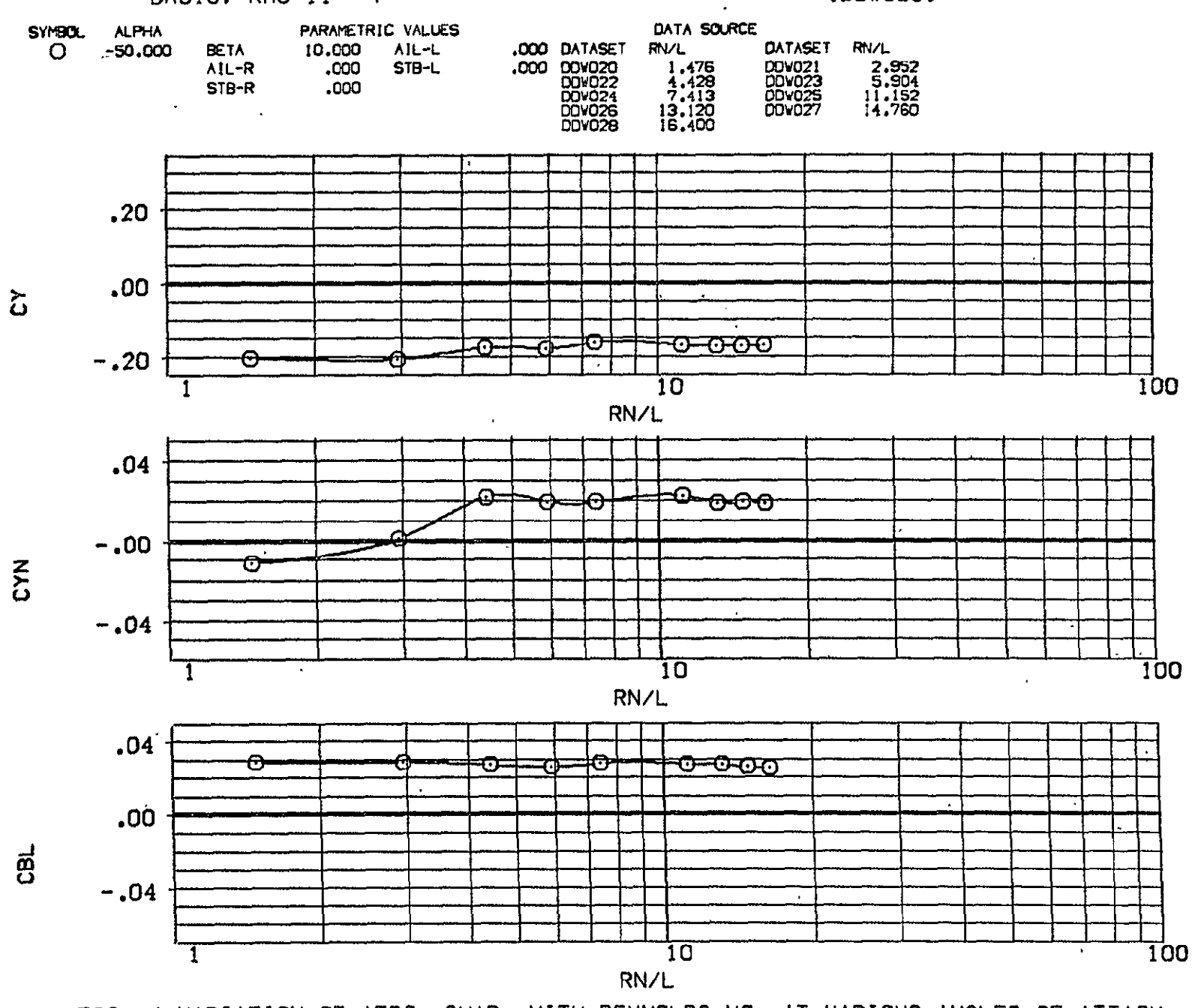

FIG. 4 VARIATION OF AERO. CHAR. WITH REYNOLDS NO. AT VARIOUS ANGLES OF ATTACK.

ORIGINAL PAGE IS
OF POOR QUALITY

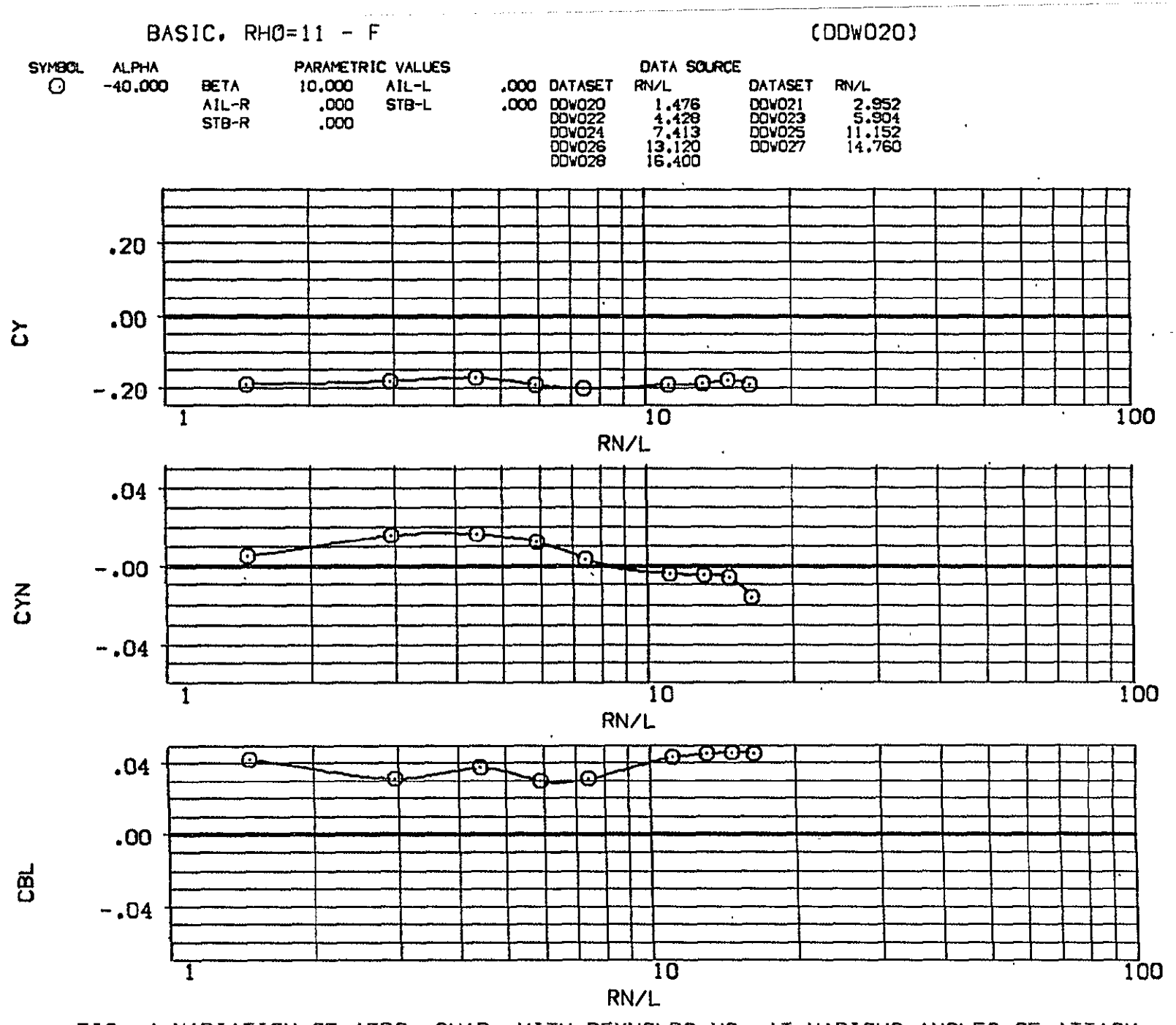

FIG. 4 VARIATION OF AERO. CHAR. WITH REYNOLDS NO. AT VARIOUS ANGLES OF ATTACK.

DATA SET	SYMBOL	CONFIGURATION DESCRIPTION	AIL-L	AIL-R	STB-L	STB-R
(BDW001)	○	BASIC, RHO=0 + GRIT	.000	.000	.000	.000
(BDW009)	□	BASIC, RHO=11 + GRIT	.000	.000	.000	.000

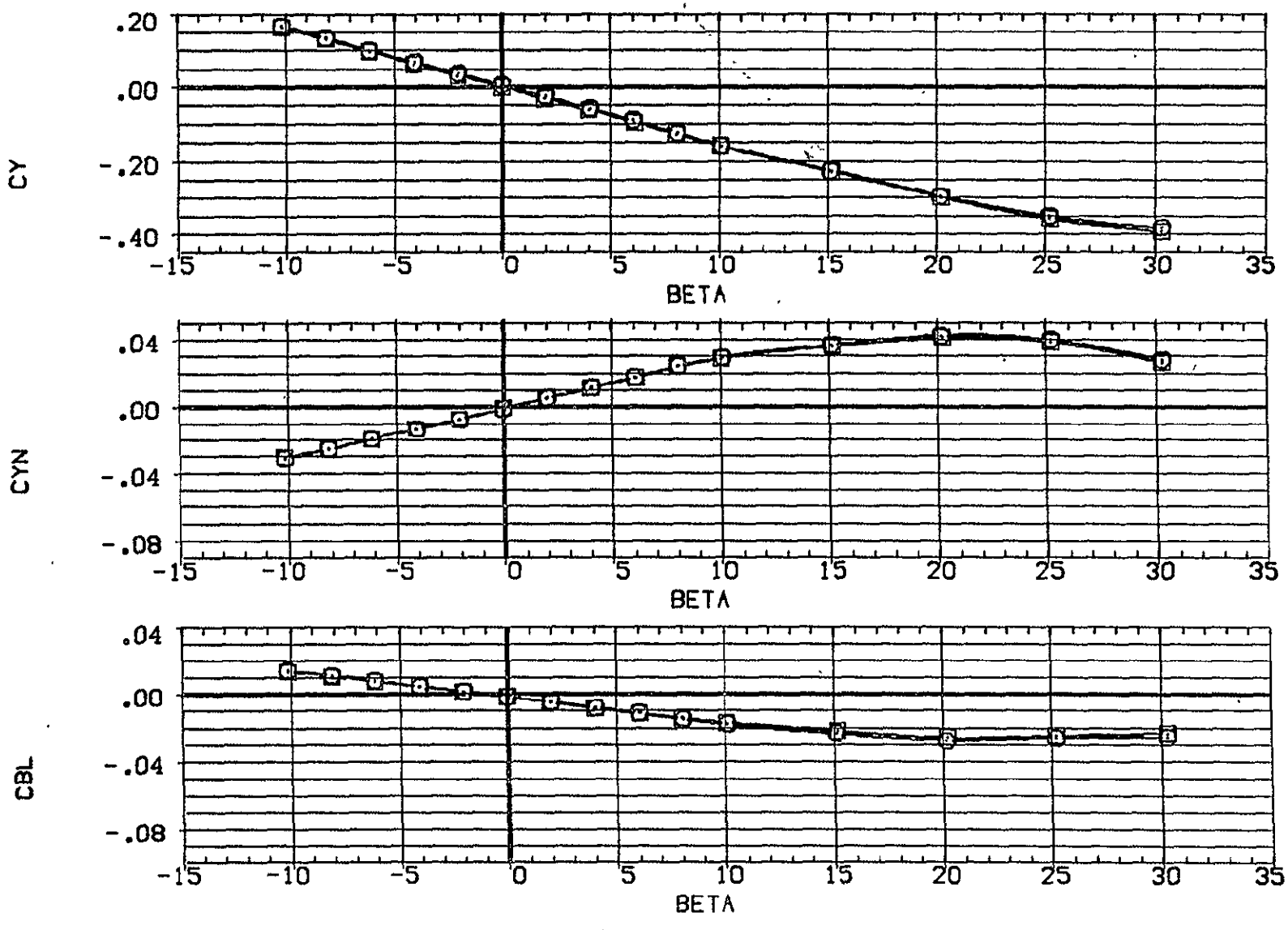

FIG. 5 EFFECT OF RAMP ANGLE ON AERODYNAMIC CHAR., REYNOLDS NO.= 13.12 MIL.

(A)ALPHA = -.11

ORIGINAL PAGE IS OF POOR QUALITY

DATA SET	SYMBOL	CONFIGURATION DESCRIPTION	AIL-L	AIL-R	STB-L	STB-R
(BDW001)	○	BASIC, RHO=0 + GRIT	.000	.000	.000	.000
(BDW009)	□	BASIC, RHO=11 + GRIT	.000	.000	.000	.000

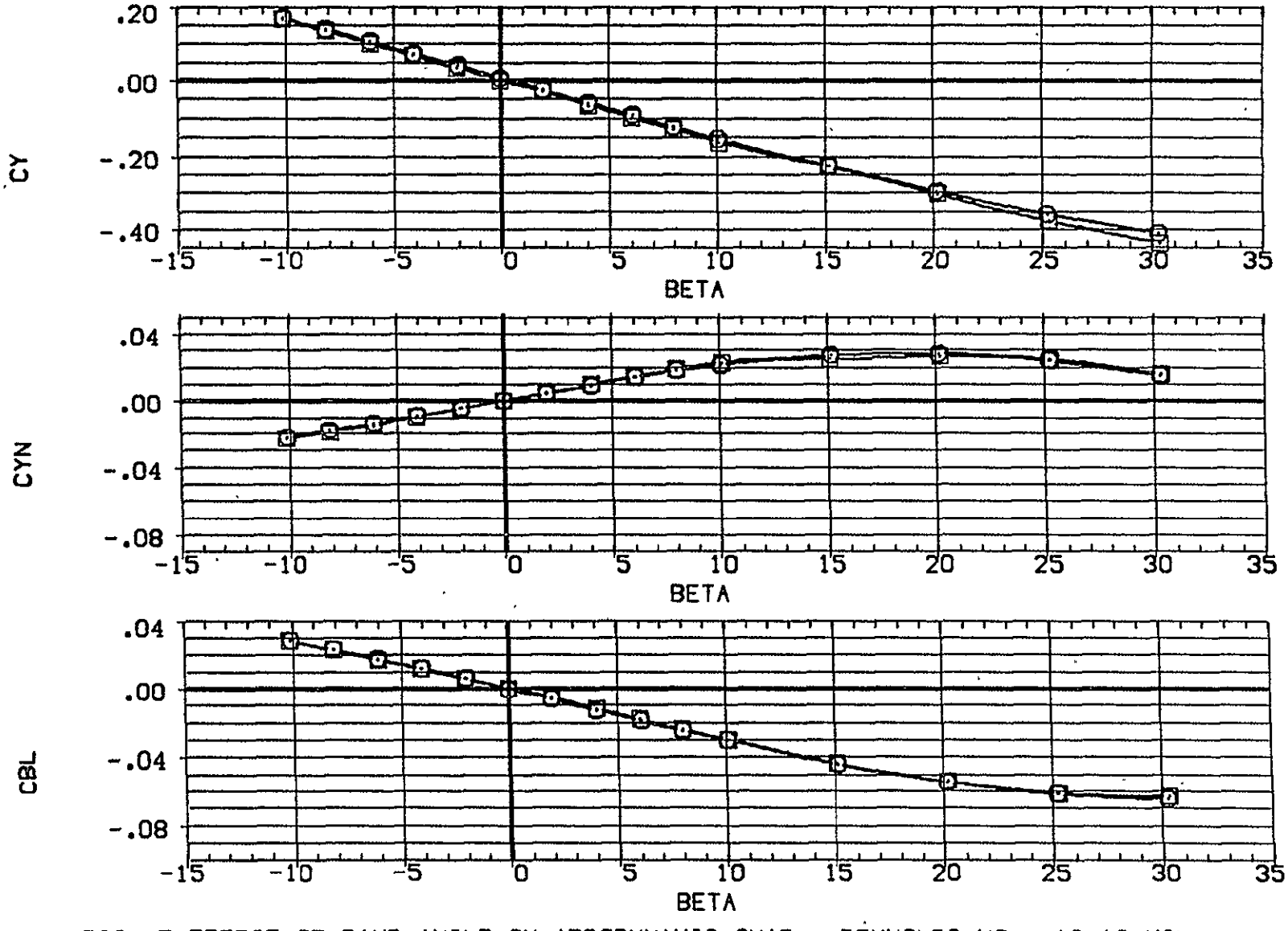

FIG. 5 EFFECT OF RAMP ANGLE ON AERODYNAMIC CHAR., REYNOLDS NO.= 13.12 MIL.

(B)ALPHA = 10.46

DATA SET	SYMBOL	CONFIGURATION DESCRIPTION	AIL-L	AIL-R	STB-L	STB-R
(BDW001)	○	BASIC, RHO=0 + GRIT	.000	.000	.000	.000
(BDW009)	□	BASIC, RHO=11 + GRIT	.000	.000	.000	.000

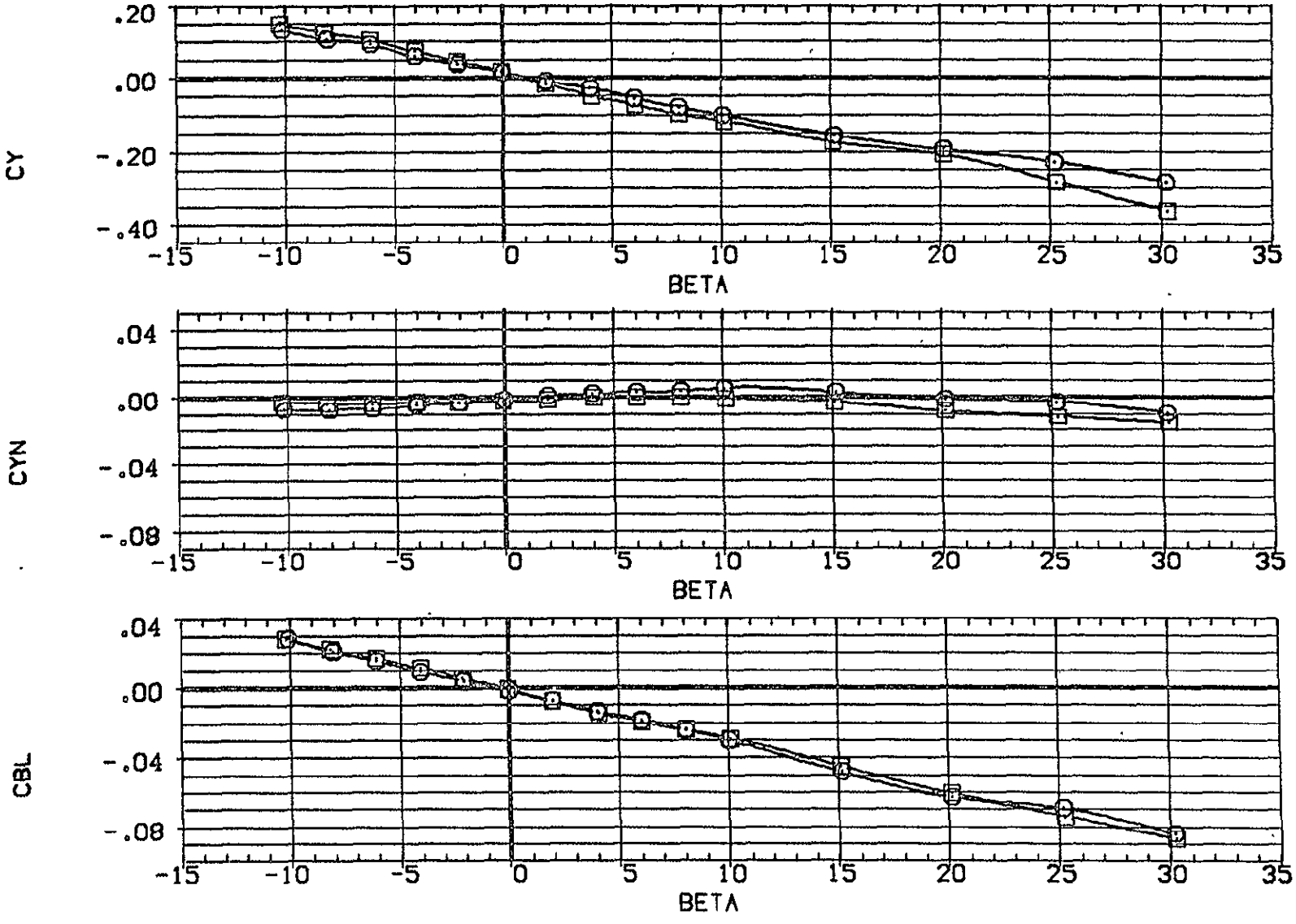

FIG. 5 EFFECT OF RAMP ANGLE ON AERODYNAMIC CHAR., REYNOLDS NO.= 13.12 MIL.

(C)ALPHA = 21.00

ORIGINAL PAGE IS
OF POOR QUALITY

74

DATA SET	SYMBOL	CONFIGURATION DESCRIPTION	AIL-L	AIL-R	STB-L	STB-R
(BDW001)	○	BASIC, RHO=0 + GRIT	.000	.000	.000	.000
(BDW009)	□	BASIC, RHO=11 + GRIT	.000	.000	.000	.000

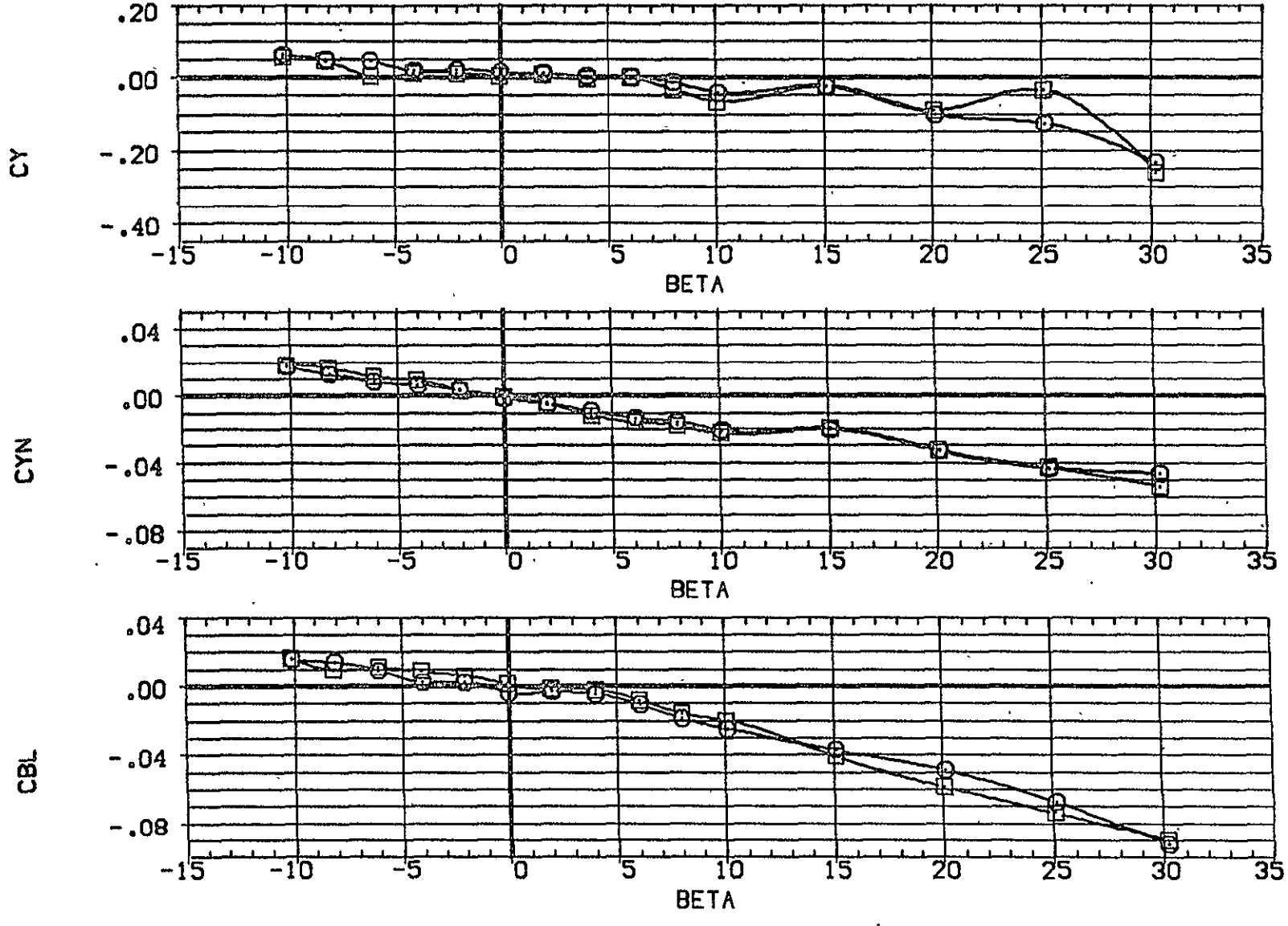

FIG. 5 EFFECT OF RAMP ANGLE ON AERODYNAMIC CHAR., REYNOLDS NO.= 13.12 MIL.

(D)ALPHA = 31.29

ORIGINAL PAGE IS
OF POOR QUALITY

DATA SET	SYMBOL	CONFIGURATION DESCRIPTION	AIL-L	AIL-R	STB-L	STB-R
(BDW001)	○	DATA NOT AVAILABLE	.000	.000	.000	.000
(BDW009)	□	BASIC. RHO=11 + GRIT	.000	.000	.000	.000

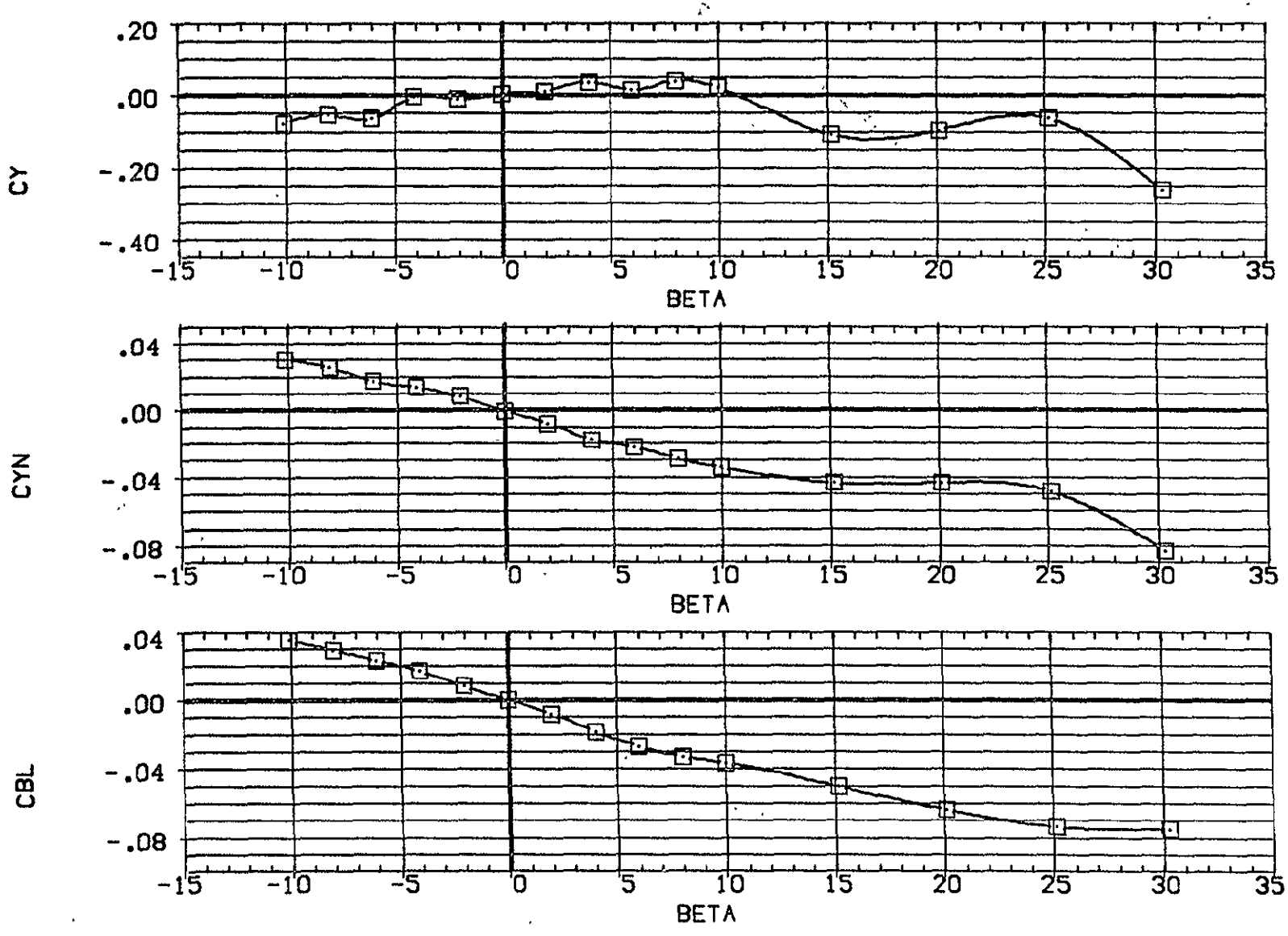

FIG. 5 EFFECT OF RAMP ANGLE ON AERODYNAMIC CHAR., REYNOLDS NO.= 13.12 MIL.

(E)ALPHA = 41.34

DATA SET	SYMBOL	CONFIGURATION DESCRIPTION	AIL-L	AIL-R	STB-L	STB-R
(BDV001)	○	BASIC, RHO=0 + GRIT	.000	.000	.000	.000
(BDV009)	□	BASIC, RHO=11 + GRIT	.000	.000	.000	.000

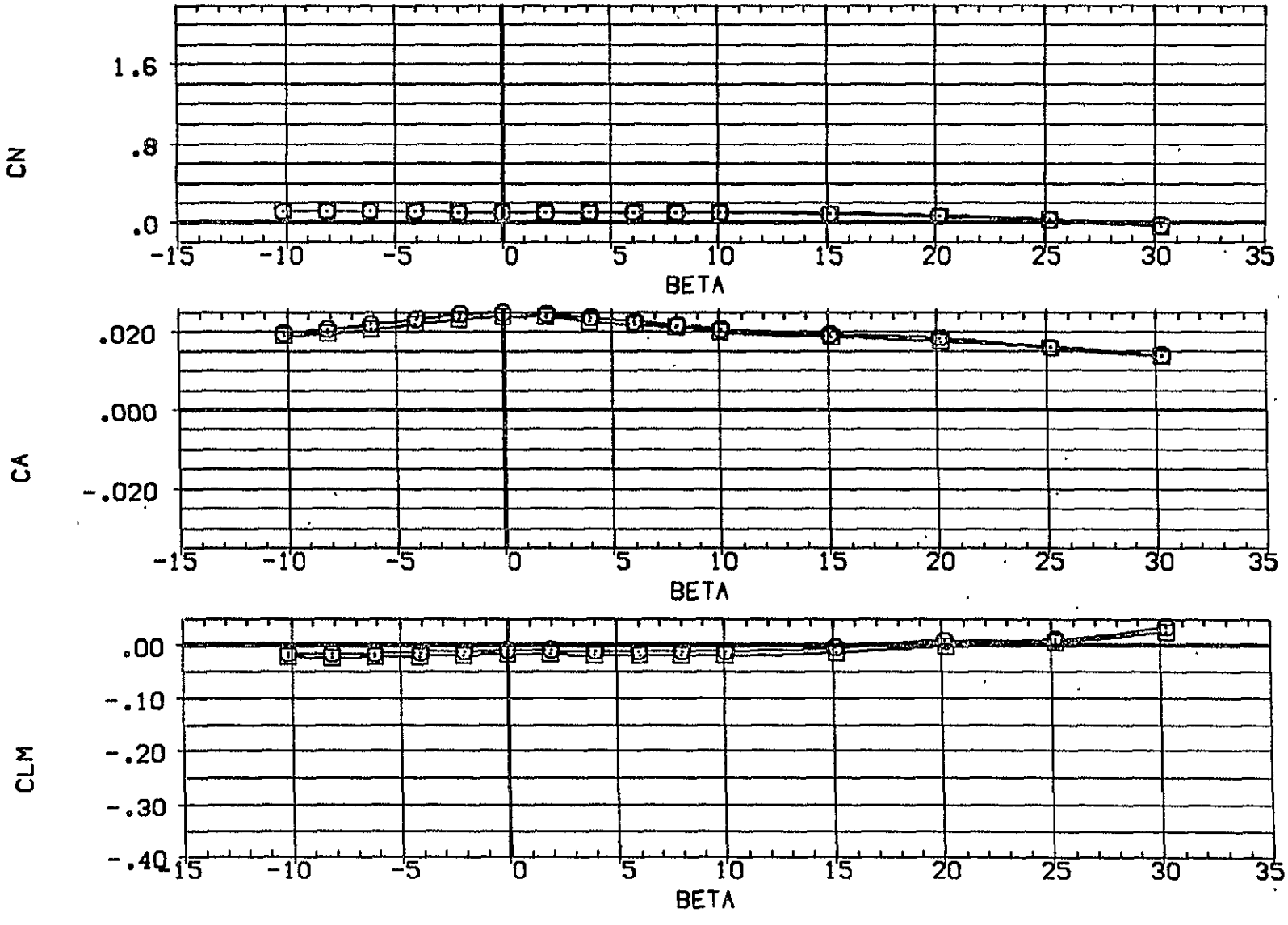

FIG. 5 EFFECT OF RAMP ANGLE ON AERODYNAMIC CHAR., REYNOLDS NO.= 13.12 MIL.

(A)ALPHA = -.11

DATA SET	SYMBOL	CONFIGURATION DESCRIPTION	AIL-L	AIL-R	STB-L	STB-R
(BDV001)	○	BASIC, RHO=0 + GRIT	.000	.000	.000	.000
(BDV009)	□	BASIC, RHO=11 + GRIT	.000	.000	.000	.000

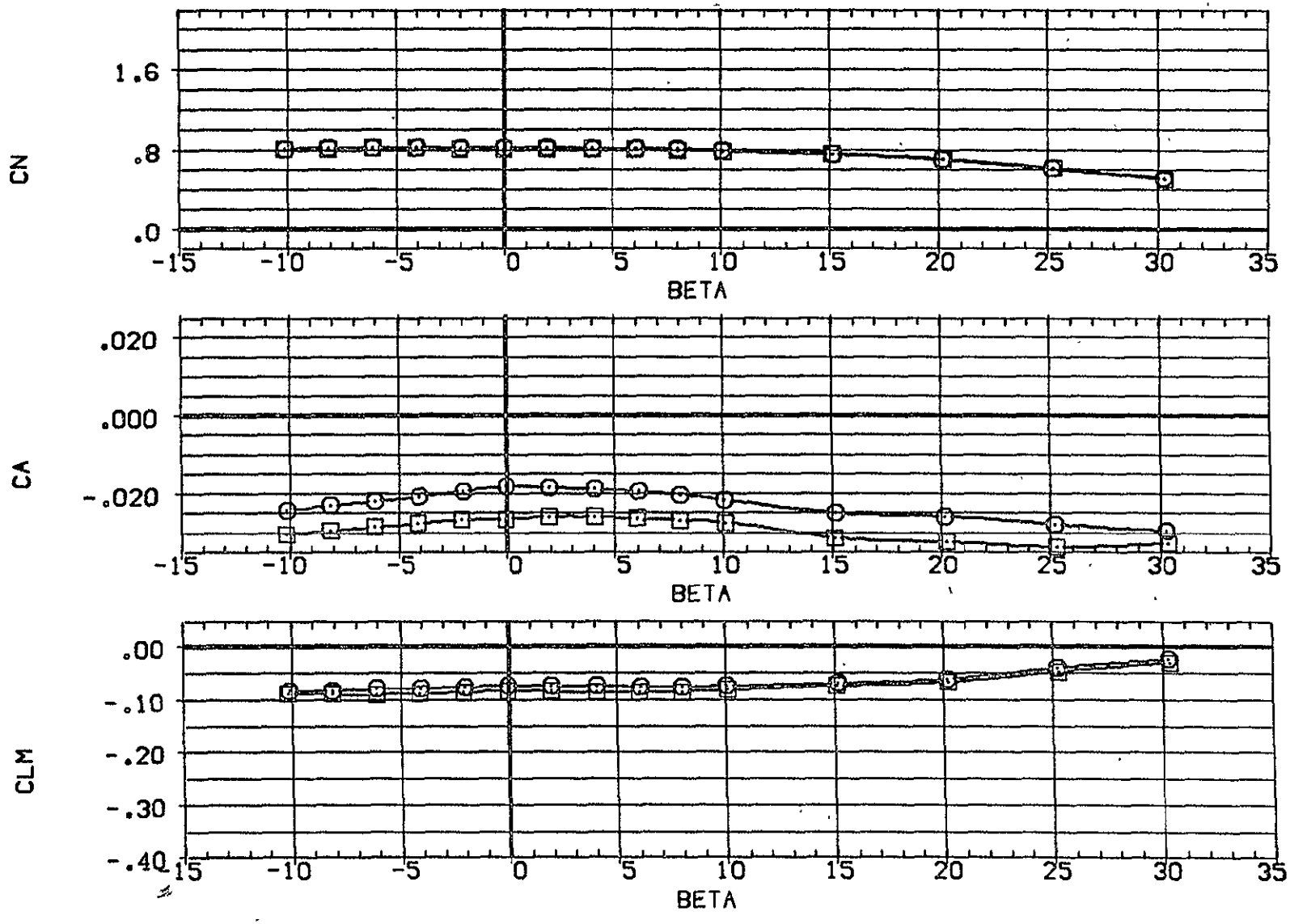

FIG. 5 EFFECT OF RAMP ANGLE ON AERODYNAMIC CHAR., REYNOLDS NO.= 13.12 MIL.

(B)ALPHA = 10.46

ORIGINAL PAGE IS
OF POOR QUALITY

78

DATA SET	SYMBOL	CONFIGURATION DESCRIPTION	AIL-L	AIL-R	STB-L	STB-R
(BDW001)	○	BASIC, RHO=0 + GRIT	.000	.000	.000	.000
(BDW009)	□	BASIC, RHO=11 + GRIT	.000	.000	.000	.000

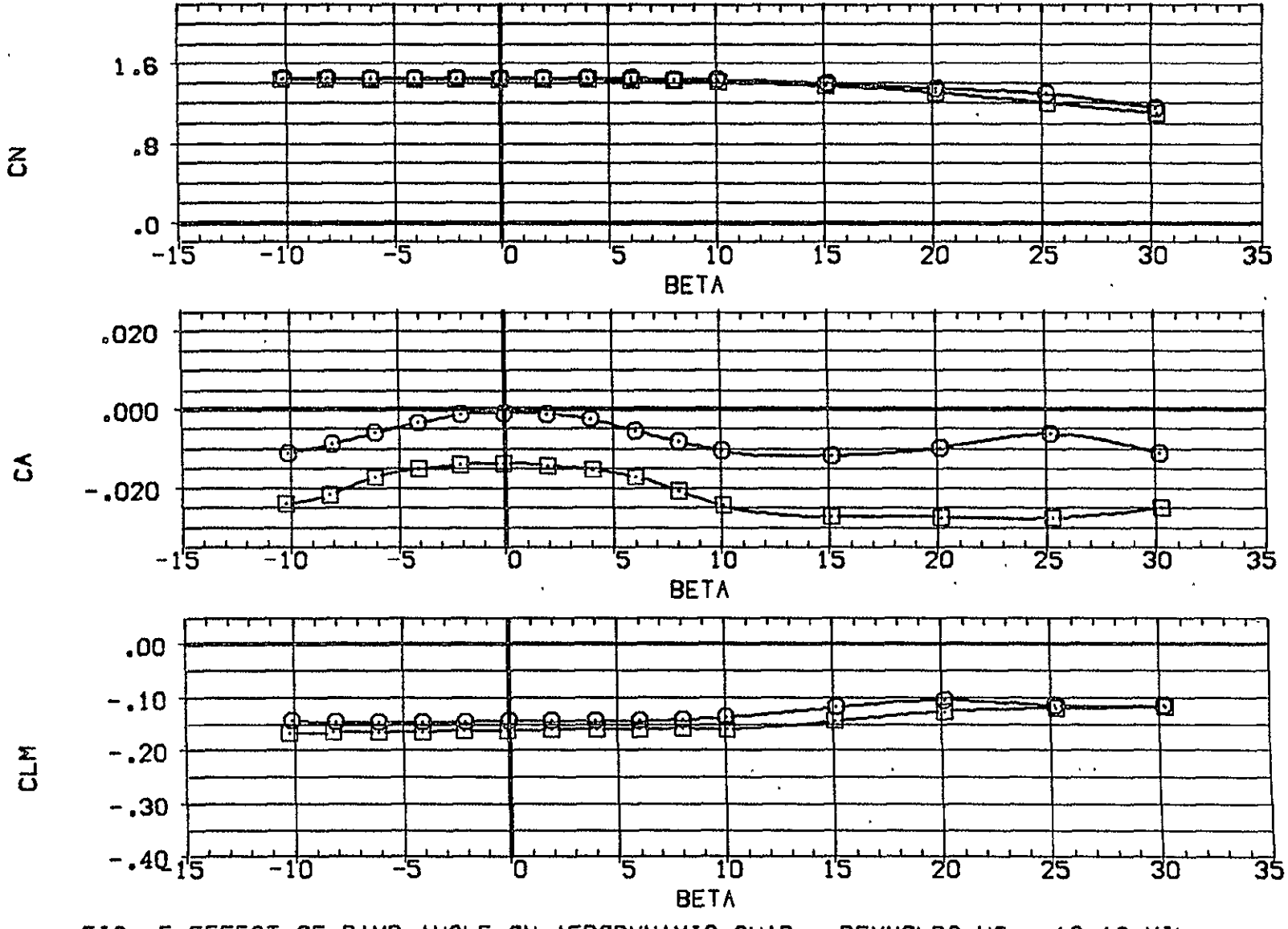

FIG. 5 EFFECT OF RAMP ANGLE ON AERODYNAMIC CHAR., REYNOLDS NO.= 13.12 MIL.

(C)ALPHA = 21.00

DATA SET	SYMBOL	CONFIGURATION DESCRIPTION	AIL-L	AIL-R	STB-L	STB-R
(BDWC01)	○	BASIC, RHO=0 + GRIT	.000	.000	.000	.000
(BDWC09)	□	BASIC, RHO=11 + GRIT	.000	.000	.000	.000

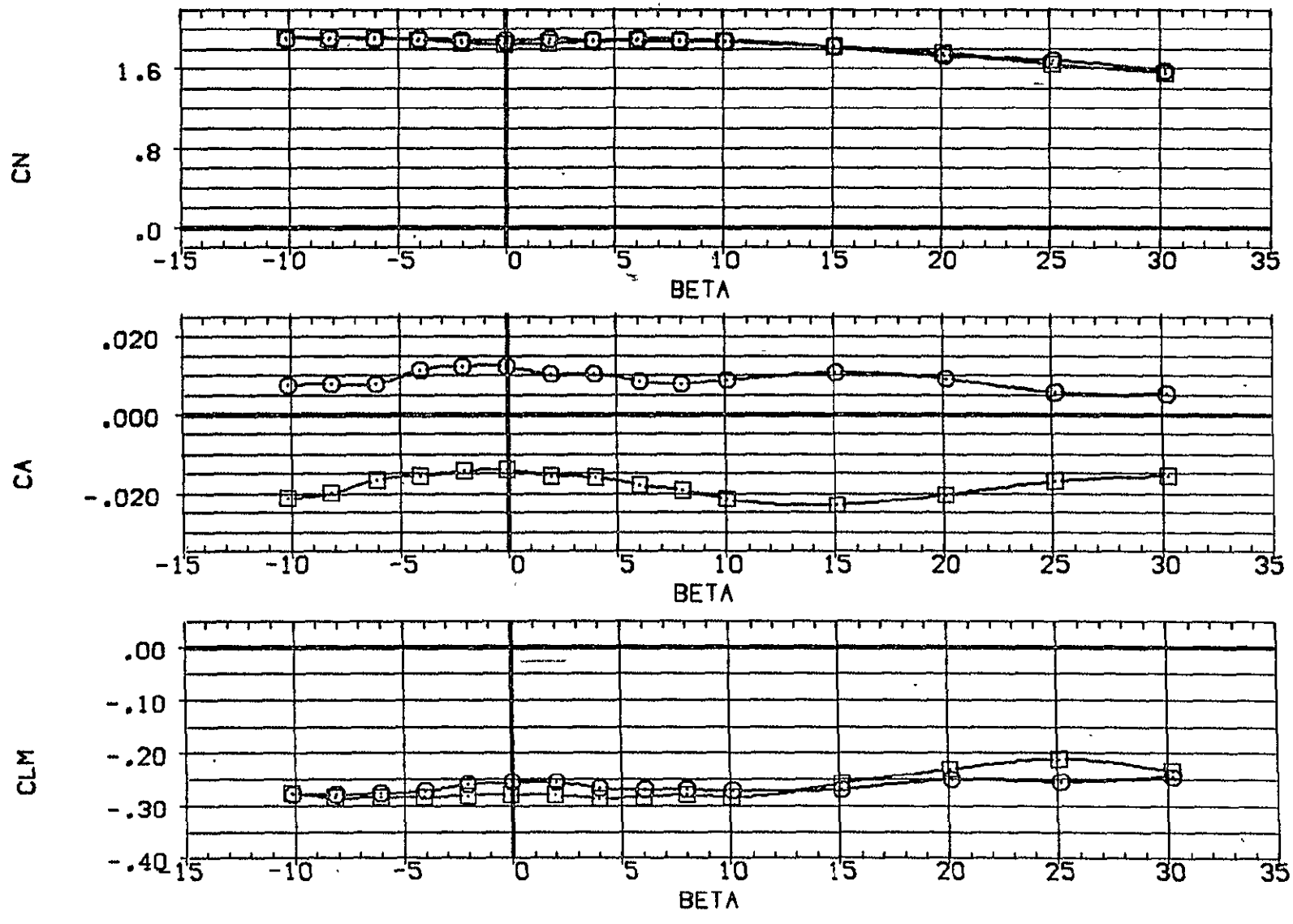

FIG. 5 EFFECT OF RAMP ANGLE ON AERODYNAMIC CHAR., REYNOLDS NO.= 13.12 MIL.

(D)ALPHA = 31.29

ORIGINAL PAGE IS
OF POOR QUALITY

80

DATA SET SYMBOL		CONFIGURATION DESCRIPTION	AIL-L	AIL-R	STB-L	STB-R
(BOV001)	○	DATA NOT AVAILABLE	.000	.000	.000	.000
(BOV009)	□	BASIC, RHO=11 + GRIT	.000	.000	.000	.000

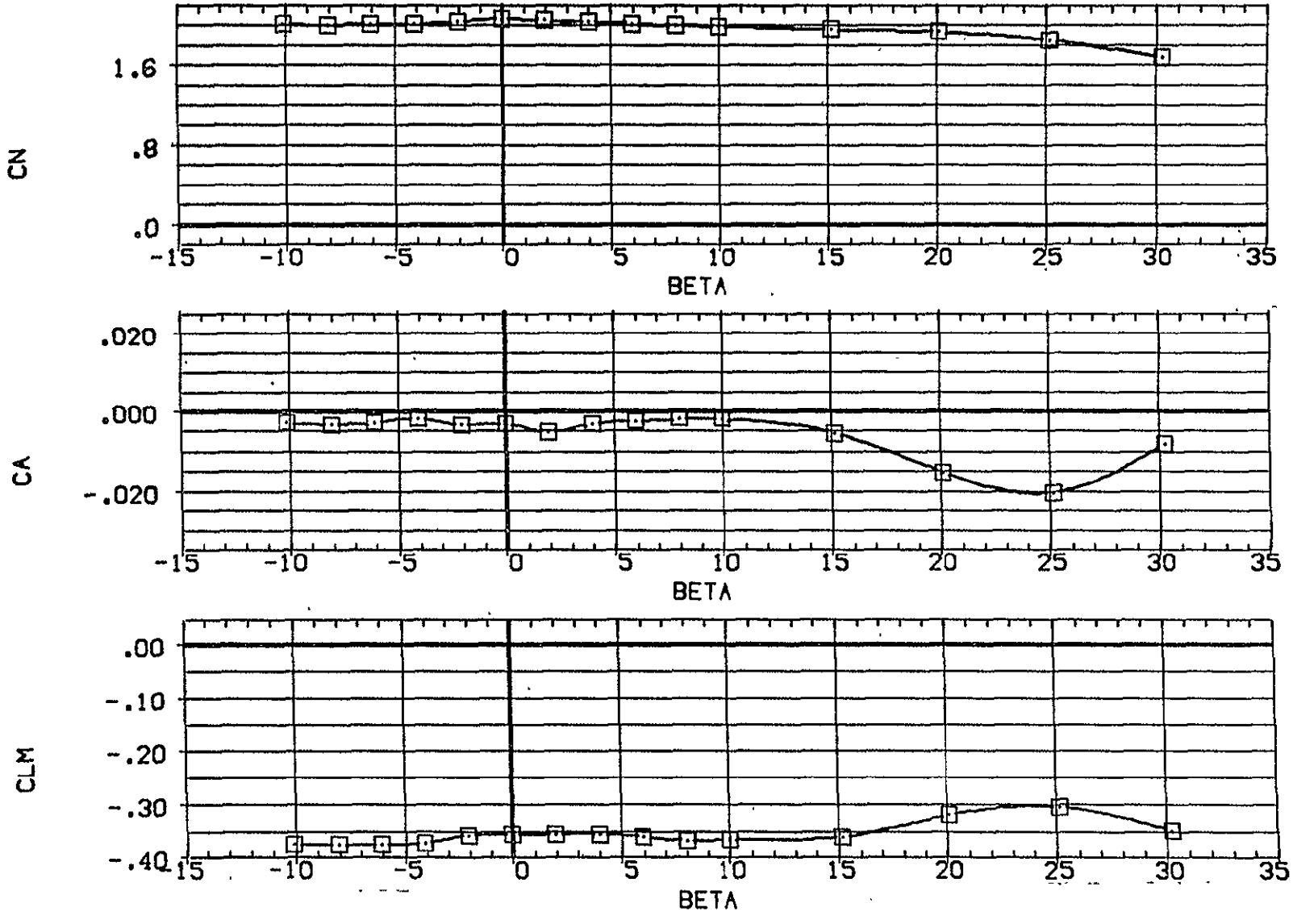

FIG. 5 EFFECT OF RAMP ANGLE ON AERODYNAMIC CHAR., REYNOLDS NO.= 13.12 MIL.

(E)ALPHA = 41.34

18

DATA SET	SYMBOL	CONFIGURATION DESCRIPTION	AIL-L	AIL-R	STB-L	STB-R
(EDW001)	○	BASIC. RHO=0 + GRIT	.000	.000	.000	.000
(EDW009)	□	BASIC. RHO=11 + GRIT	.000	.000	.000	.000

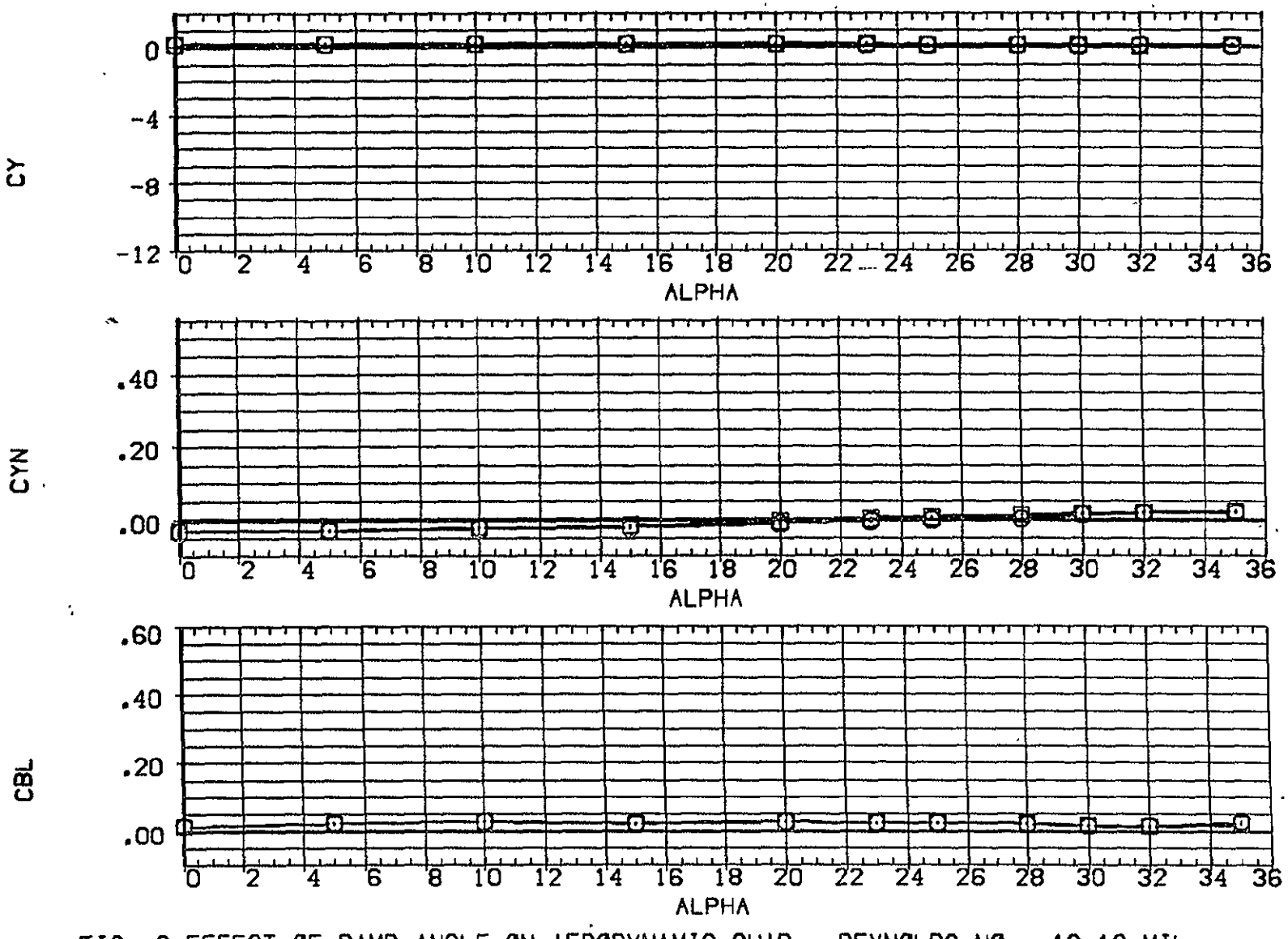

FIG. 6 EFFECT OF RAMP ANGLE ON AERODYNAMIC CHAR., REYNOLDS NO.= 13.12 MIL.

(A)BETA =-10.00

ORIGINAL PAGE IS
OF POOR QUALITY

DATA SET SYMBOL	CONFIGURATION DESCRIPTION	AIL-L	AIL-R	STB-L	STB-R
(EDW001) ○	BASIC, RH0=0 + GRIT	.000	.000	.000	.000
(EDW009) □	BASIC, RH0=11 + GRIT	.000	.000	.000	.000

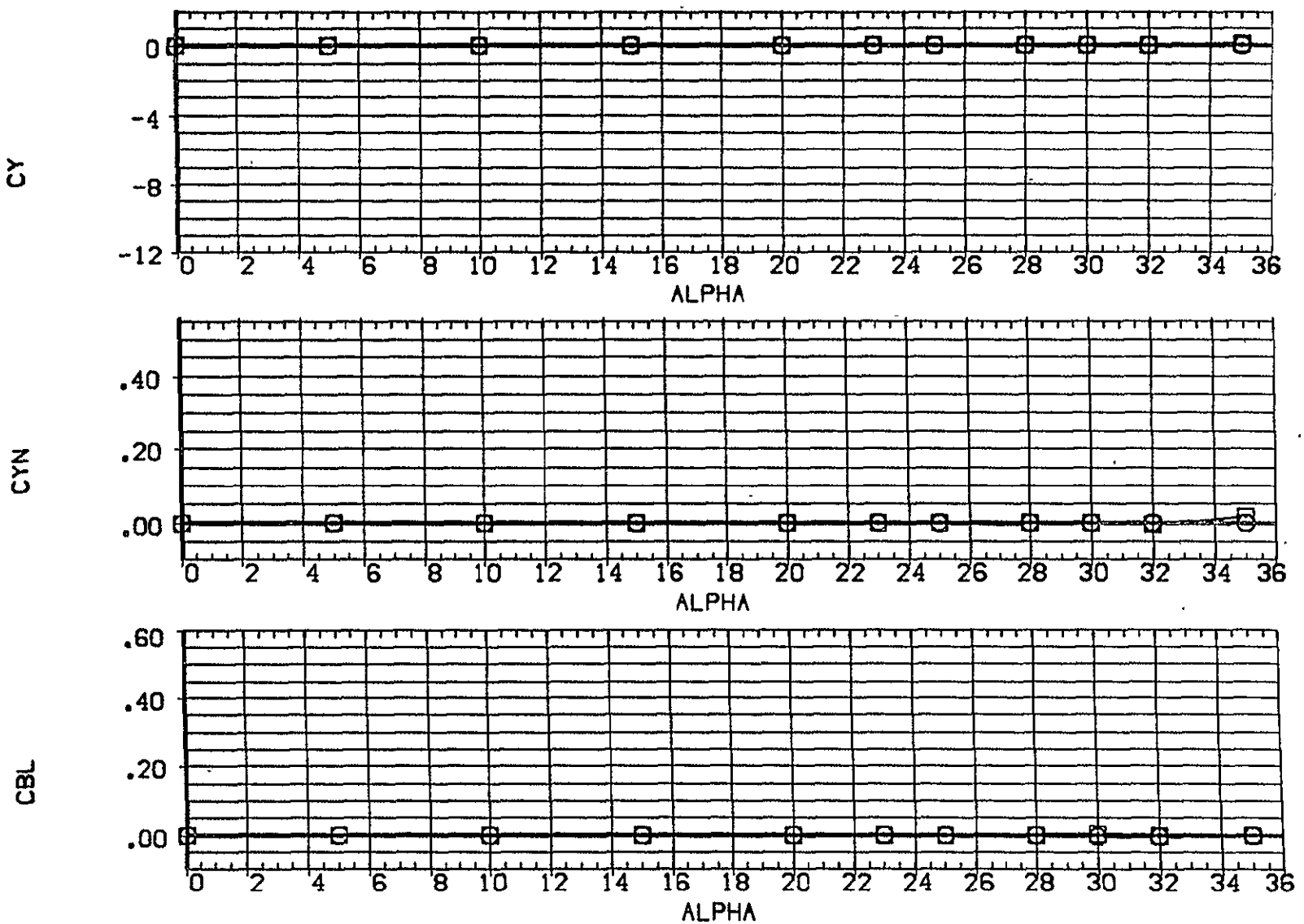

FIG. 6 EFFECT OF RAMP ANGLE ON AERODYNAMIC CHAR., REYNOLDS NO.= 13.12 MIL.

(B)BETA = .00

ORIGINAL PAGE IS
OF POOR QUALITY

DATA SET	SYMBOL	CONFIGURATION DESCRIPTION	AIL-L	AIL-R	STB-L	STB-R
(EDW001)	○	BASIC, RHO=0 + GRIT	.000	.000	.000	.000
(EDW009)	□	BASIC, RHO=11 + GRIT	.000	.000	.000	.000

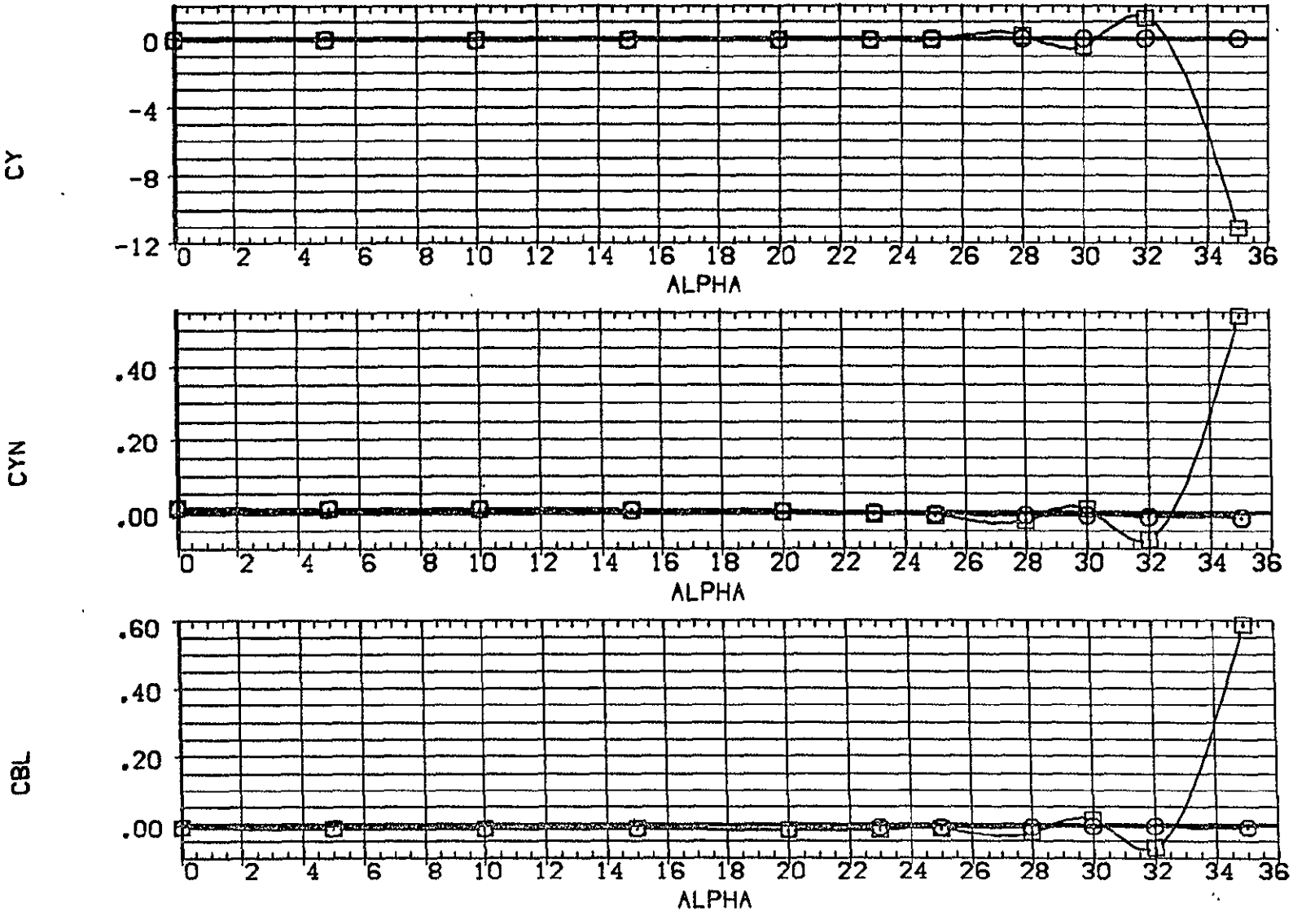

FIG. 6 EFFECT OF RAMP ANGLE ON AERODYNAMIC CHAR., REYNOLDS NO.= 13.12 MIL.

(C)BETA = 4.00

DATA SET SYMBOL	CONFIGURATION DESCRIPTION	AIL-L	AIL-R	STB-L	STB-R
(EDW001) ○	BASIC, RHO=0 + GRIT	.000	.000	.000	.000
(EDW009) □	BASIC, RHO=11 + GRIT	.000	.000	.000	.000

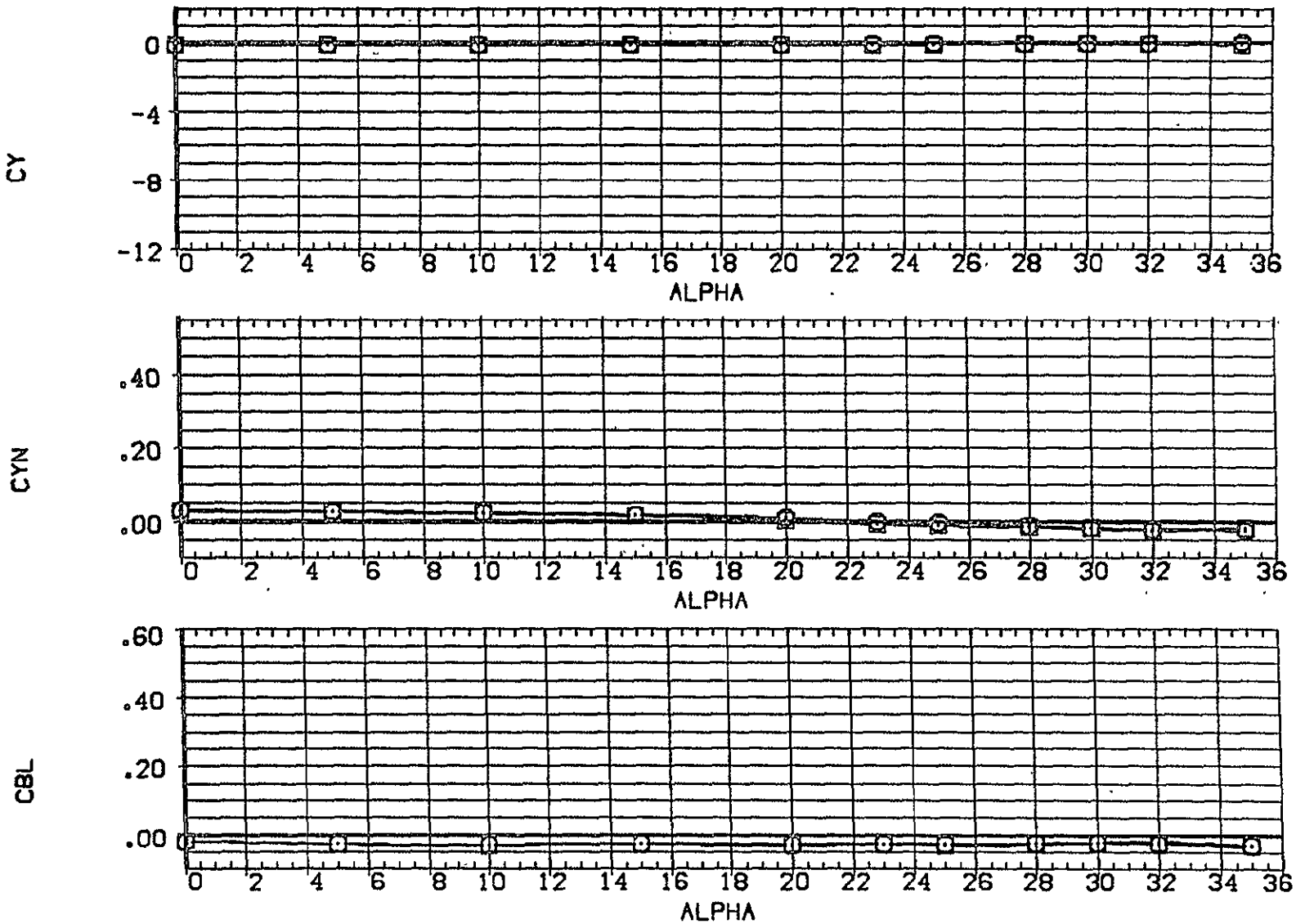

FIG. 6 EFFECT OF RAMP ANGLE ON AERODYNAMIC CHAR., REYNOLDS NO.= 13.12 MIL.

(D)BETA = 10.00

DATA SET	SYMBOL	CONFIGURATION DESCRIPTION	AIL-L	AIL-R	STB-L	STB-R
(EDW001)	○	BASIC, RH0=0 + GRIT	.000	.000	.000	.000
(EDW009)	□	BASIC, RH0=11 + GRIT	.000	.000	.000	.000

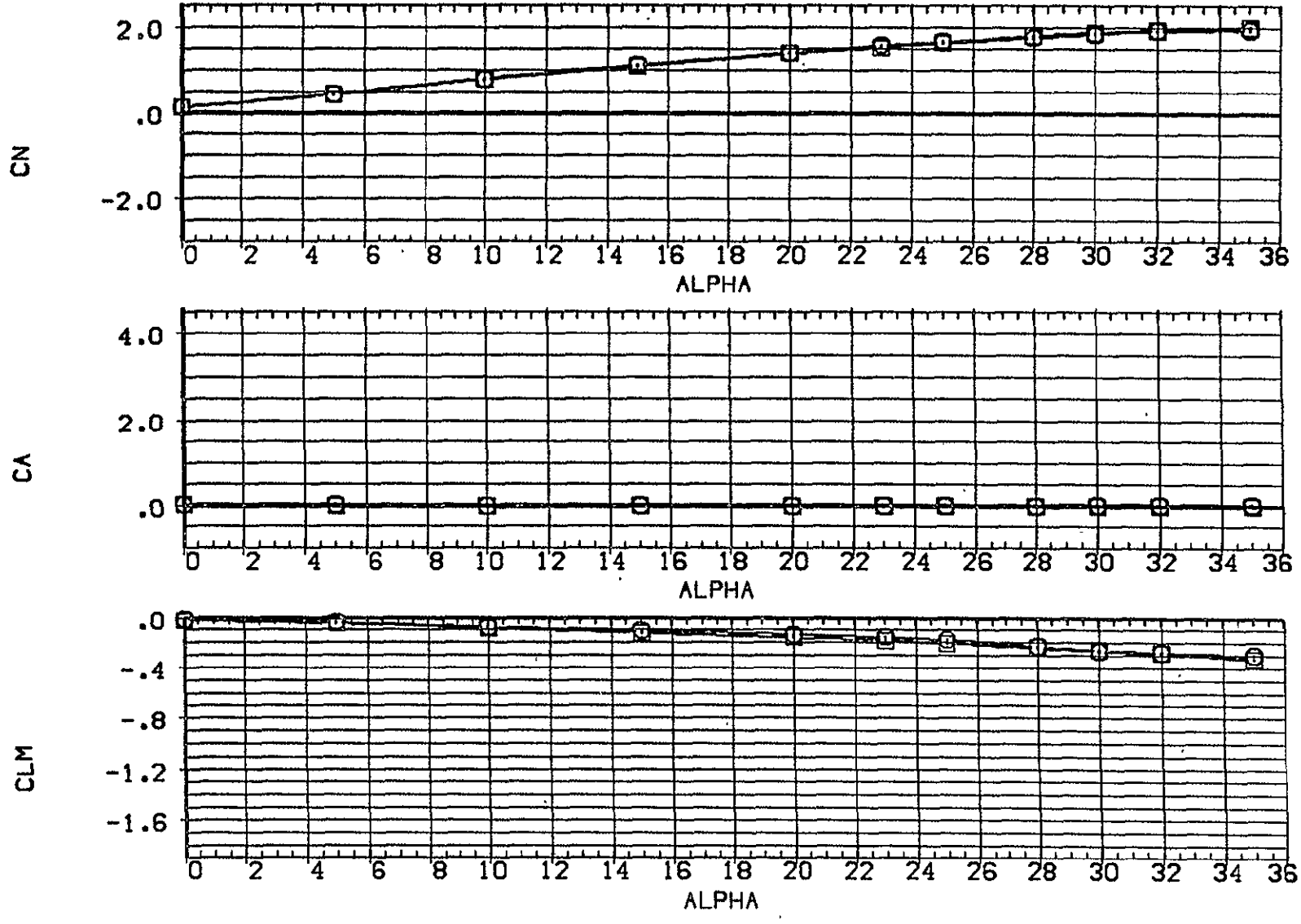

FIG. 6 EFFECT OF RAMP ANGLE ON AERODYNAMIC CHAR., REYNOLDS NO.= 13.12 MIL.

(A)BETA =-10.00

ORIGINAL PAGE IS OF POOR QUALITY

DATA SET	SYMBOL	CONFIGURATION DESCRIPTION	AIL-L	AIL-R	STB-L	STB-R
(E0W001)	○	BASIC, RHO=0 + GRIT	.000	.000	.000	.000
(E0W009)	□	BASIC, RHO=11 + GRIT	.000	.000	.000	.000

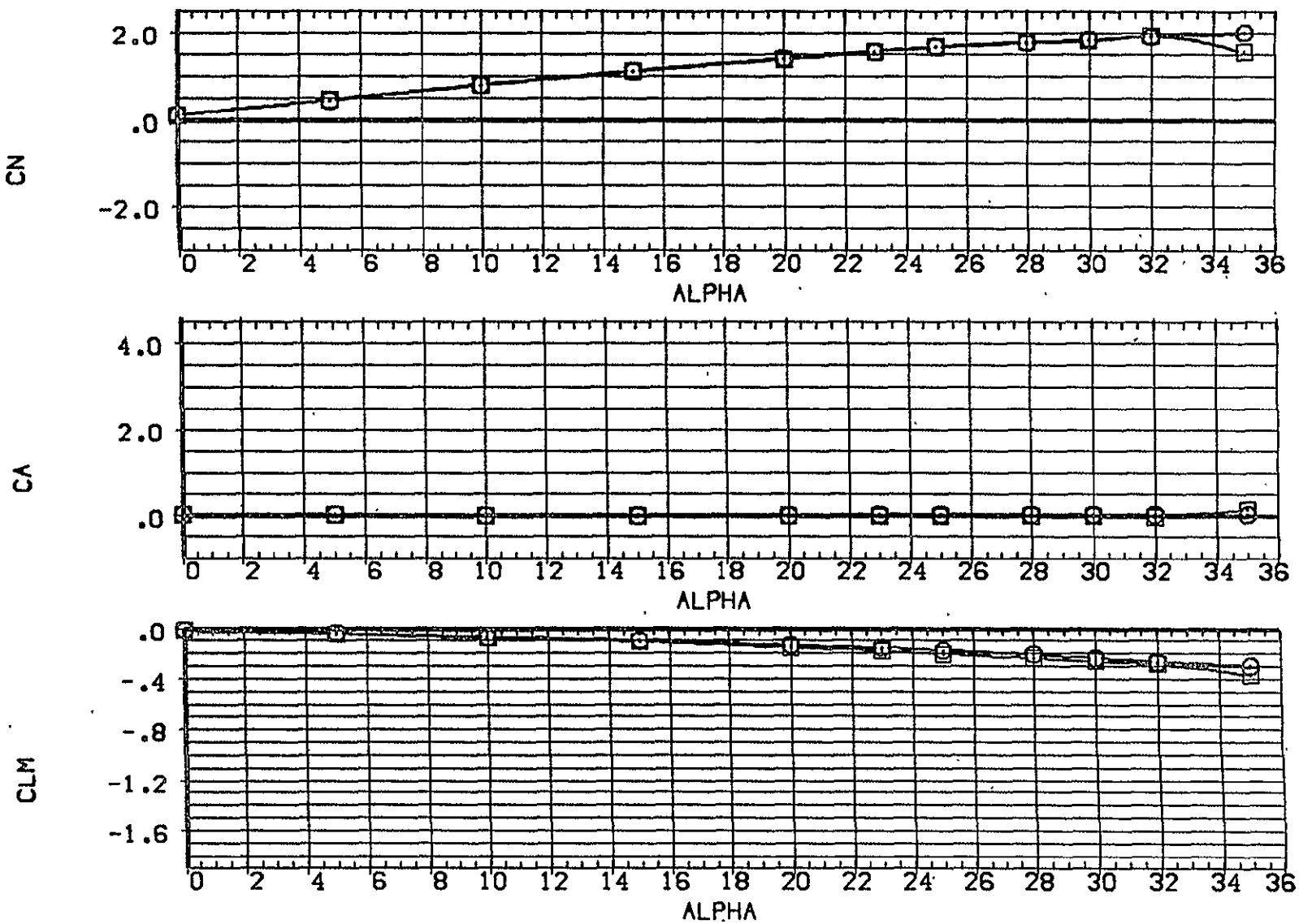

FIG. 6 EFFECT OF RAMP ANGLE ON AERODYNAMIC CHAR., REYNOLDS NO.= 13.12 MIL.

(B)BETA = .00

DATA SET	SYMBOL	CONFIGURATION DESCRIPTION	AIL-L	AIL-R	STB-L	STB-R
(EDW001)	○	BASIC, RHO=0 + GRIT	.000	.000	.000	.000
(EDW009)	□	BASIC, RHO=11 + GRIT	.000	.000	.000	.000

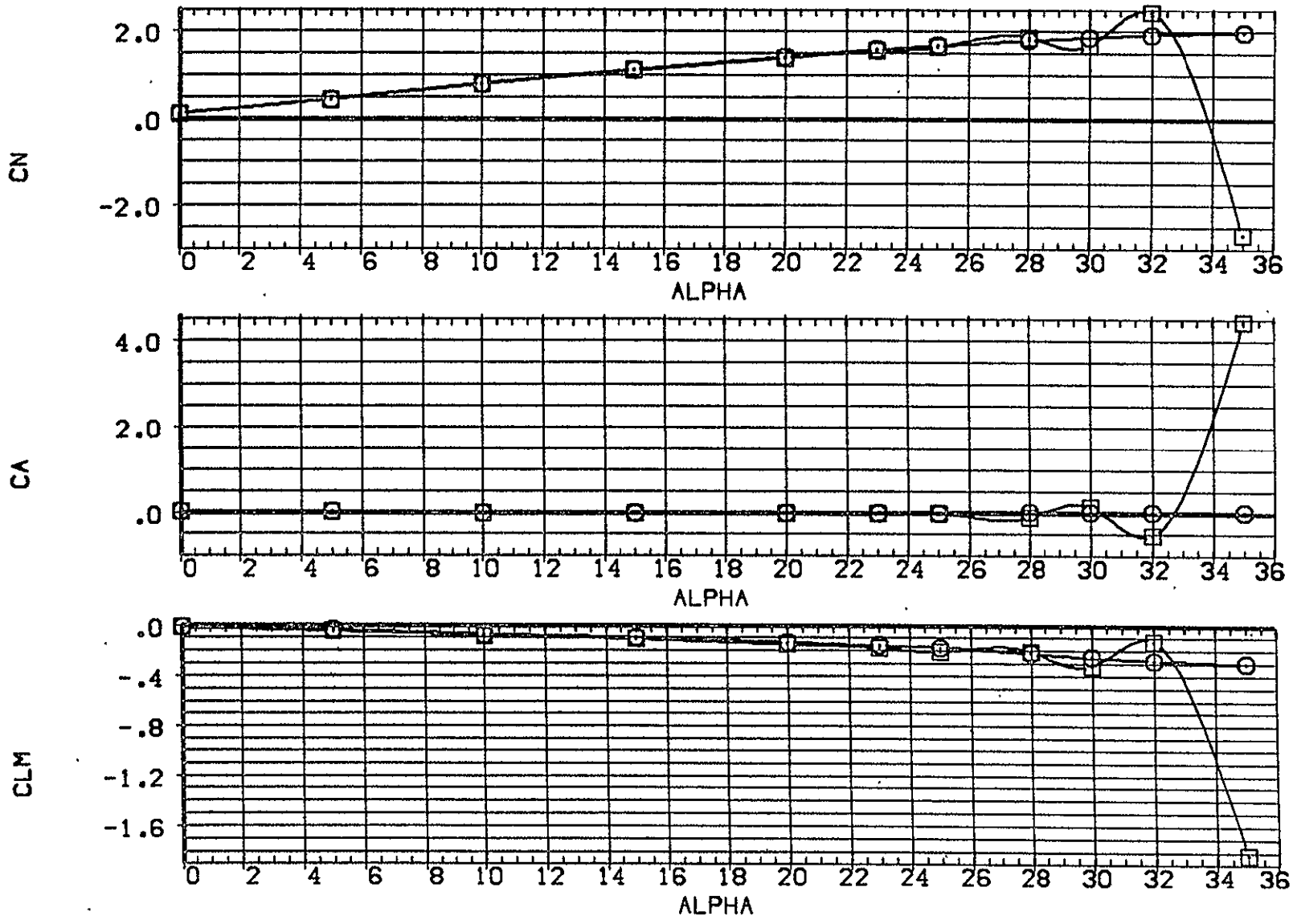

FIG. 6 EFFECT OF RAMP ANGLE ON AERODYNAMIC CHAR., REYNOLDS NO.= 13.12 MIL.

(C)BETA = 4.00

ORIGINAL PAGE IS
OF POOR QUALITY

88

DATA SET	SYMBOL	CONFIGURATION DESCRIPTION	AIL-L	AIL-R	STB-L	STB-R
(EDW001)	○	BASIC, RHO=0 + GRIT	.000	.000	.000	.000
(EDW009)	□	BASIC, RHO=11 + GRIT	.000	.000	.000	.000

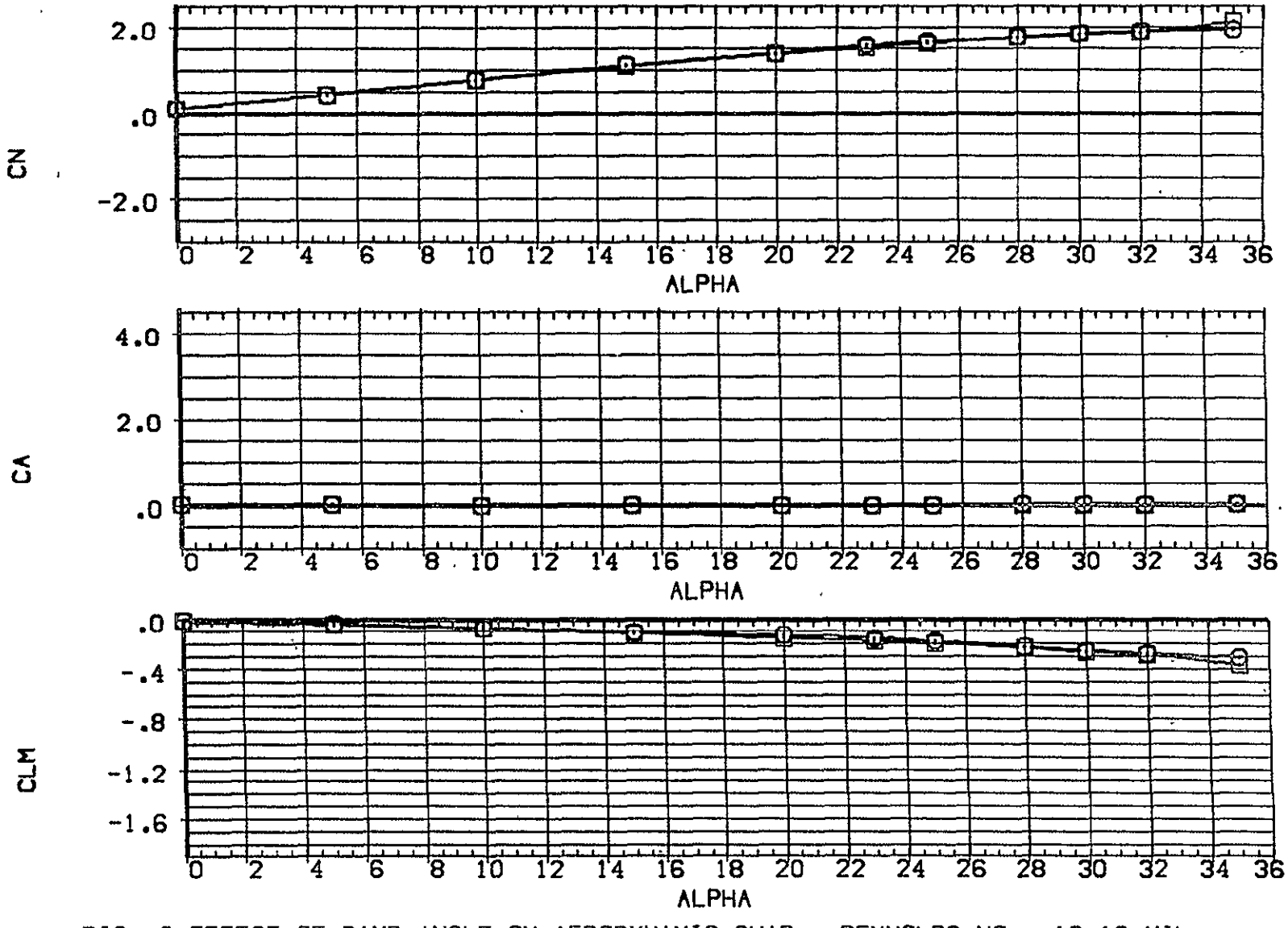

FIG. 6 EFFECT OF RAMP ANGLE ON AERODYNAMIC CHAR., REYNOLDS NO.= 13.12 MIL.

(D)BETA = 10.00

DATA SET	SYMBOL	CONFIGURATION DESCRIPTION	AIL-L	AIL-R	STB-L	STB-R
(CDW009)	○	BASIC, RHO=11 + GRIT	.000	.000	.000	.000
(CDW010)	□	BASIC, RHO=11 + GRIT	.000	.000	-25.000	-25.000
(CDW011)	◇	DATA NOT AVAILABLE	.000	.000	5.000	-5.000

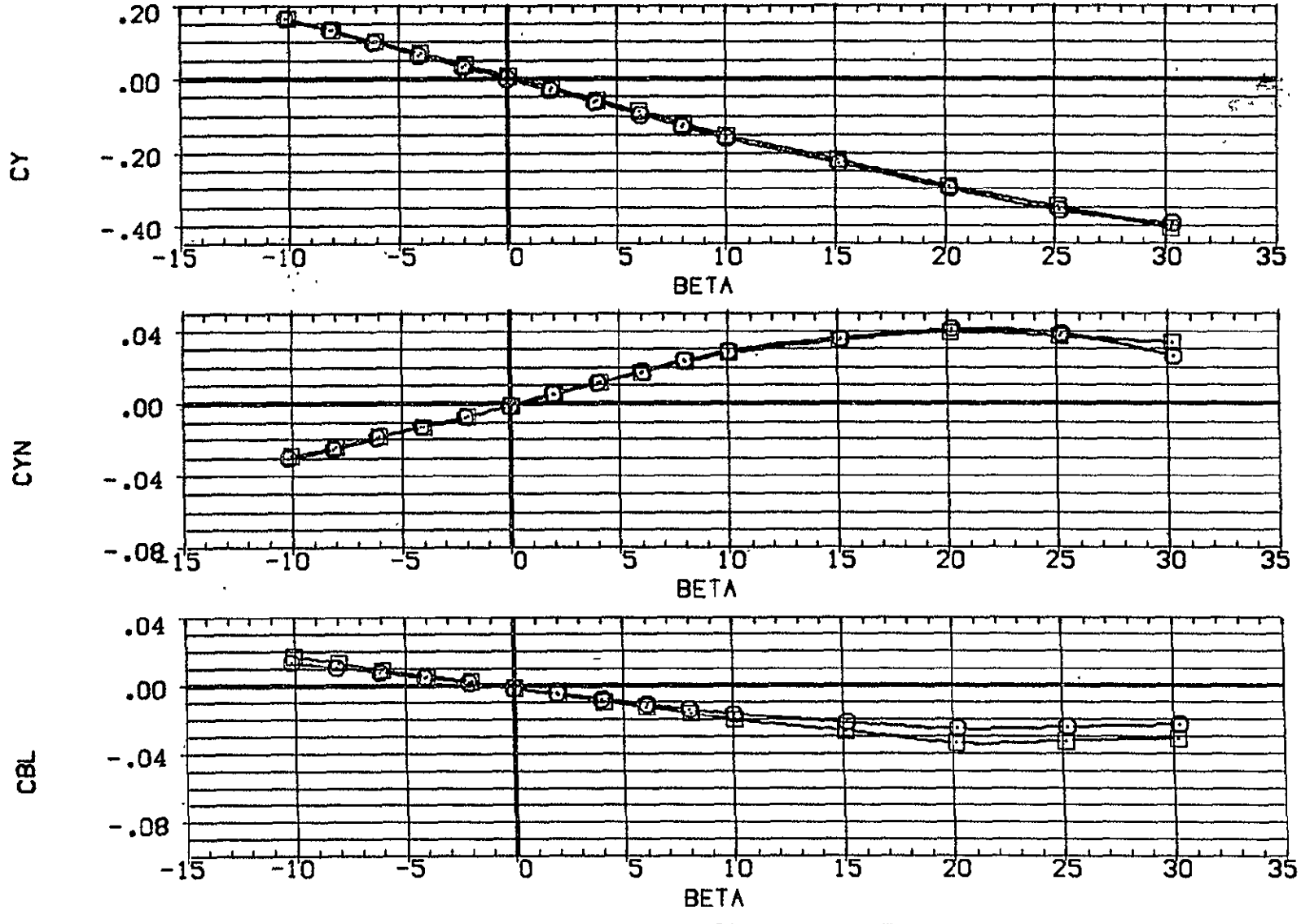

FIG. 7 EFFECT OF STABILATORS ON AERODYNAMIC CHAR., REYNOLDS NO.= 13.12 MIL.

(A)ALPHA = -.10

ORIGINAL PAGE IS
OF POOR QUALITY

DATA SET	SYMBOL	CONFIGURATION DESCRIPTION	AIL-L	AIL-R	STB-L	STB-R
(CDV009)	○	BASIC, RHO=11 + GRIT	.000	.000	.000	.000
(CDV010)	□	BASIC, RHO=11 + GRIT	.000	.000	-25.000	-25.000
(CDV011)	◇	DATA NOT AVAILABLE	.000	.000	5.000	-5.000

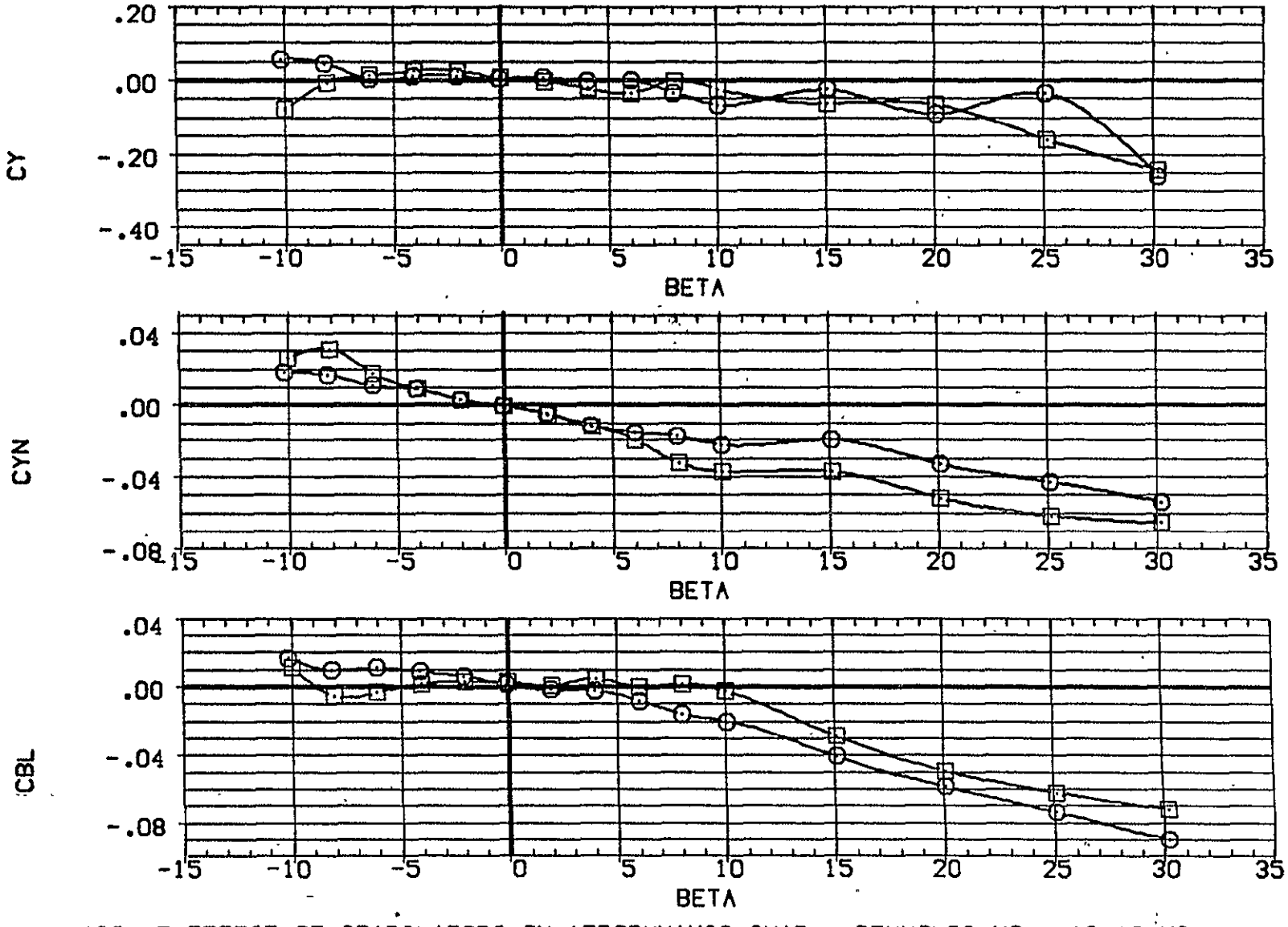

16

FIG. 7 EFFECT OF STABILATORS ON AERODYNAMIC CHAR., REYNOLDS NO.= 13.12 MIL.

(B)ALPHA = 31.33

DATA SET	SYMBOL	CONFIGURATION DESCRIPTION	AIL-L	AIL-R	STB-L	STB-R
(CDW009)	○	BASIC, RHO=11 + GRIT	.000	.000	.000	.000
(CDW010)	□	BASIC, RHO=11 + GRIT	.000	.000	-25.000	-25.000
(CDW011)	◇	BASIC, RHO=11 + GRIT	.000	.000	5.000	-5.000

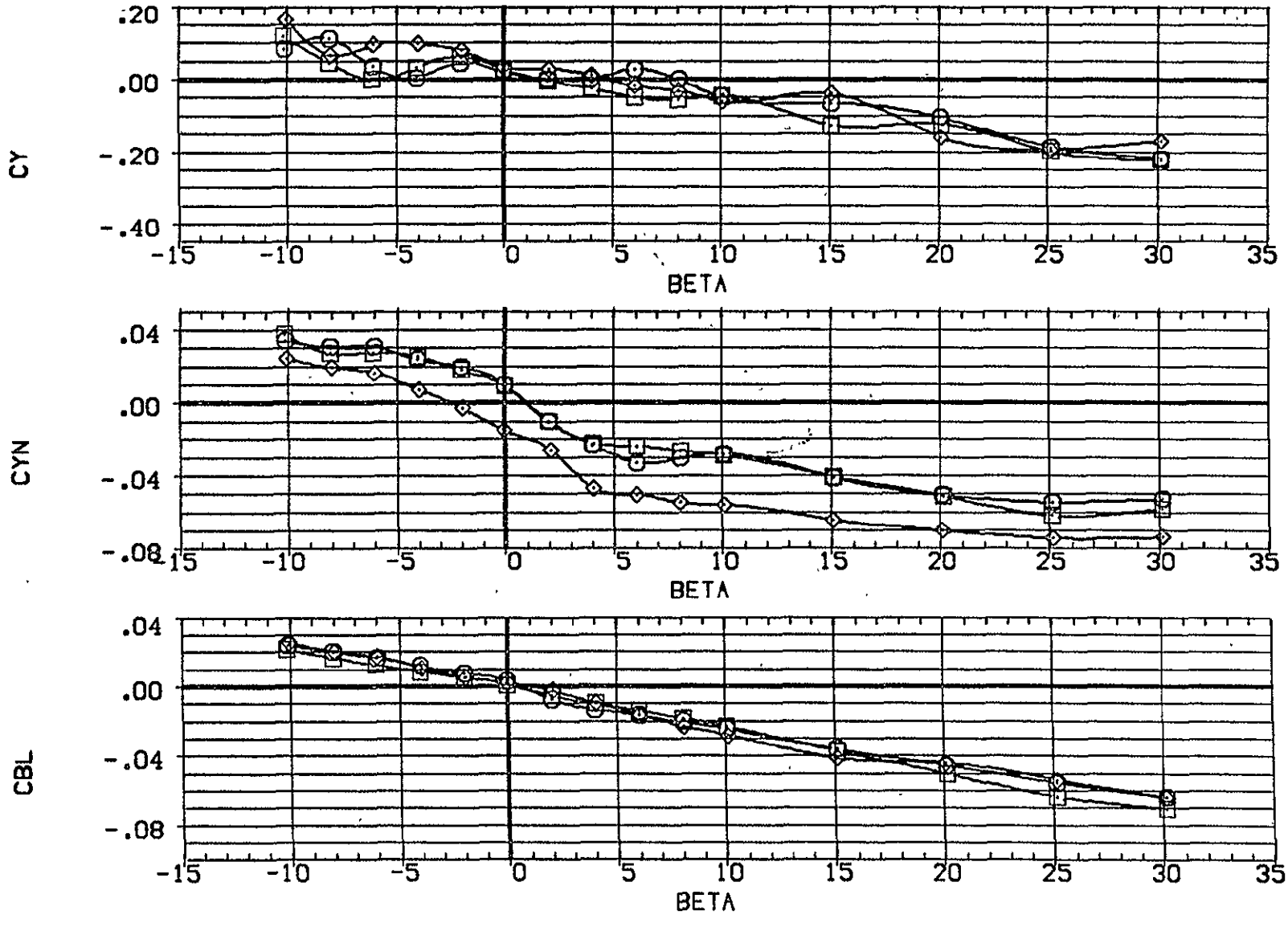

FIG. 7 EFFECT OF STABILATORS ON AERODYNAMIC CHAR., REYNOLDS NO.= 13.12 MIL.

(C)ALPHA = 51.37

ORIGINAL PAGE IS
OF POOR QUALITY

DATA SET	SYMBOL	CONFIGURATION DESCRIPTION	AIL-L	AIL-R	STB-L	STB-R
(CDV009)	○	BASIC, RHO=11 + GRIT	.000	.000	.000	.000
(CDV010)	□	BASIC, RHO=11 + GRIT	.000	.000	-25.000	-25.000
(CDV011)	◇	BASIC, RHO=11 + GRIT	.000	.000	5.000	-5.000

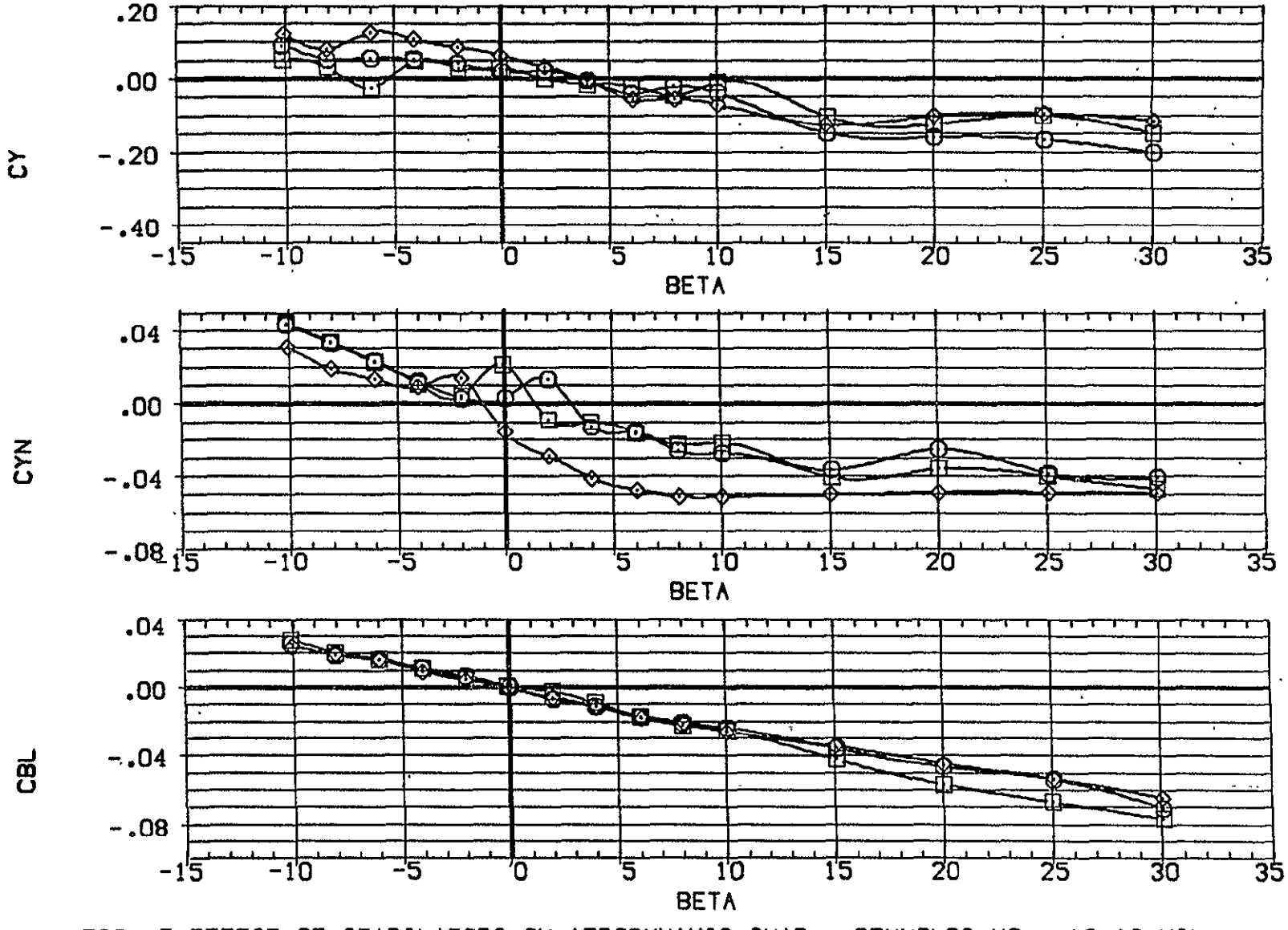

93

FIG. 7 EFFECT OF STABILATORS ON AERODYNAMIC CHAR., REYNOLDS NO.= 13.12 MIL.

(D)ALPHA = 61.28

DATA SET	SYMBOL	CONFIGURATION DESCRIPTION	AIL-L	AIL-R	STB-L	STB-R
(CDW009)	○	BASIC. RHO=11 + GRIT	.000	.000	.000	.000
(CDW010)	□	BASIC. RHO=11 + GRIT	.000	.000	-25.000	-25.000
(CDW011)	◇	BASIC. RHO=11 + GRIT	.000	.000	5.000	-5.000

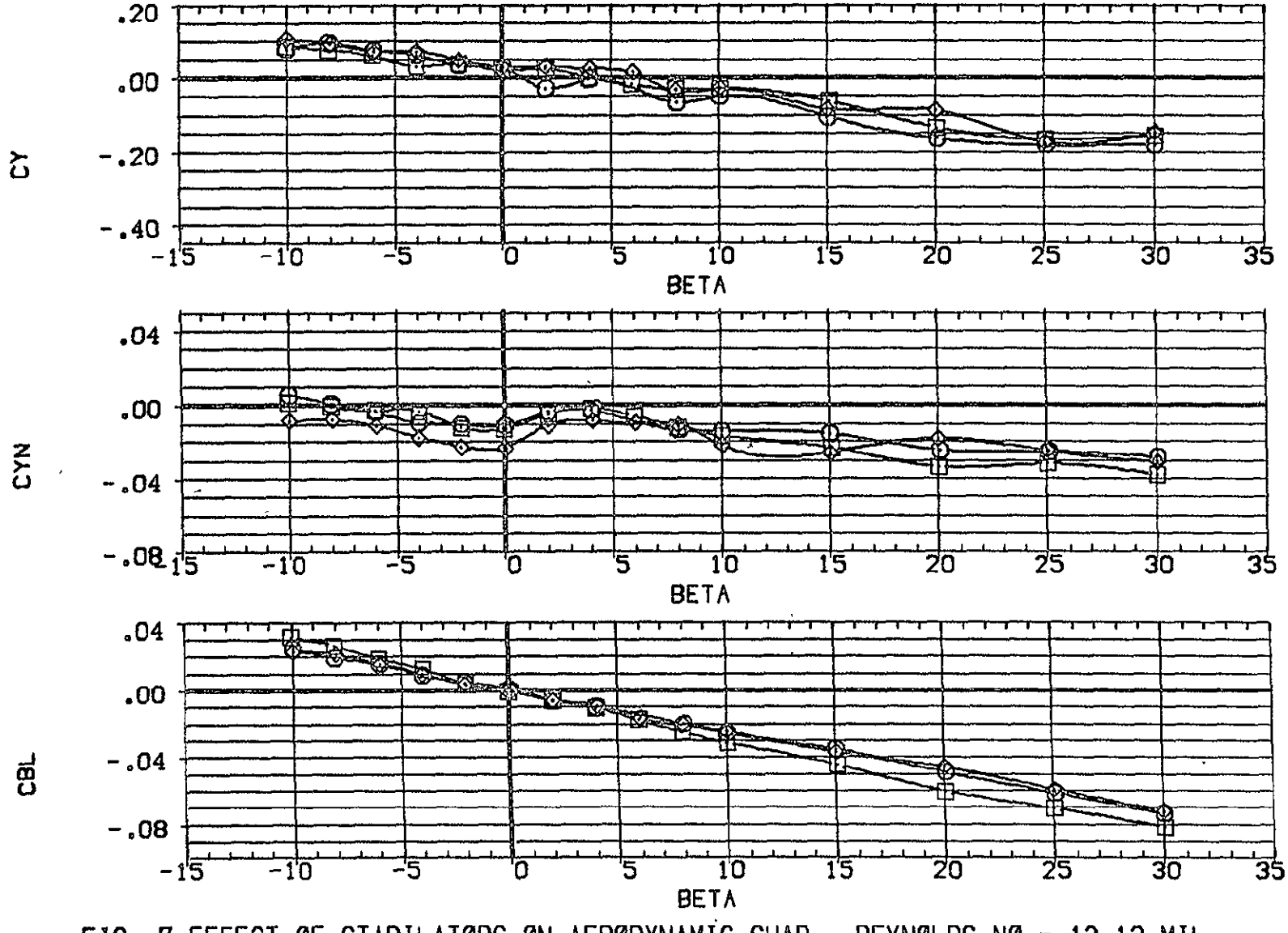

FIG. 7 EFFECT OF STABILATORS ON AERODYNAMIC CHAR., REYNOLDS NO.= 13.12 MIL.

(E)ALPHA = 71.30

ORIGINAL PAGE IS
OF POOR QUALITY

DATA SET	SYMBOL	CONFIGURATION DESCRIPTION	AIL-L	AIL-R	STB-L	STB-R
(CQV009)	○	BASIC, RHO=11 + GRIT	.000	.000	.000	.000
(CQV010)	□	BASIC, RHO=11 + GRIT	.000	.000	-25.000	-25.000
(CQV011)	◇	BASIC, RHO=11 + GRIT	.000	.000	5.000	-5.000

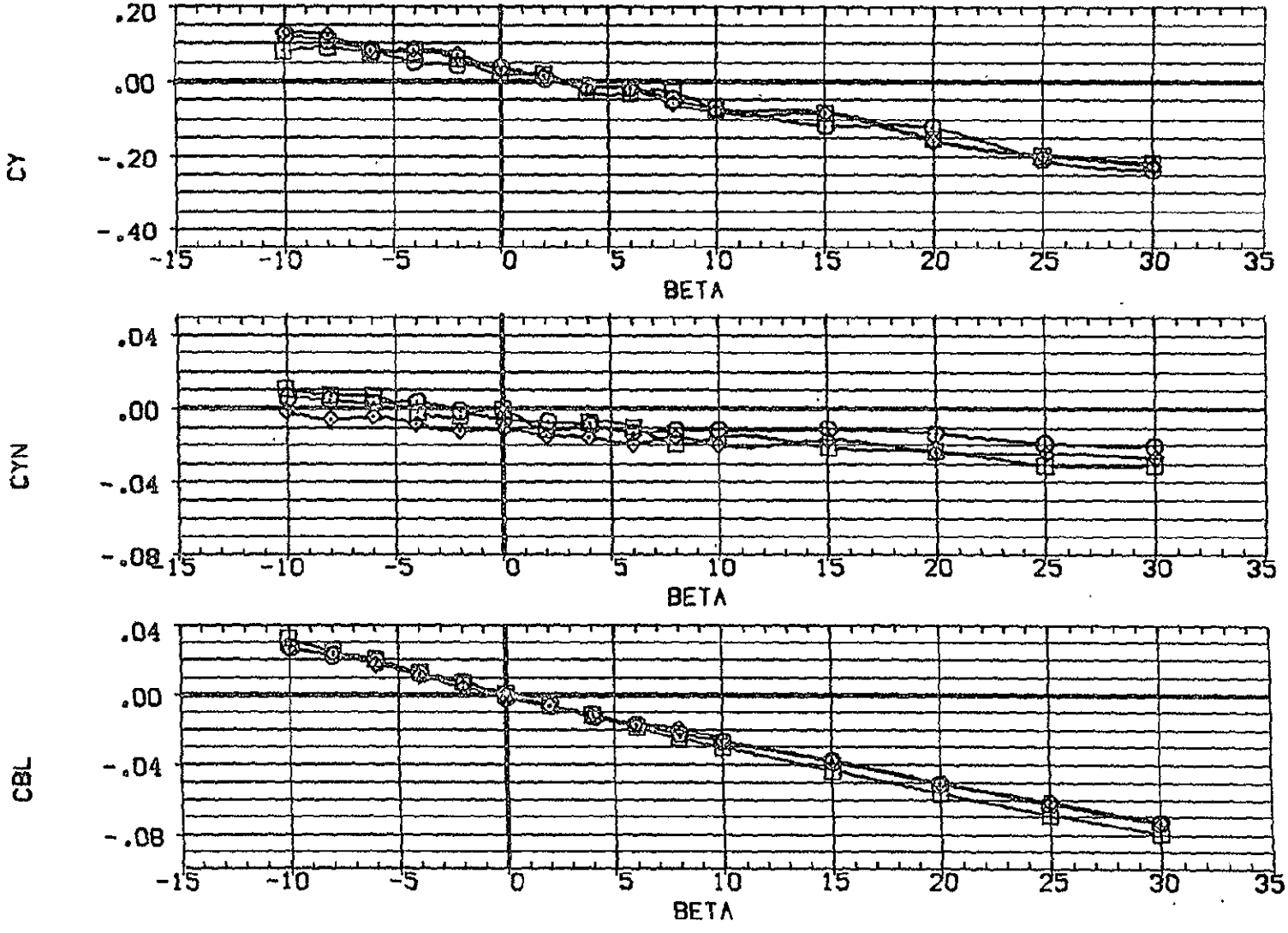

FIG. 7 EFFECT OF STABILATORS ON AERODYNAMIC CHAR., REYNOLDS NO.= 13.12 MIL.

(F)ALPHA = 88.24

DATA SET	SYMBOL	CONFIGURATION DESCRIPTION	AIL-L	AIL-R	STB-L	STB-R
(CDW009)	○	BASIC, RHO=11 + GRIT	.000	.000	.000	.000
(CDW010)	□	BASIC, RHO=11 + GRIT	.000	.000	-25.000	-25.000
(CDW011)	◇	DATA NOT AVAILABLE	.000	.000	5.000	-5.000

ORIGINAL PAGE IS
OF POOR QUALITY

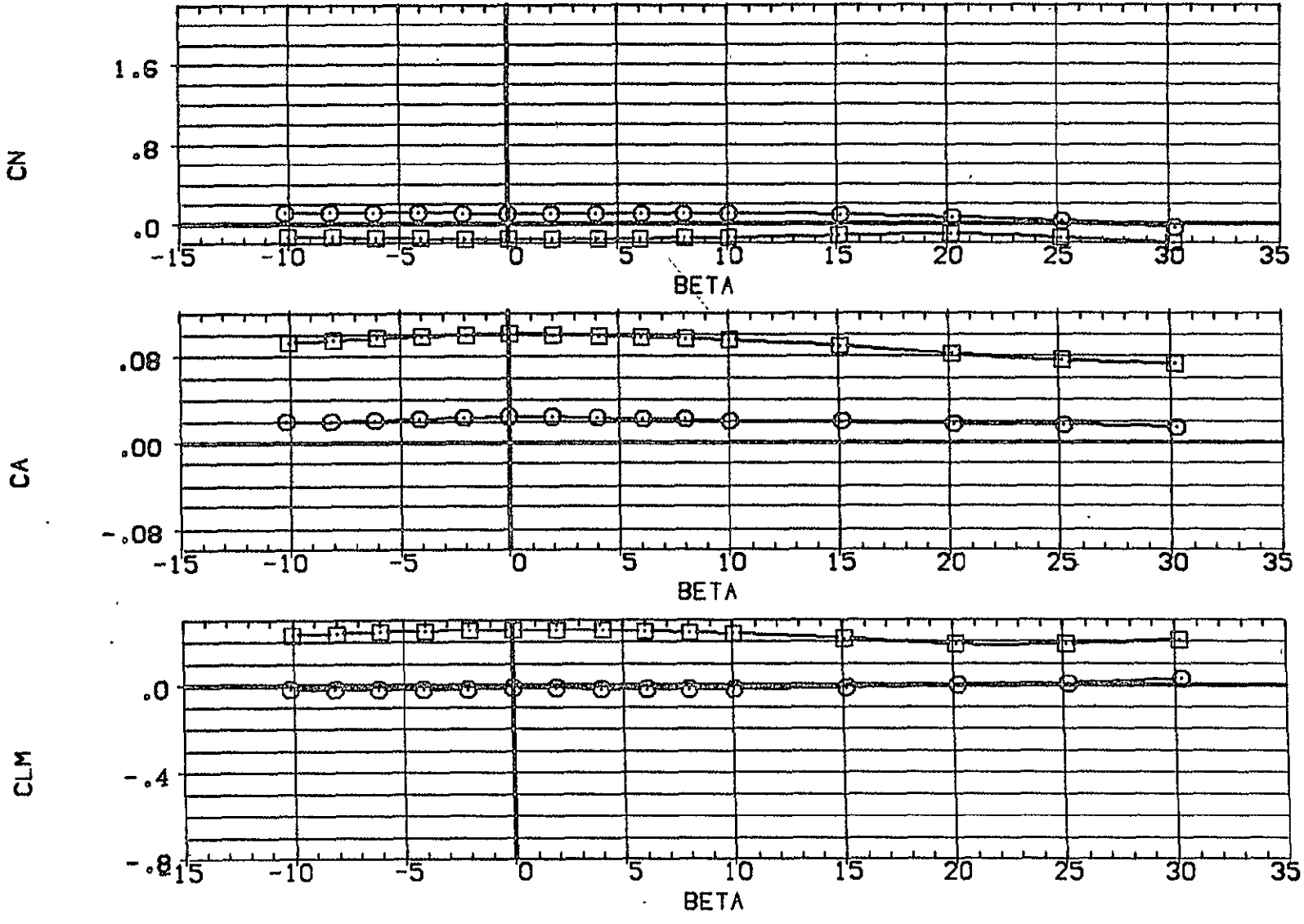

FIG. 7 EFFECT OF STABILATORS ON AERODYNAMIC CHAR., REYNOLDS NO.= 13.12 MIL.

(A)ALPHA = -.10

DATA SET	SYMBOL	CONFIGURATION DESCRIPTION	AIL-L	AIL-R	STB-L	STB-R
(CDW009)	○	BASIC, RHO=11 + GRIT	.000	.000	.000	.000
(CDW010)	□	BASIC, RHO=11 + GRIT	.000	.000	-25.000	-25.000
(CDW011)	◇	DATA NOT AVAILABLE	.000	.000	5.000	-5.000

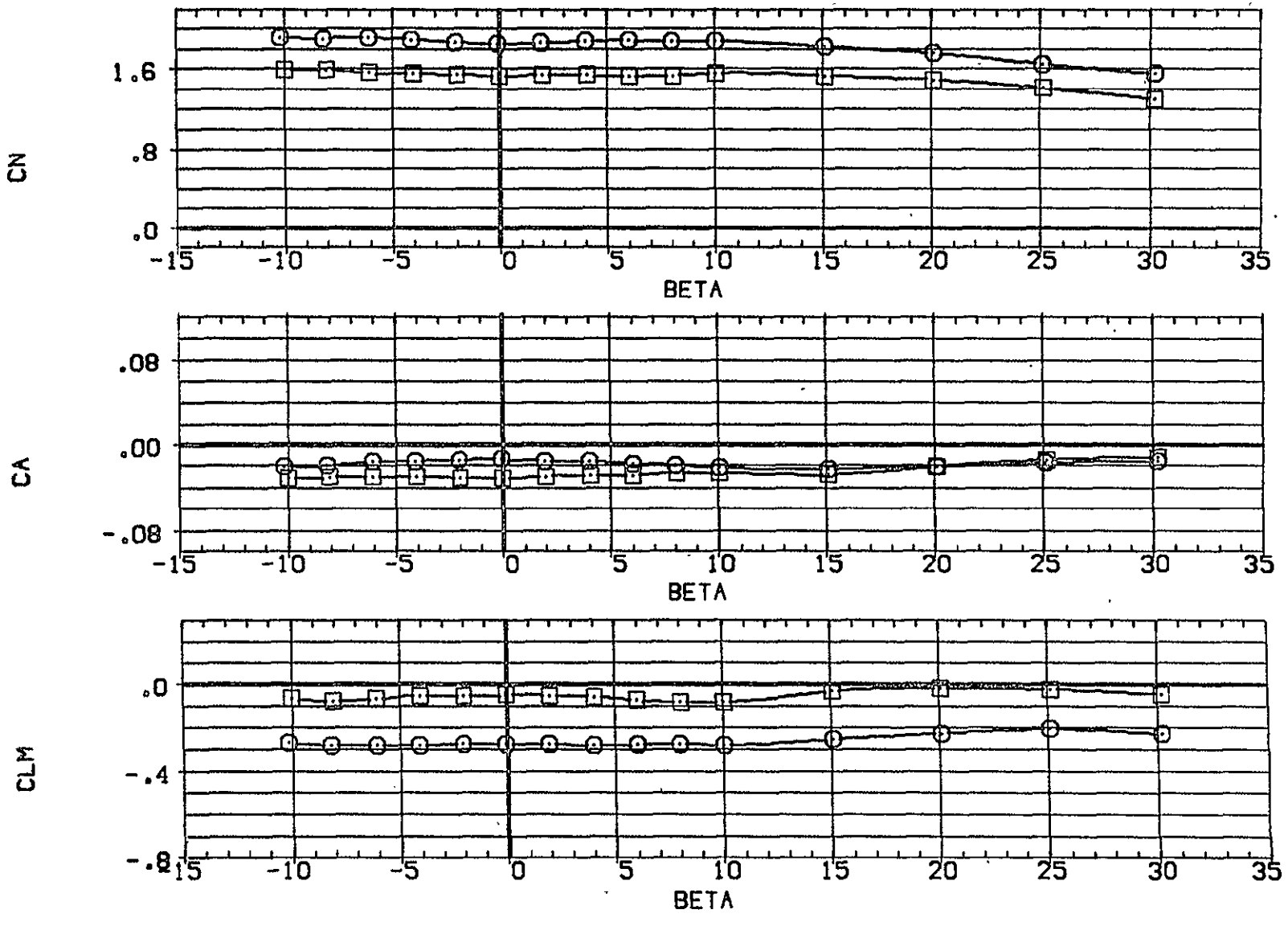

FIG. 7 EFFECT OF STABILATORS ON AERODYNAMIC CHAR., REYNOLDS NO.= 13.12 MIL.

(B)ALPHA = 31.33

DATA SET	SYMBOL	CONFIGURATION DESCRIPTION	AIL-L	AIL-R	STB-L	STB-R
(CDW009)	○	BASIC, RHO=11 + GRIT	.000	.000	.000	.000
(CDW010)	□	BASIC, RHO=11 + GRIT	.000	.000	-25.000	-25.000
(CDW011)	◇	BASIC, RHO=11 + GRIT	.000	.000	5.000	-5.000

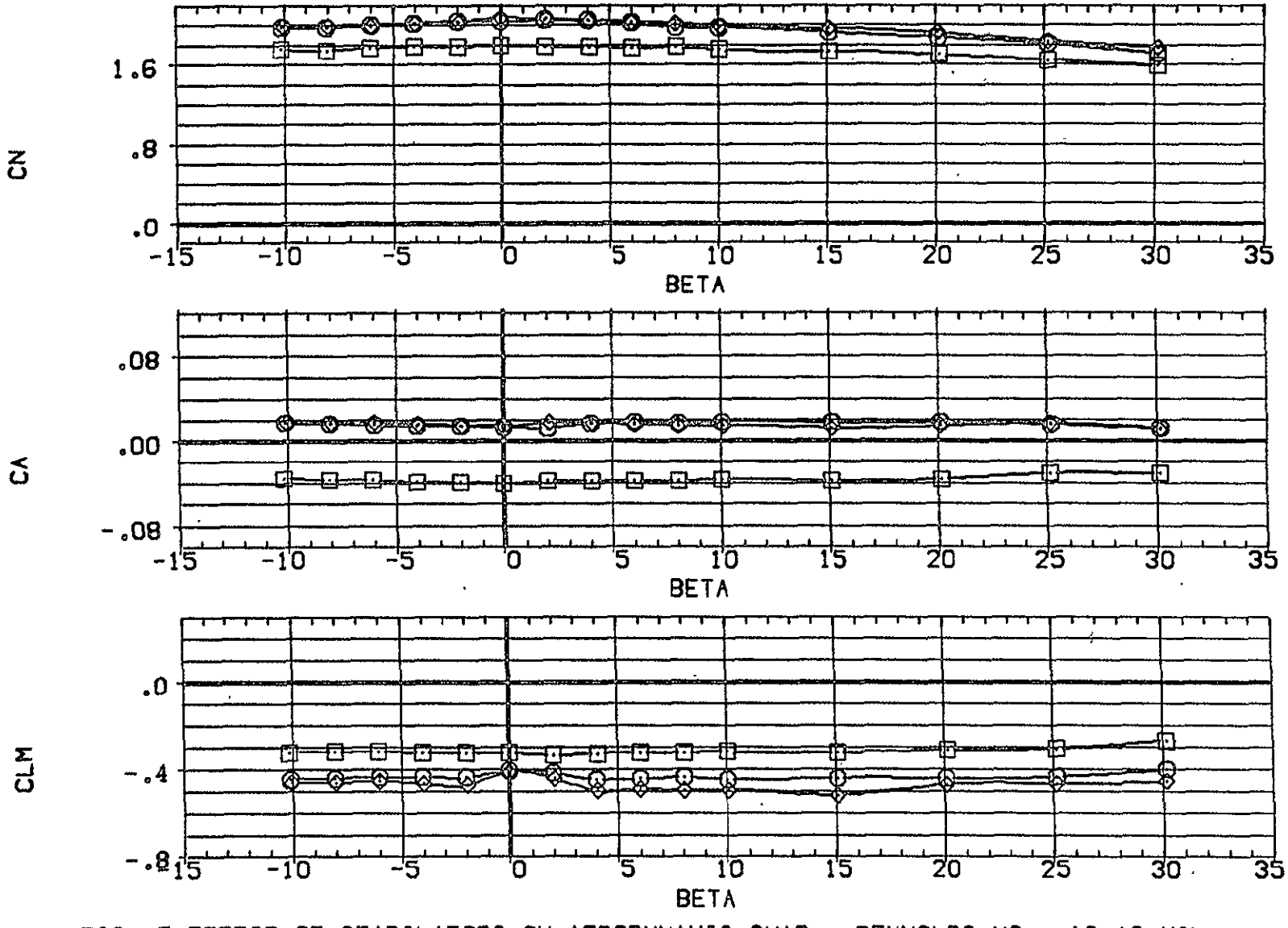

FIG. 7 EFFECT OF STABILATORS ON AERODYNAMIC CHAR., REYNOLDS NO.= 13.12 MIL.

(C)ALPHA = 51.37

ORIGINAL PAGE IS
OF POOR QUALITY

DATA SET	SYMBOL	CONFIGURATION DESCRIPTION	AIL-L	AIL-R	STB-L	STB-R
(CDW009)	○	BASIC, RHO=11 + GRIT	.000	.000	.000	.000
(CDW010)	□	BASIC, RHO=11 + GRIT	.000	.000	-25.000	-25.000
(CDW011)	◇	BASIC, RHO=11 + GRIT	.000	.000	5.000	-5.000

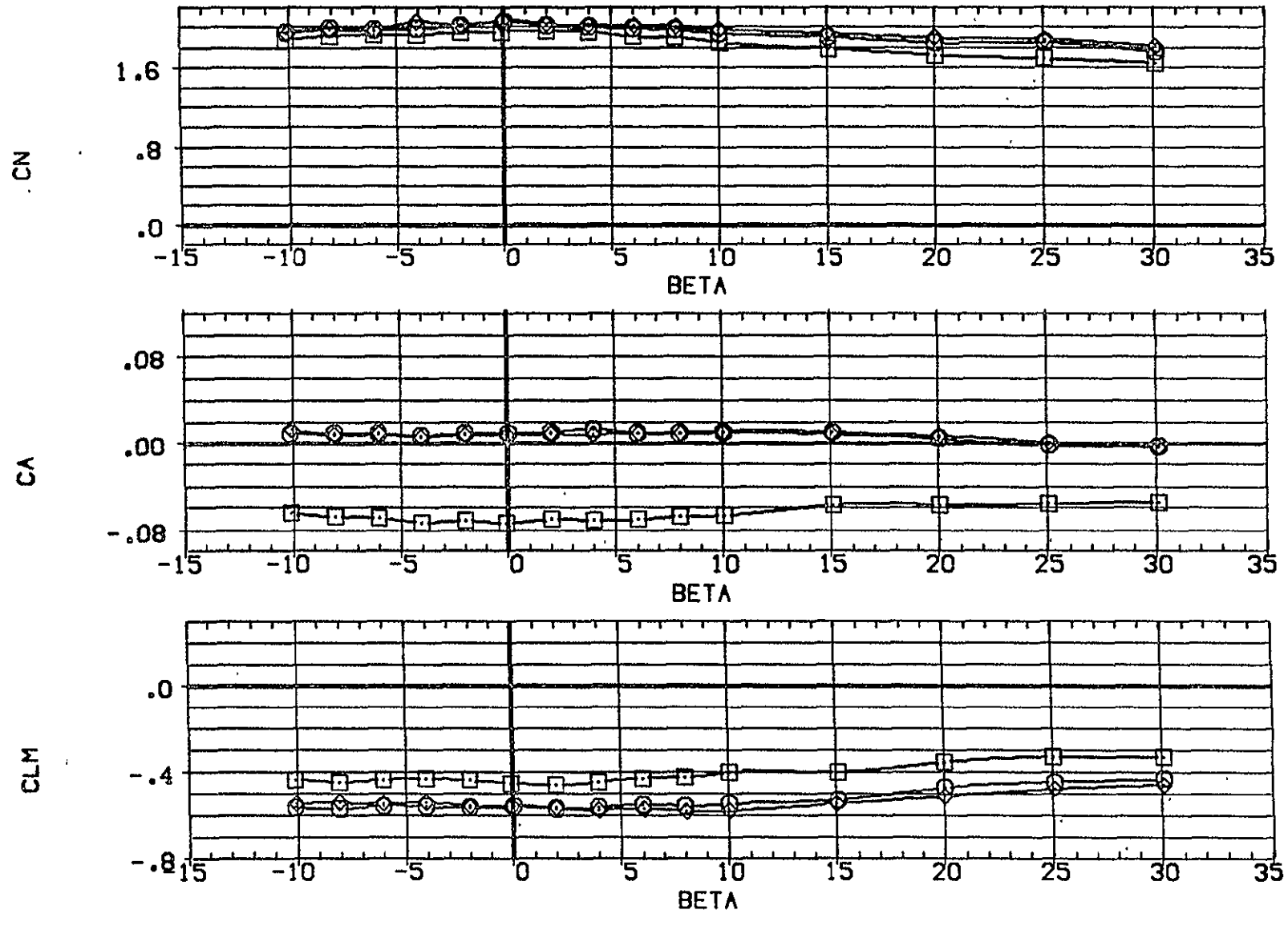

FIG. 7 EFFECT OF STABILATORS ON AERODYNAMIC CHAR., REYNOLDS NO.= 13.12 MIL.

(D)ALPHA = 61.28

ORIGINAL PAGE IS
OF POOR QUALITY

DATA SET-SYMBOL	CONFIGURATION DESCRIPTION	AIL-L	AIL-R	STB-L	STB-R
(CDW009) ○	BASIC, RHO=11 + GRIT	.000	.000	.000	.000
(CDW010) □	BASIC, RHO=11 + GRIT	.000	.000	-25.000	-25.000
(CDW011) ◇	BASIC, RHO=11 + GRIT	.000	.000	5.000	-5.000

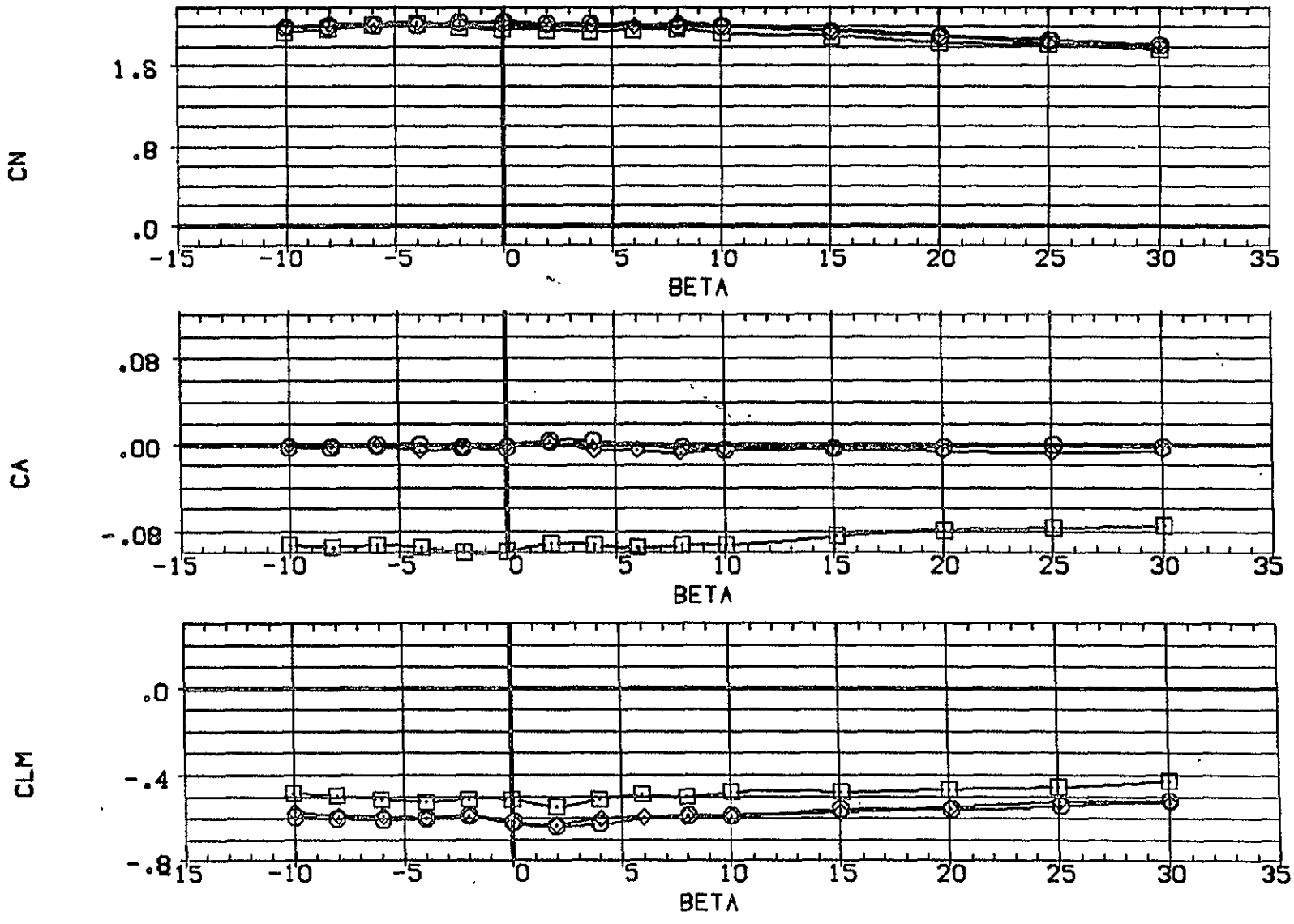

FIG. 7 EFFECT OF STABILATORS ON AERODYNAMIC CHAR., REYNOLDS NO.= 13.12 MIL.

(E)ALPHA = 71.30

DATA SET	SYMBOL	CONFIGURATION DESCRIPTION	AIL-L	AIL-R	STB-L	STB-R
(CDW009)	○	BASIC, RHO=11 + GRIT	.000	.000	.000	.000
(CDW010)	□	BASIC, RHO=11 + GRIT	.000	.000	-25.000	-25.000
(CDW011)	◇	BASIC, RHO=11 + GRIT	.000	.000	5.000	-5.000

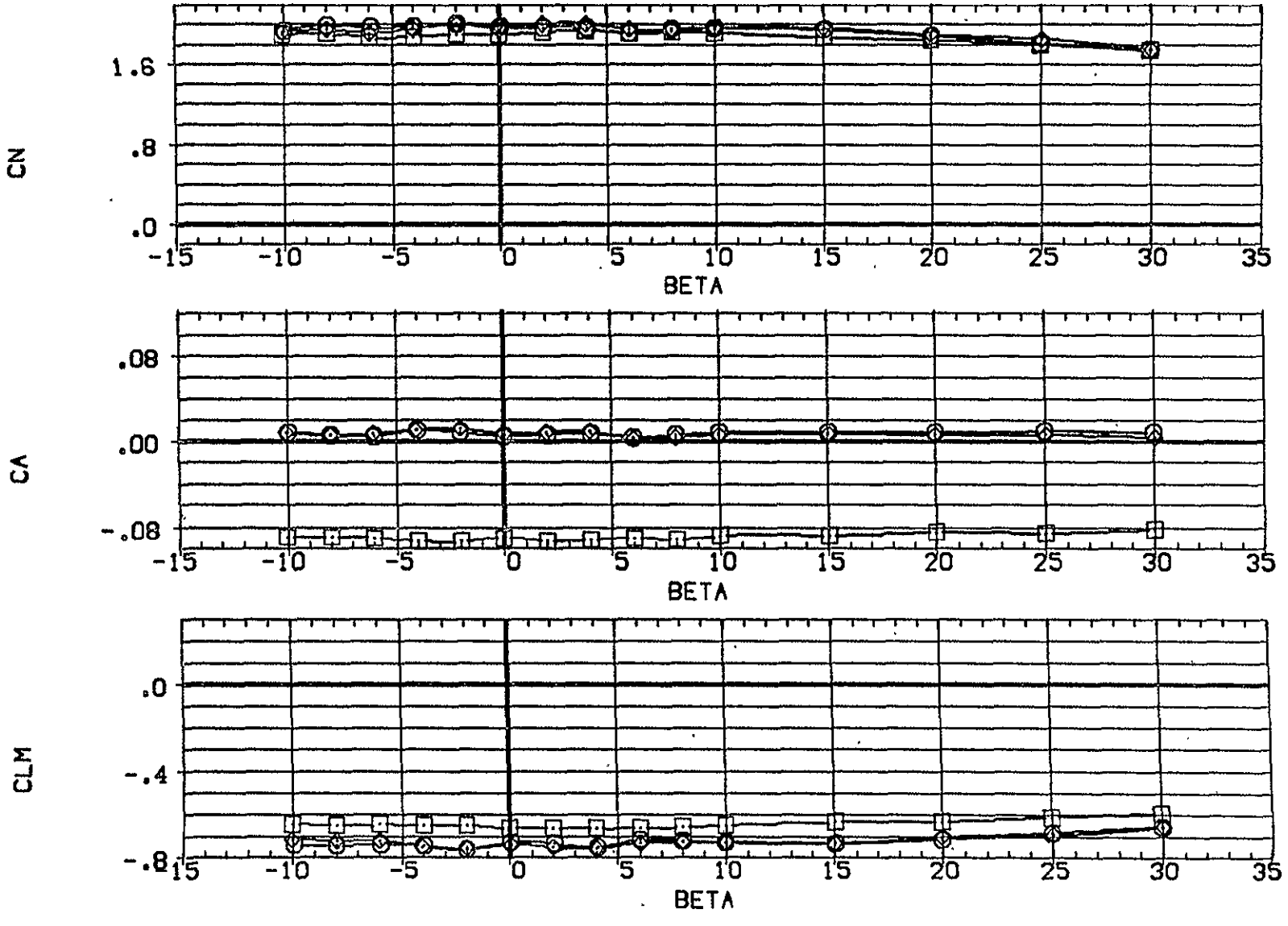

FIG. 7 EFFECT OF STABILATORS ON AERODYNAMIC CHAR., REYNOLDS NO.= 13.12 MIL.

(F)ALPHA = 88.24

DATA SET	SYMBOL	CONFIGURATION DESCRIPTION	AIL-L	AIL-R	STB-L	STB-R
(CDW010)	○	BASIC, RHO=11 + GRIT	.000	.000	-25.000	-25.000
(CDW012)	□	BASIC, RHO=11 + GRIT + A + B + C	.000	.000	-25.000	-25.000
(CDW014)	◇	DATA NOT AVAILABLE	.000	.000	-25.000	-25.000
(CDW015)	△	DATA NOT AVAILABLE	.000	.000	-25.000	-25.000

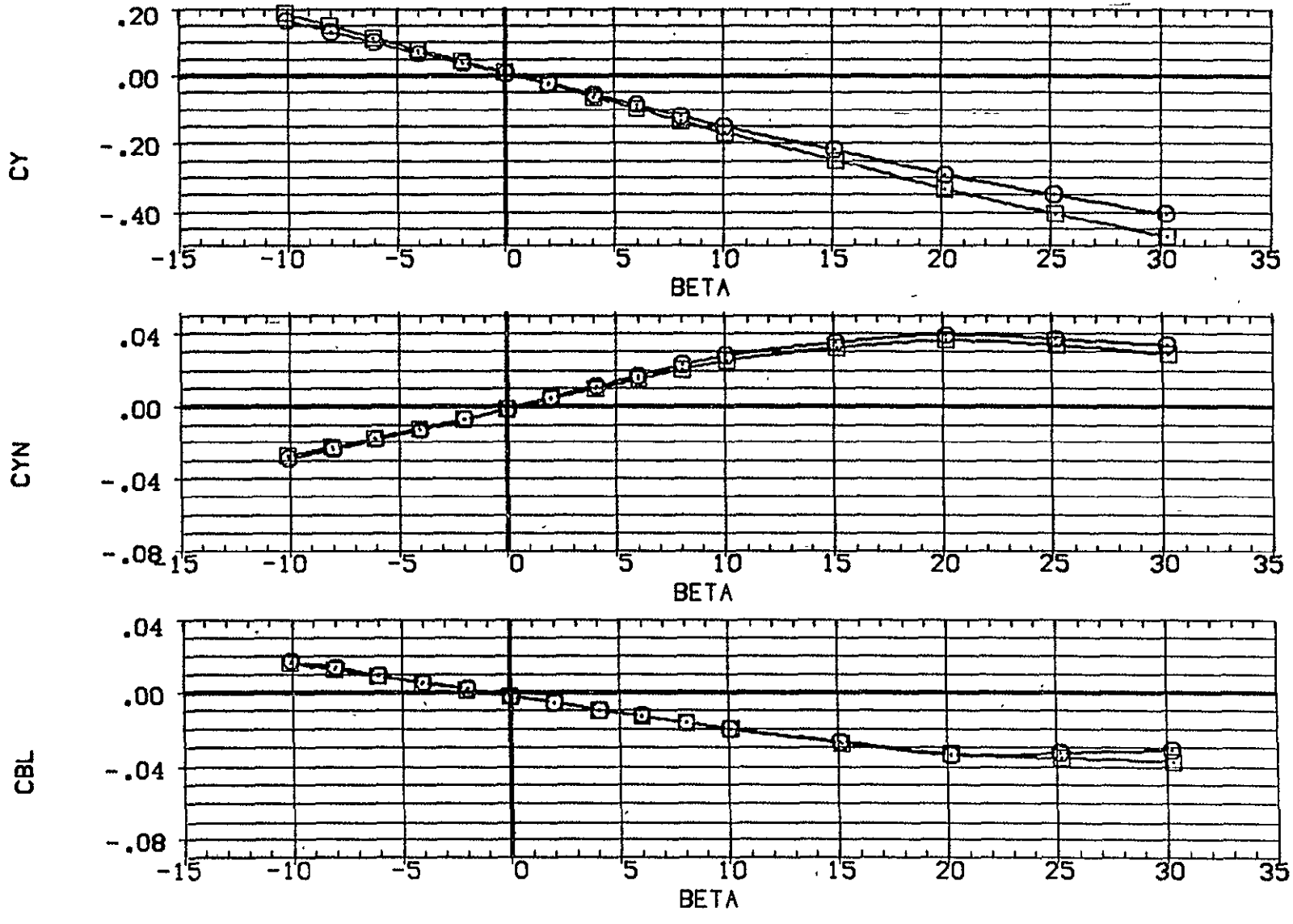

FIG. 8 EFFECT OF STORES ON AERODYNAMIC CHAR., REYNOLDS NO.= 13.12 MIL.

(A)ALPHA = -.24

DATA SET	SYMBOL	CONFIGURATION DESCRIPTION	AIL-L	AIL-R	STB-L	STB-R
(CDW010)	○	BASIC, RHO=11 + GRIT	.000	.000	-25.000	-25.000
(CDW012)	□	BASIC, RHO=11 + GRIT + A + B + C	.000	.000	-25.000	-25.000
(CDW014)	◇	DATA NOT AVAILABLE	.000	.000	-25.000	-25.000
(CDW015)	△	DATA NOT AVAILABLE	.000	.000	-25.000	-25.000

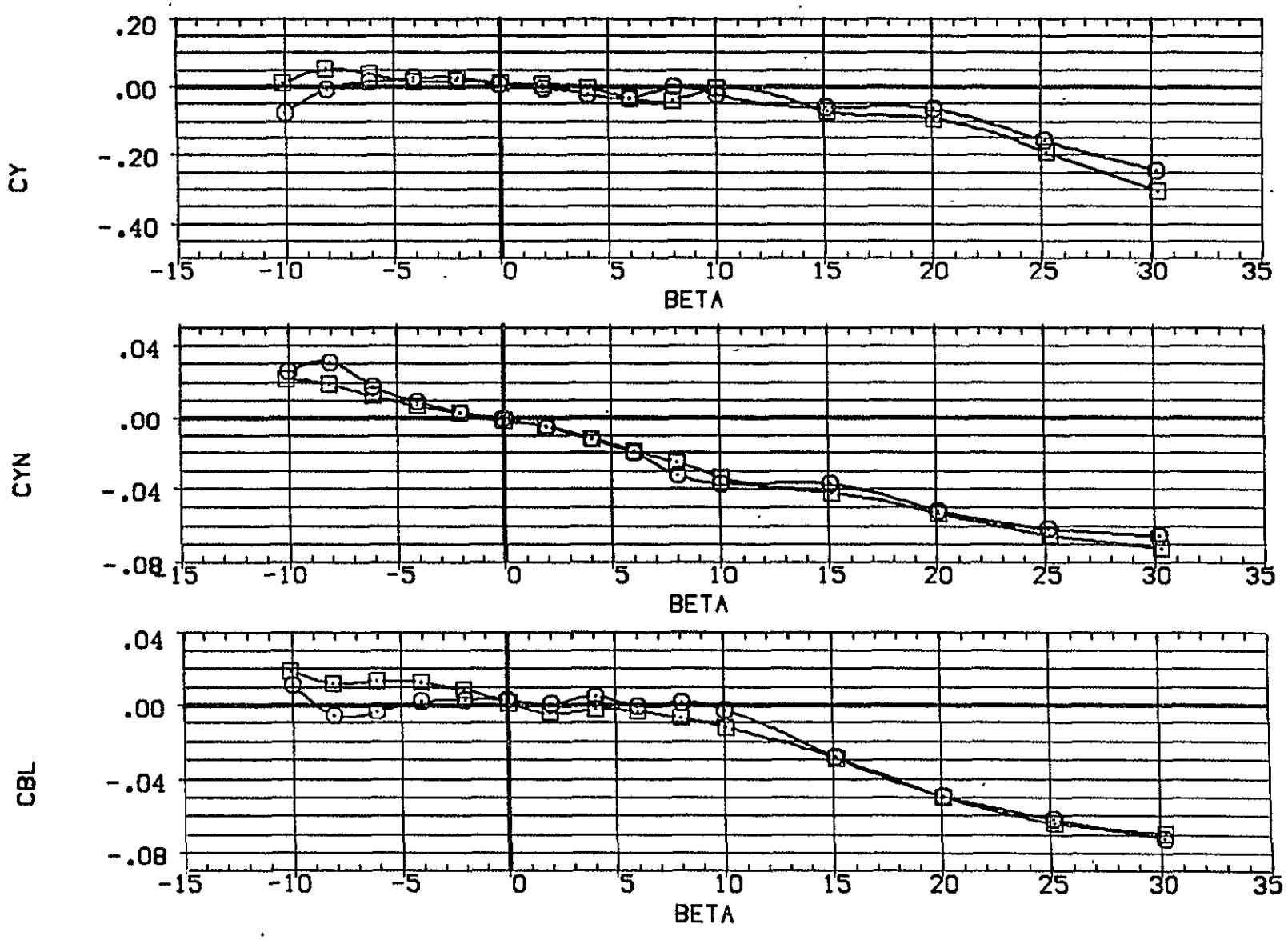

FIG. 8 EFFECT OF STORES ON AERODYNAMIC CHAR., REYNOLDS NO.= 13.12 MIL.

(B)ALPHA = 31.24

ORIGINAL PAGE IS
OF POOR QUALITY

DATA SET	SYMBOL	CONFIGURATION DESCRIPTION	AIL-L	AIL-R	STB-L	STB-R
(CDW010)	○	BASIC, RHO=11 + GRIT	.000	.000	-25.000	-25.000
(CDW012)	□	BASIC, RHO=11 + GRIT + A + B + C	.000	.000	-25.000	-25.000
(CDW014)	◇	BASIC, RHO=11 + GRIT + D	.000	.000	-25.000	-25.000
(CDW015)	△	BASIC, RHO=11 + GRIT + E	.000	.000	-25.000	-25.000

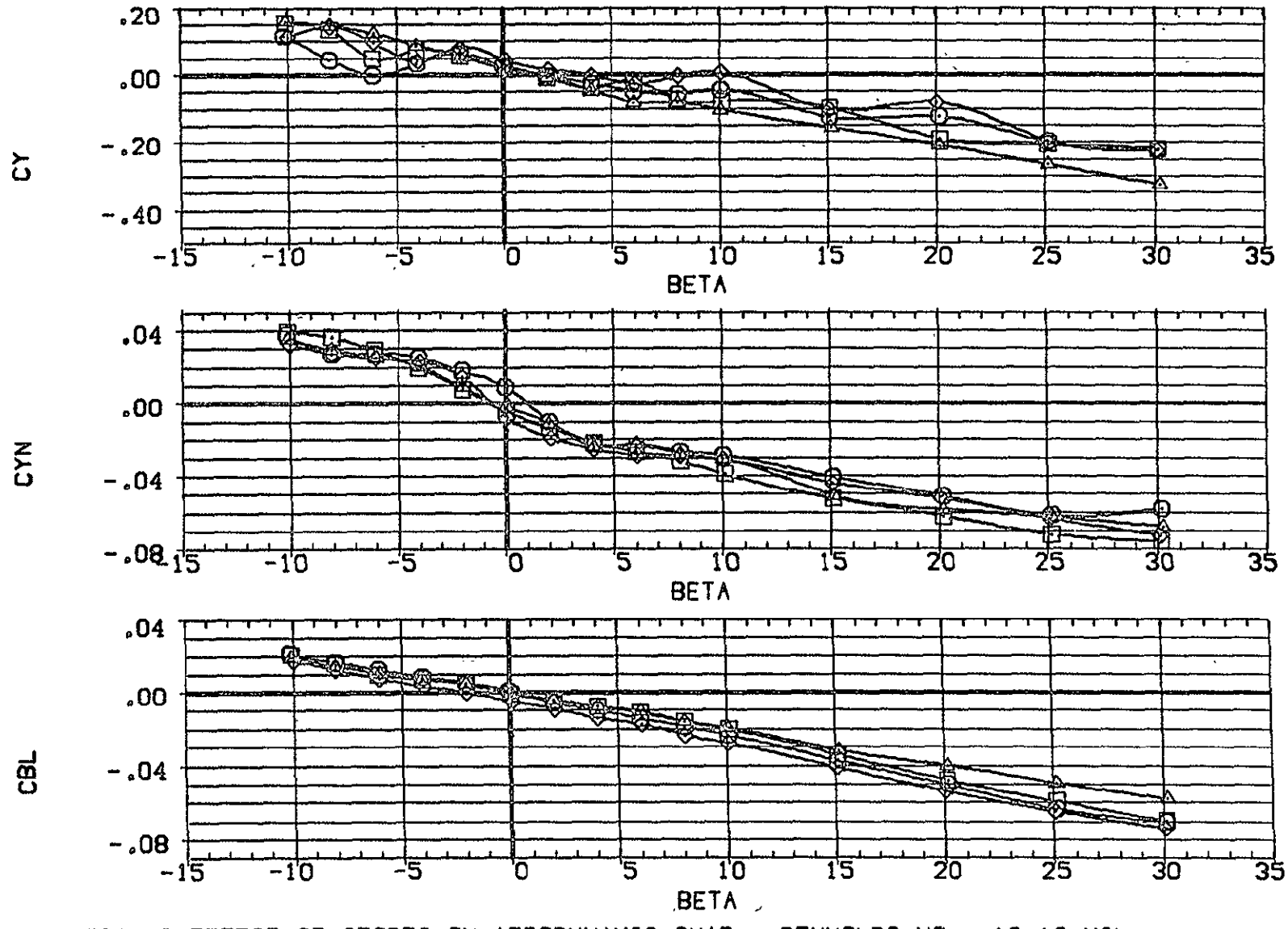

FIG. 8 EFFECT OF STORES ON AERODYNAMIC CHAR., REYNOLDS NO.= 13.12 MIL.

(C)ALPHA = 51.33

ORIGINAL PAGE IS OF POOR QUALITY

DATA SET	SYMBOL	CONFIGURATION DESCRIPTION	AIL-L	AIL-R	STB-L	STB-R
(CDW010)	○	BASIC, RHO=11 + GRIT	.000	.000	-25.000	-25.000
(CDW012)	□	BASIC, RHO=11 + GRIT + A + B + C	.000	.000	-25.000	-25.000
(CDW014)	◇	BASIC, RHO=11 + GRIT + D	.000	.000	-25.000	-25.000
(CDW015)	△	BASIC, RHO=11 + GRIT + E	.000	.000	-25.000	-25.000

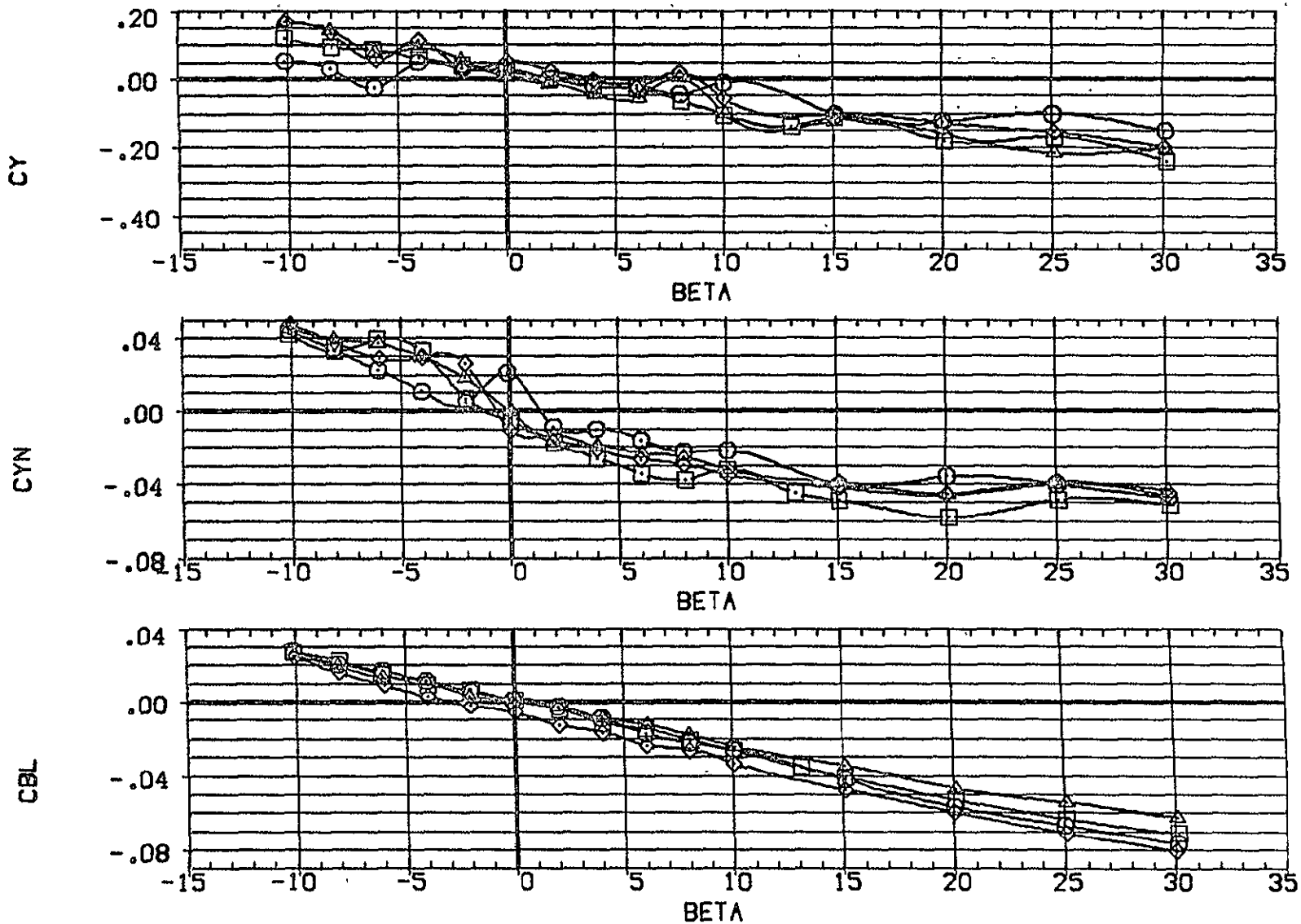

FIG. 8 EFFECT OF STORES ON AERODYNAMIC CHAR., REYNOLDS NO.= 13.12 MIL.

(D)ALPHA = 61.31

DATA SET	SYMBOL	CONFIGURATION DESCRIPTION	AIL-L	AIL-R	STB-L	STB-R
(CDW010)	○	BASIC, RHO=11 + GRIT	.000	.000	-25.000	-25.000
(CDW012)	□	BASIC, RHO=11 + GRIT + A + B + C	.000	.000	-25.000	-25.000
(CDW014)	◇	BASIC, RHO=11 + GRIT + D	.000	.000	-25.000	-25.000
(CDW015)	△	BASIC, RHO=11 + GRIT + E	.000	.000	-25.000	-25.000

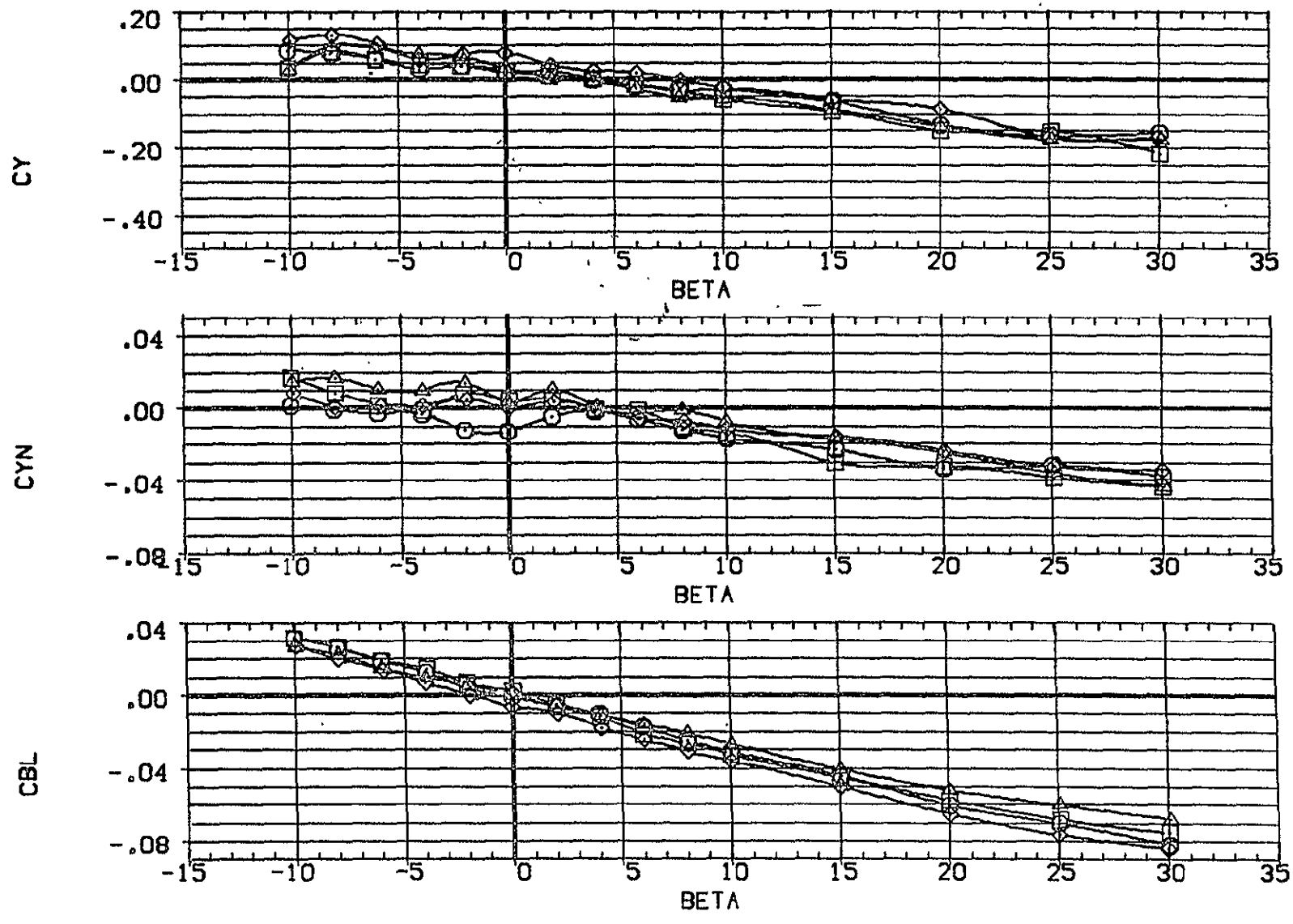

FIG. 8 EFFECT OF STORES ON AERODYNAMIC CHAR., REYNOLDS NO.= 13.12 MIL.

(E)ALPHA = 71.35

ORIGINAL PAGE IS
OF POOR QUALITY

101

DATA SET	SYMBOL	CONFIGURATION DESCRIPTION	AIL-L	AIL-R	STB-L	STB-R
(CDW010)	○	BASIC, RHO=11 + GRIT	.000	.000	-25.000	-25.000
(CDW012)	□	BASIC, RHO=11 + GRIT + A + B + C	.000	.000	-25.000	-25.000
(CDW014)	◇	BASIC, RHO=11 + GRIT + D	.000	.000	-25.000	-25.000
(CDW015)	△	BASIC, RHO=11 + GRIT + E	.000	.000	-25.000	-25.000

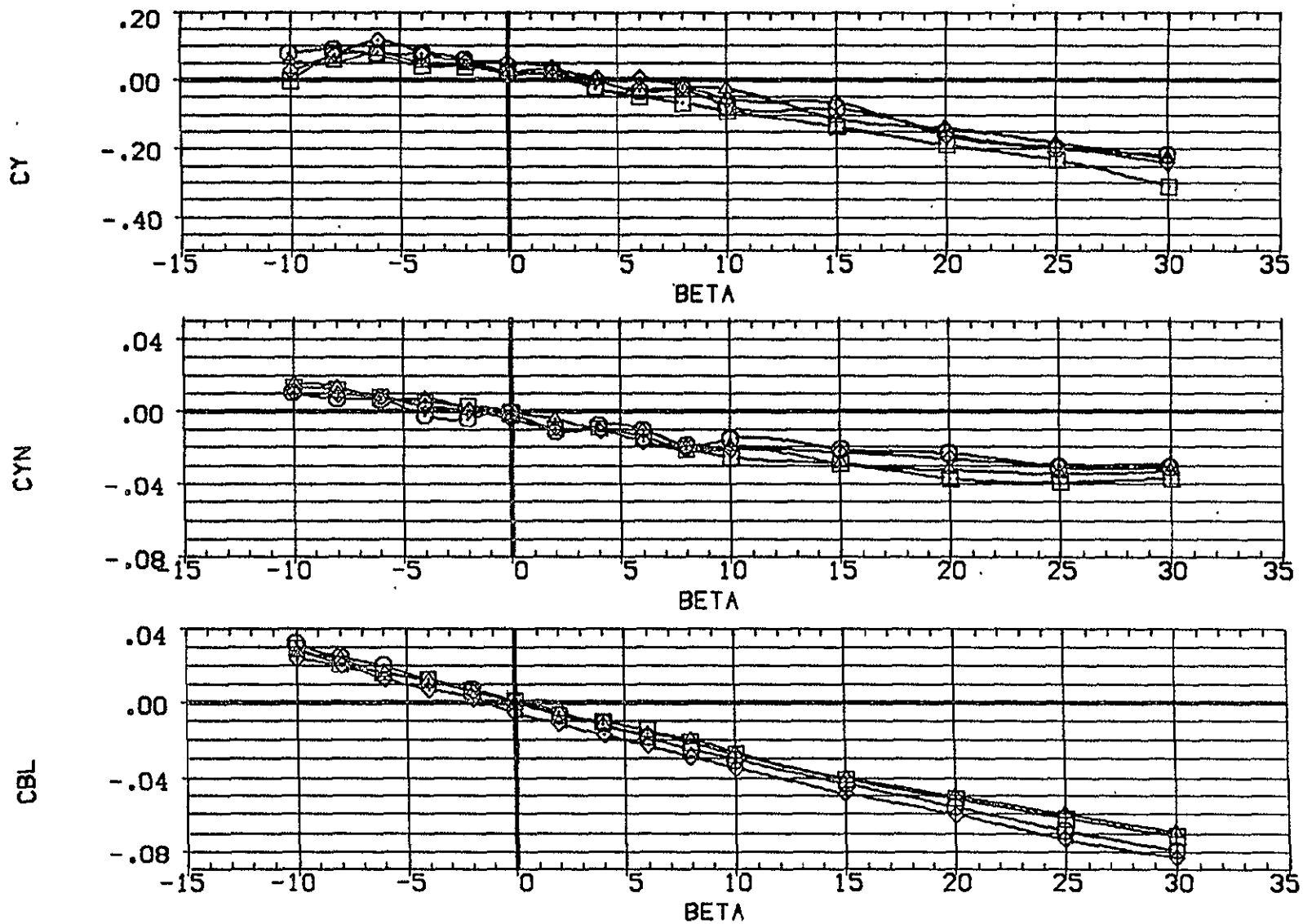

FIG. 8 EFFECT OF STORES ON AERODYNAMIC CHAR., REYNOLDS NO.= 13.12 MIL.

(F)ALPHA = 88.25

DATA SET	SYMBOL	CONFIGURATION DESCRIPTION	AIL-L	AIL-R	STB-L	STB-R
(CDV010)	○	BASIC, RHO=11 + GRIT	.000	.000	-25.000	-25.000
(CDV012)	□	BASIC, RHO=11 + GRIT + A + B + C	.000	.000	-25.000	-25.000
(CDV014)	◇	DATA NOT AVAILABLE	.000	.000	-25.000	-25.000
(CDV015)	△	DATA NOT AVAILABLE	.000	.000	-25.000	-25.000

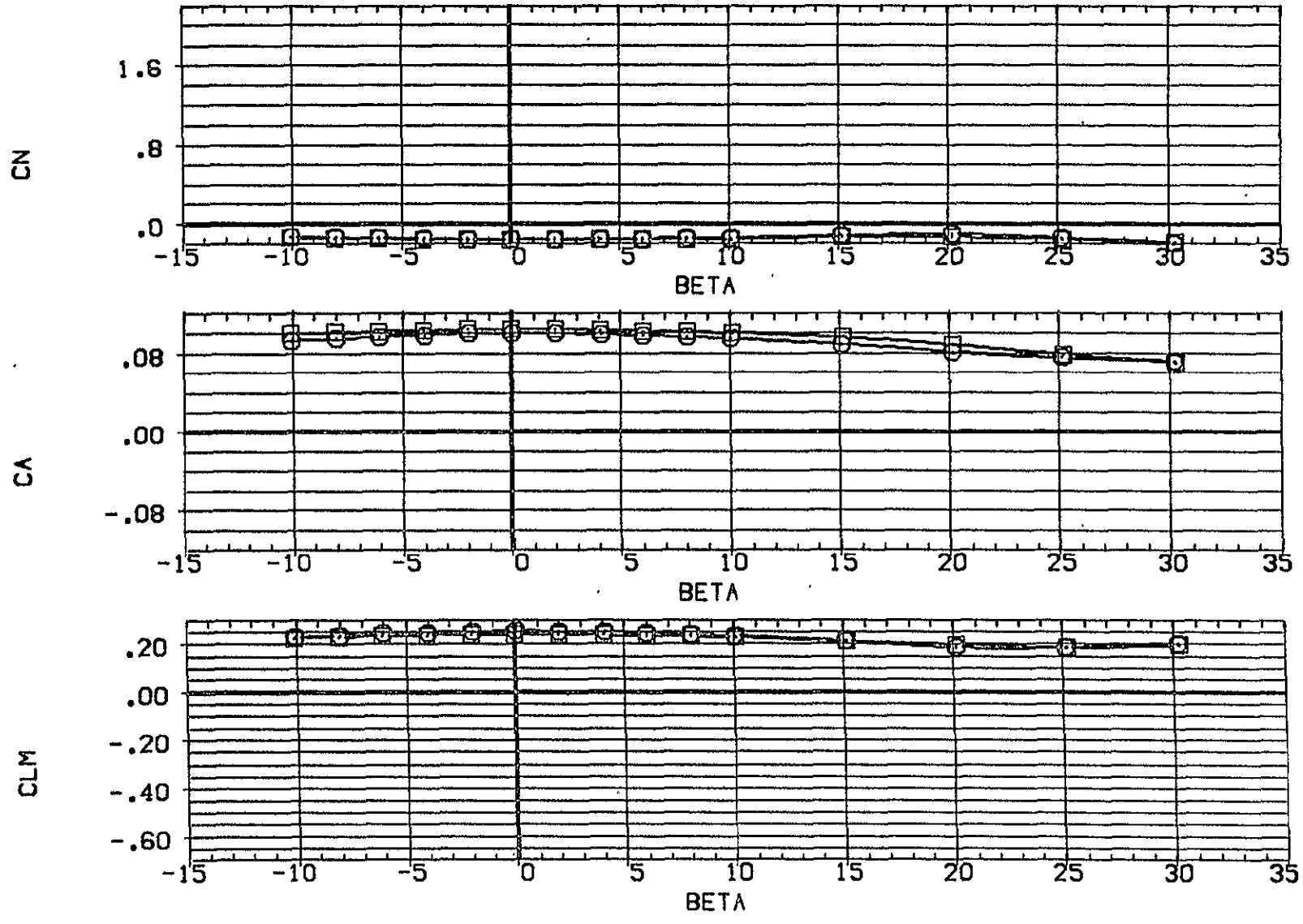

FIG. 8 EFFECT OF STORES ON AERODYNAMIC CHAR., REYNOLDS NO.= 13.12 MIL.

(A)ALPHA = -.24

ORIGINAL PAGE IS
OF POOR QUALITY

8 of 8

DATA SET	SYMBOL	CONFIGURATION DESCRIPTION	AIL-L	AIL-R	STB-L	STB-R
(CDW010)	○	BASIC, RHO=11 + GRIT	.000	.000	-25.000	-25.000
(CDW012)	□	BASIC, RHO=11 + GRIT + A + B + C	.000	.000	-25.000	-25.000
(CDW014)	◇	DATA NOT AVAILABLE	.000	.000	-25.000	-25.000
(CDW015)	△	DATA NOT AVAILABLE	.000	.000	-25.000	-25.000

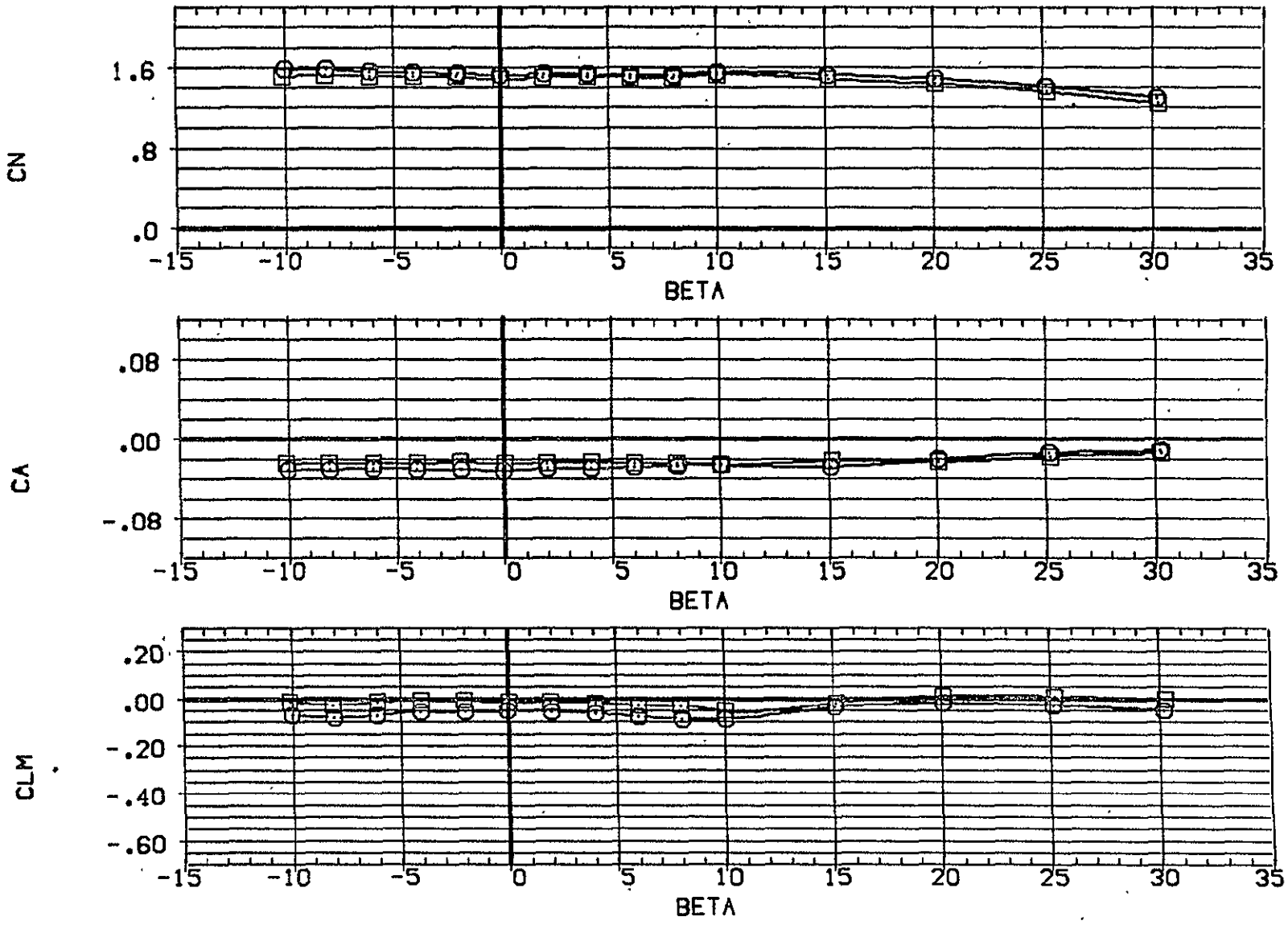

FIG. 8 EFFECT OF STORES ON AERODYNAMIC CHAR., REYNOLDS NO.= 13.12 MIL.

(B)ALPHA = 31.24

DATA SET	SYMBOL	CONFIGURATION DESCRIPTION	AIL-L	AIL-R	STB-L	STB-R
(CDW010)	○	BASIC, RHO=11 + GRIT	.000	.000	-25.000	-25.000
(CDW012)	□	BASIC, RHO=11 + GRIT + A + B + C	.000	.000	-25.000	-25.000
(CDW014)	◇	BASIC, RHO=11 + GRIT + D	.000	.000	-25.000	-25.000
(CDW015)	△	BASIC, RHO=11 + GRIT + E	.000	.000	-25.000	-25.000

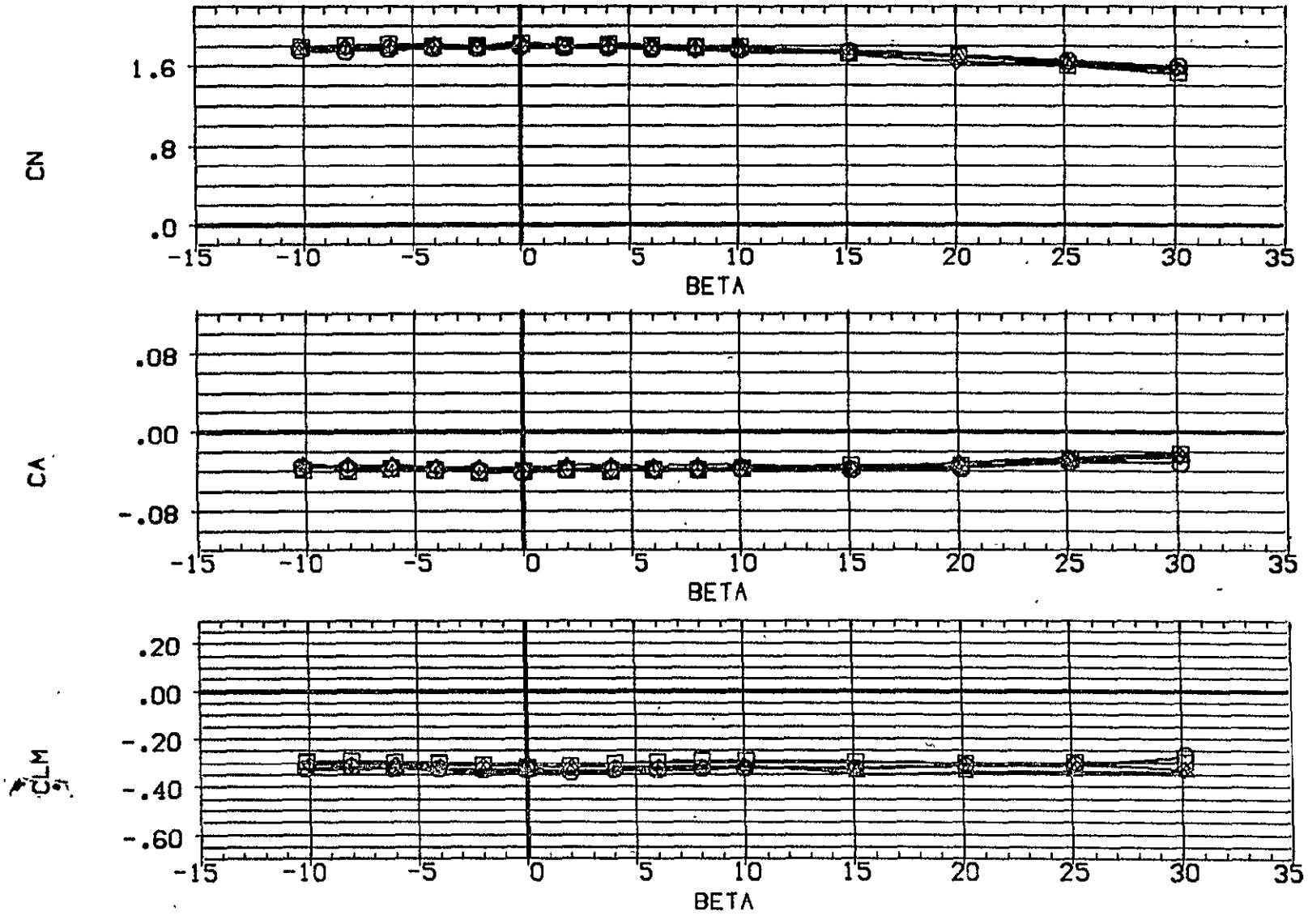

FIG. 8 EFFECT OF STORES ON AERODYNAMIC CHAR., REYNOLDS NO.= 13.12 MIL.

(C)ALPHA = 51.33

ORIGINAL PAGE IS
OF POOR QUALITY

DATA SET	SYMBOL	CONFIGURATION DESCRIPTION	AIL-L	AIL-R	STB-L	STB-R
(CDW010)	○	BASIC, RHO=11 + GRIT	.000	.000	-25.000	-25.000
(CDW012)	□	BASIC, RHO=11 + GRIT + A + B + C	.000	.000	-25.000	-25.000
(CDW014)	◇	BASIC, RHO=11 + GRIT + D	.000	.000	-25.000	-25.000
(CDW015)	△	BASIC, RHO=11 + GRIT + E	.000	.000	-25.000	-25.000

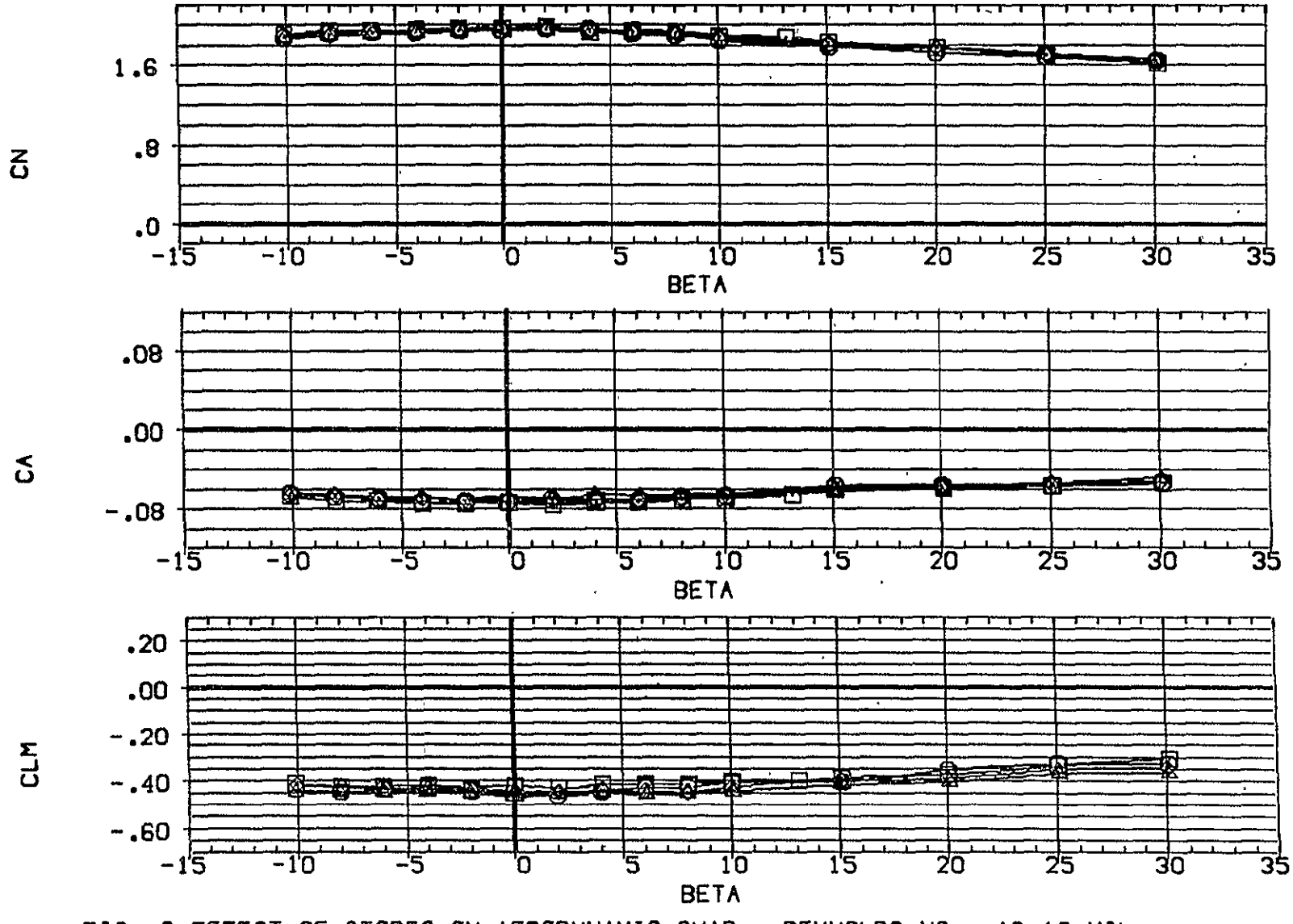

FIG. 8 EFFECT OF STORES ON AERODYNAMIC CHAR., REYNOLDS NO.= 13.12 MIL.

(D)ALPHA = 61.31

DATA SET	SYMBOL	CONFIGURATION DESCRIPTION	AIL-L	AIL-R	STB-L	STB-R
(CDW010)	○	BASIC, RHO=11 + GRIT	.000	.000	-25.000	-25.000
(CDW012)	□	BASIC, RHO=11 + GRIT + A + B + C	.000	.000	-25.000	-25.000
(CDW014)	⋈	BASIC, RHO=11 + GRIT + D	.000	.000	-25.000	-25.000
(CDW015)	△	BASIC, RHO=11 + GRIT + E	.000	.000	-25.000	-25.000

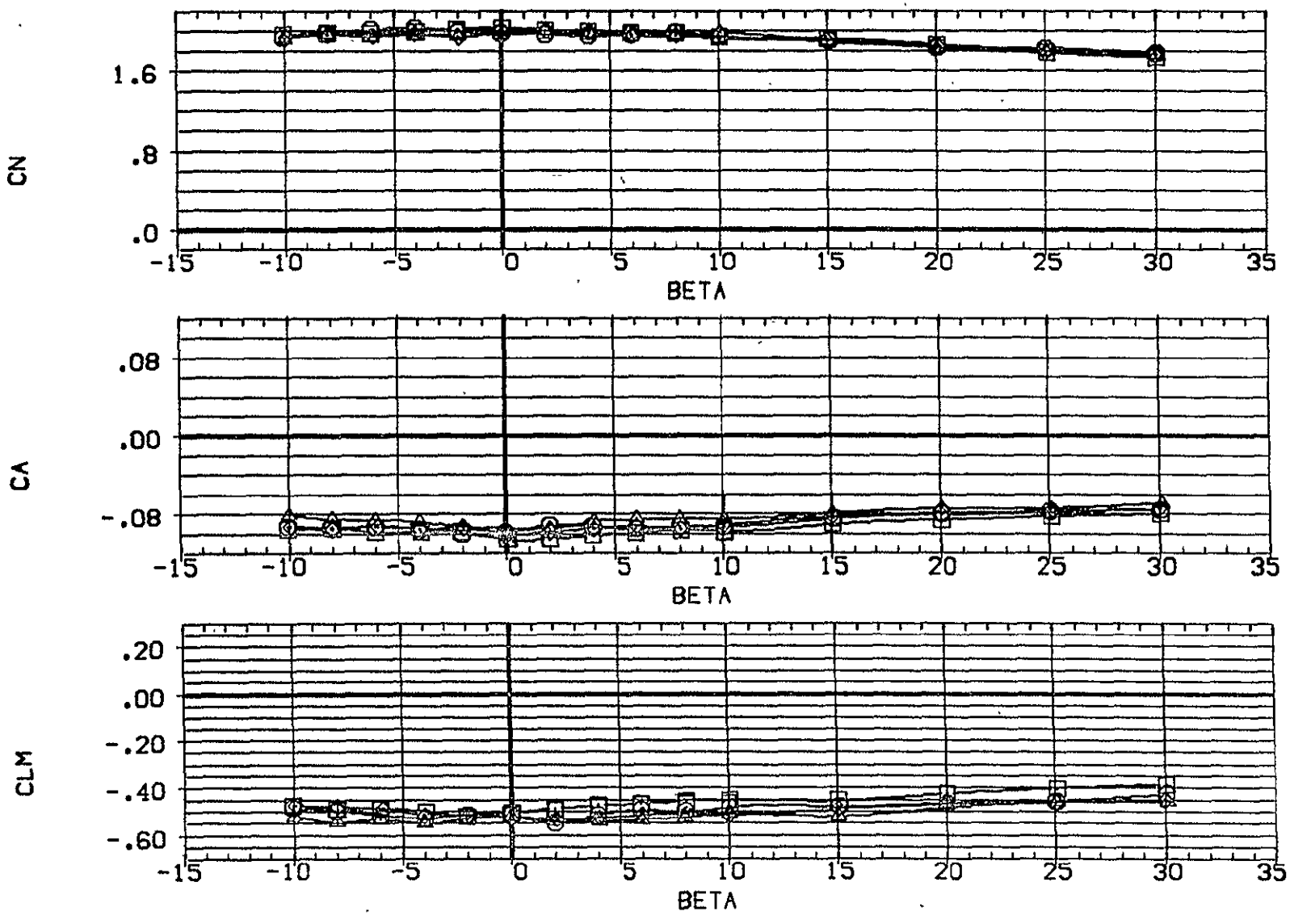

FIG. 8 EFFECT OF STORES ON AERODYNAMIC CHAR., REYNOLDS NO.= 13.12 MIL.

(E)ALPHA = 71.35

ORIGINAL PAGE IS
OF POOR QUALITY

DATA SET	SYMBOL	CONFIGURATION DESCRIPTION	AIL-L	AIL-R	STB-L	STB-R
(CDW010)	○	BASIC, RHO-11 + GRIT	.000	.000	-25.000	-25.000
(CDW012)	□	BASIC, RHO-11 + GRIT + A + B + C	.000	.000	-25.000	-25.000
(CDW014)	◇	BASIC, RHO-11 + GRIT + D	.000	.000	-25.000	-25.000
(CDW015)	△	BASIC, RHO-11 + GRIT + E	.000	.000	-25.000	-25.000

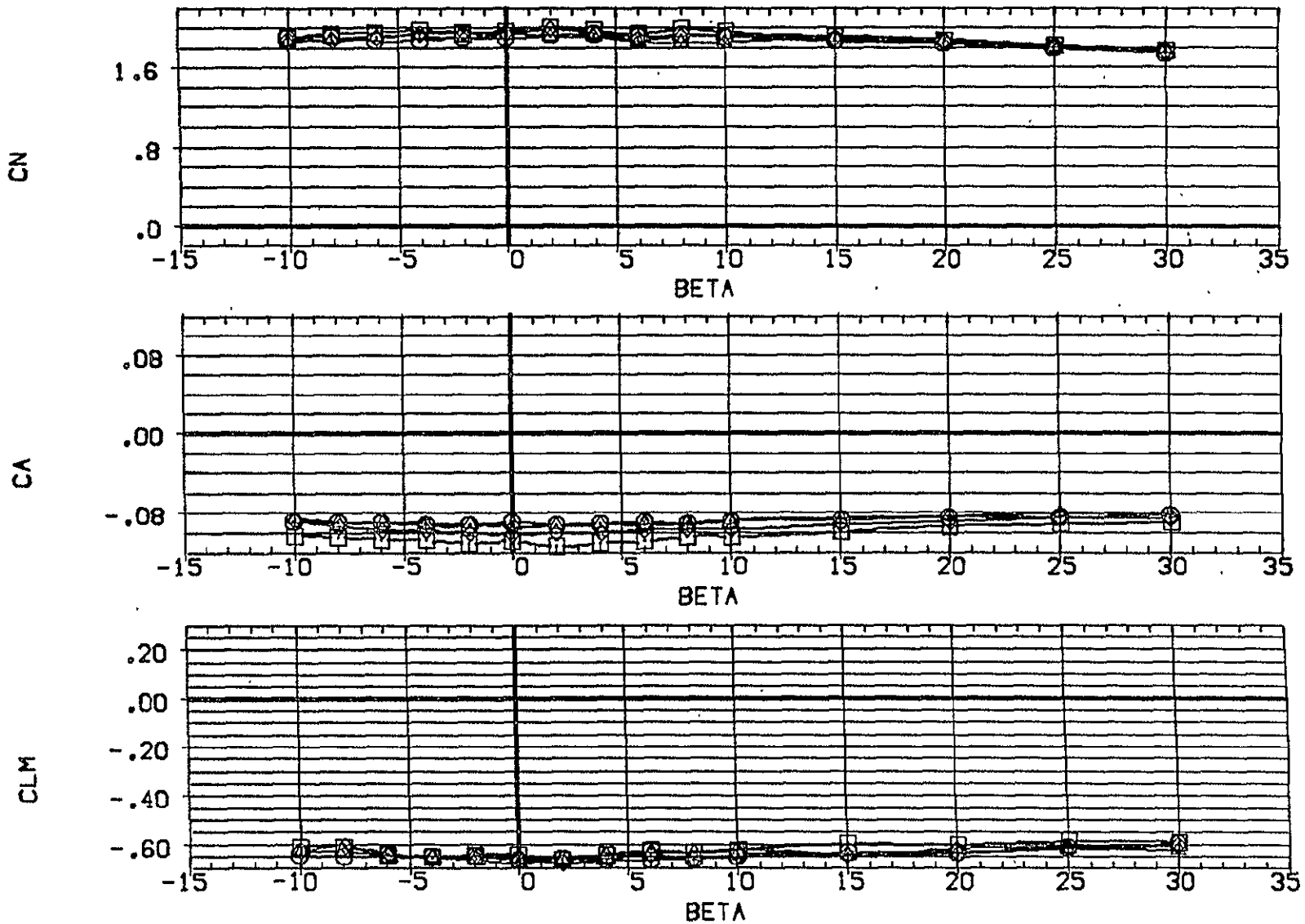

FIG. 8 EFFECT OF STORES ON AERODYNAMIC CHAR., REYNOLDS NO.= 13.12 MIL.

(F)ALPHA = 88.25

DATA SET	SYMBOL	CONFIGURATION DESCRIPTION	RN/L
(FDW020)	○	BASIC, RHO=11 - F	1.476
(FDW029)	□	BASIC, RHO=11 - F + G	1.476
(FDW032)	◇	BASIC, RHO=11 - F + H	1.476
(FDW028)	△	BASIC, RHO=11 - F	16.400
(FDW031)	▽	BASIC, RHO=11 - F + G	16.400
(FDW034)	⬠	BASIC, RHO=11 - F + H	16.400

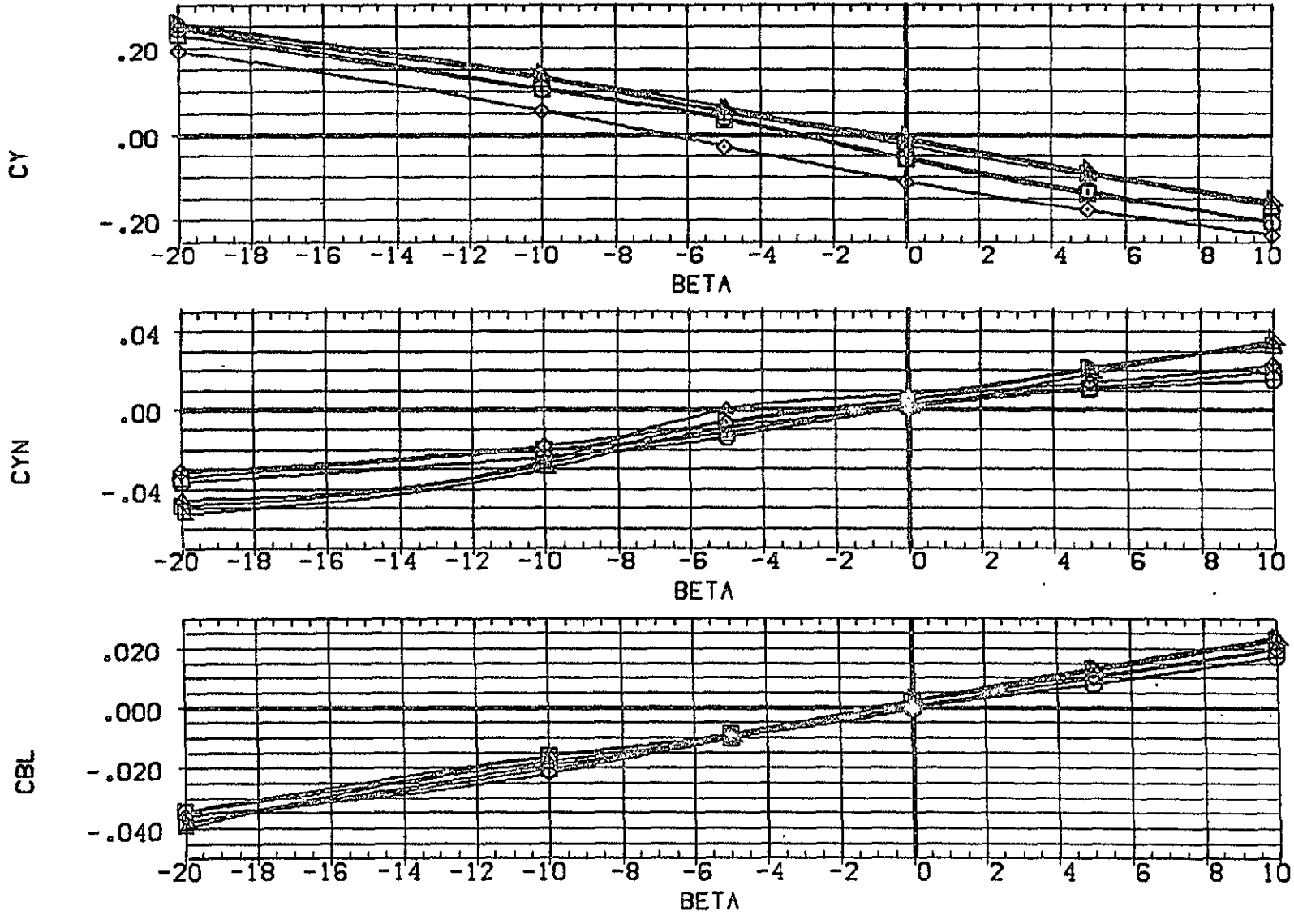

ORIGINAL PAGE IS
OF POOR QUALITY

FIG. 9 EFFECT OF NOSE SHAPE FOR 2 REYN. NOS. AT VARIOUS ALPHAS, ZERO CON. SURF.

(A)ALPHA =-80.00

DATA SET	SYMBOL	CONFIGURATION DESCRIPTION	RN/L
(FDV020)	□	BASIC, RHO=11 - F	1.476
(FDV029)	□	BASIC, RHO=11 - F + G	1.476
(FDV032)	◇	BASIC, RHO=11 - F + H	1.476
(FDV028)	△	BASIC, RHO=11 - F	16.400
(FDV031)	△	BASIC, RHO=11 - F + G	16.400
(FDV034)	△	BASIC, RHO=11 - F + H	16.400

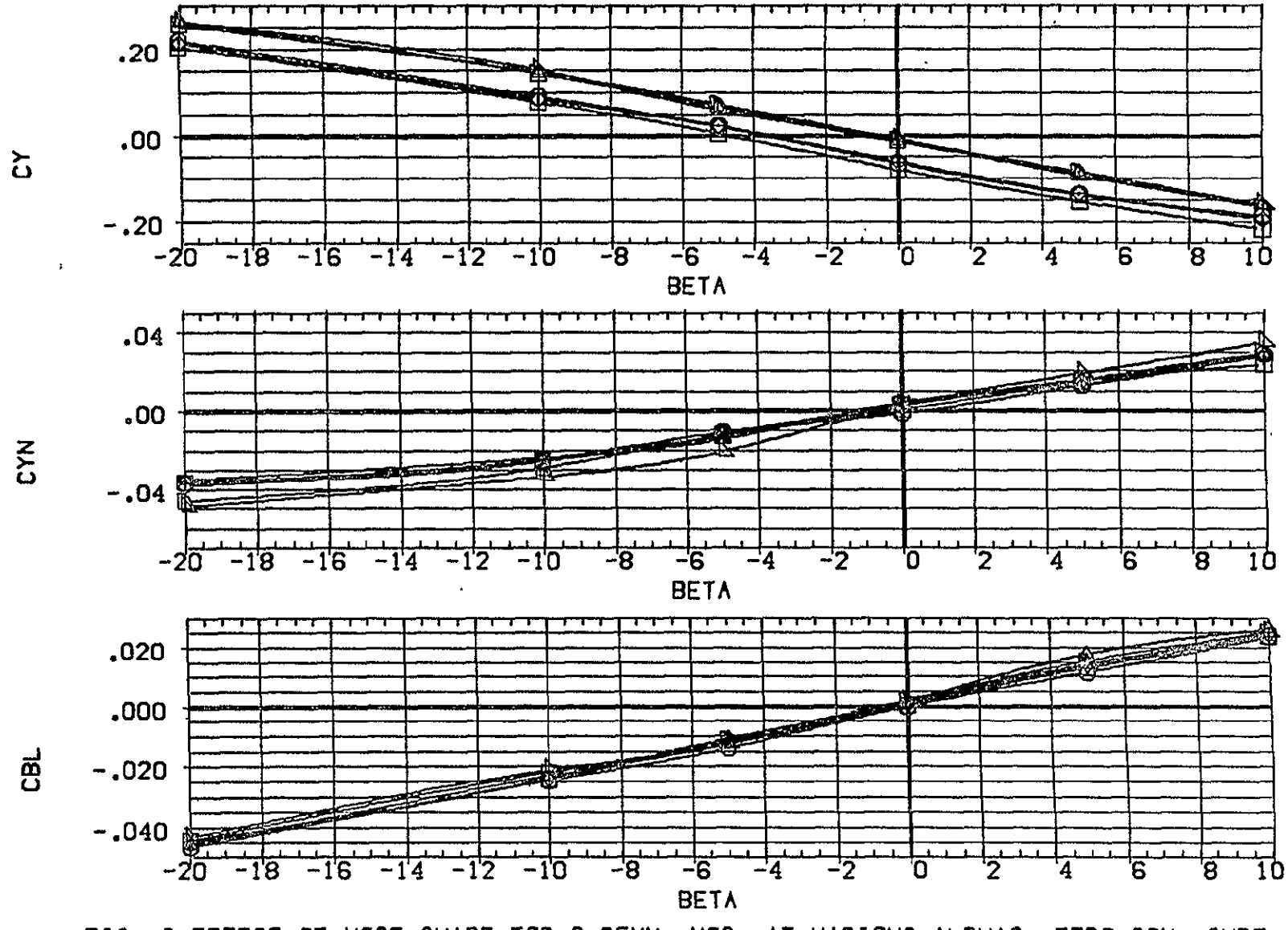

FIG. 9 EFFECT OF NOSE SHAPE FOR 2 REYN. NOS. AT VARIOUS ALPHAS, ZERO CON. SURF.

(B)ALPHA =-70.00

ORIGINAL PAGE IS
OF POOR QUALITY

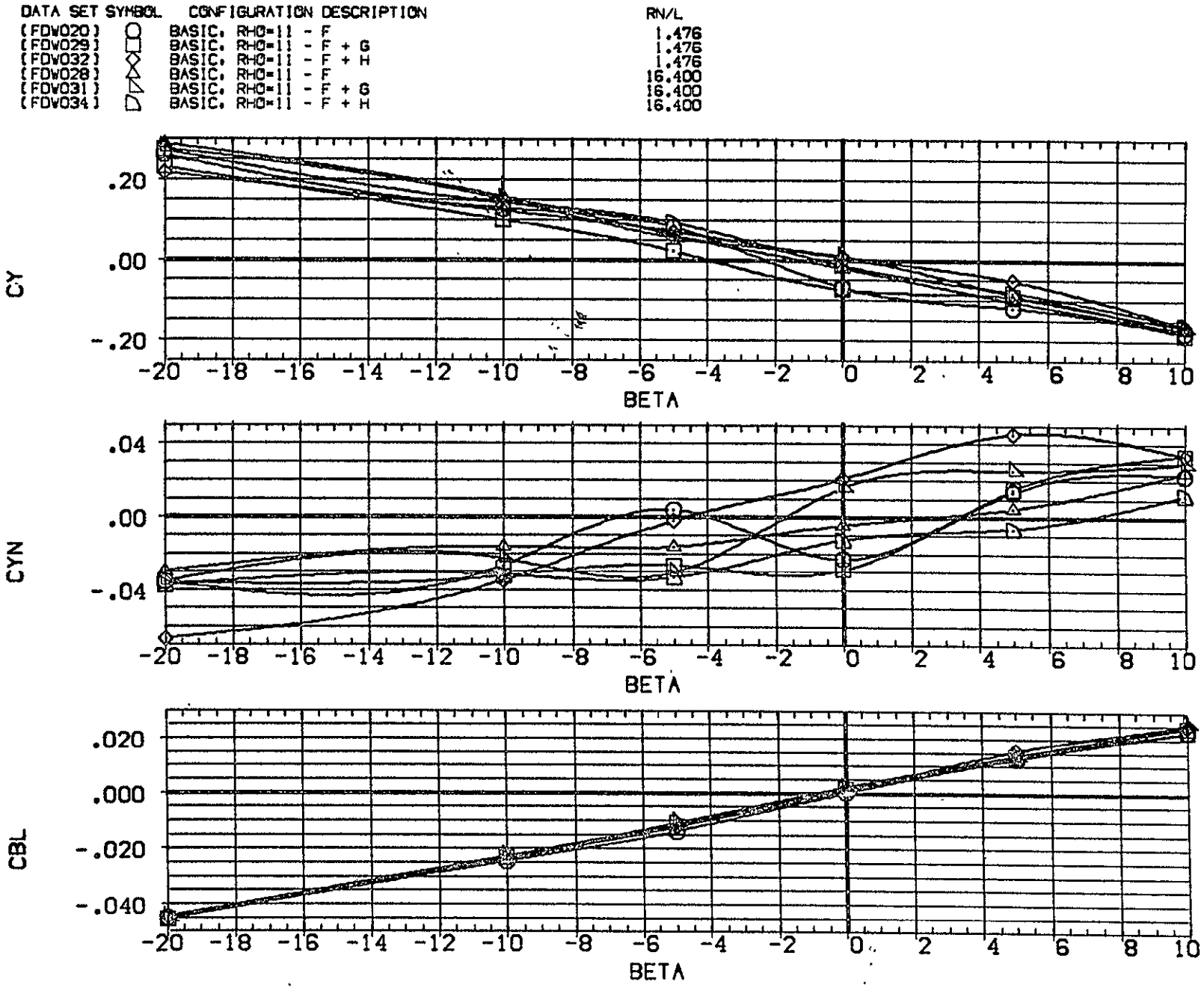

FIG. 9 EFFECT OF NOSE SHAPE FOR 2 REYN. NOS. AT VARIOUS ALPHAS, ZERO CON. SURF.

(C)ALPHA =-60.00

DATA SET	SYMBOL	CONFIGURATION DESCRIPTION	RN/L
(GDW020)	○	BASIC, RHO=11 - F	1.476
(GDW029)	□	BASIC, RHO=11 - F + G	1.476
(GDW032)	◇	BASIC, RHO=11 - F + H	1.476
(GDW028)	△	BASIC, RHO=11 - F	16.400
(GDW031)	▽	BASIC, RHO=11 - F + G	16.400
(GDW034)	▽	BASIC, RHO=11 - F + H	16.400

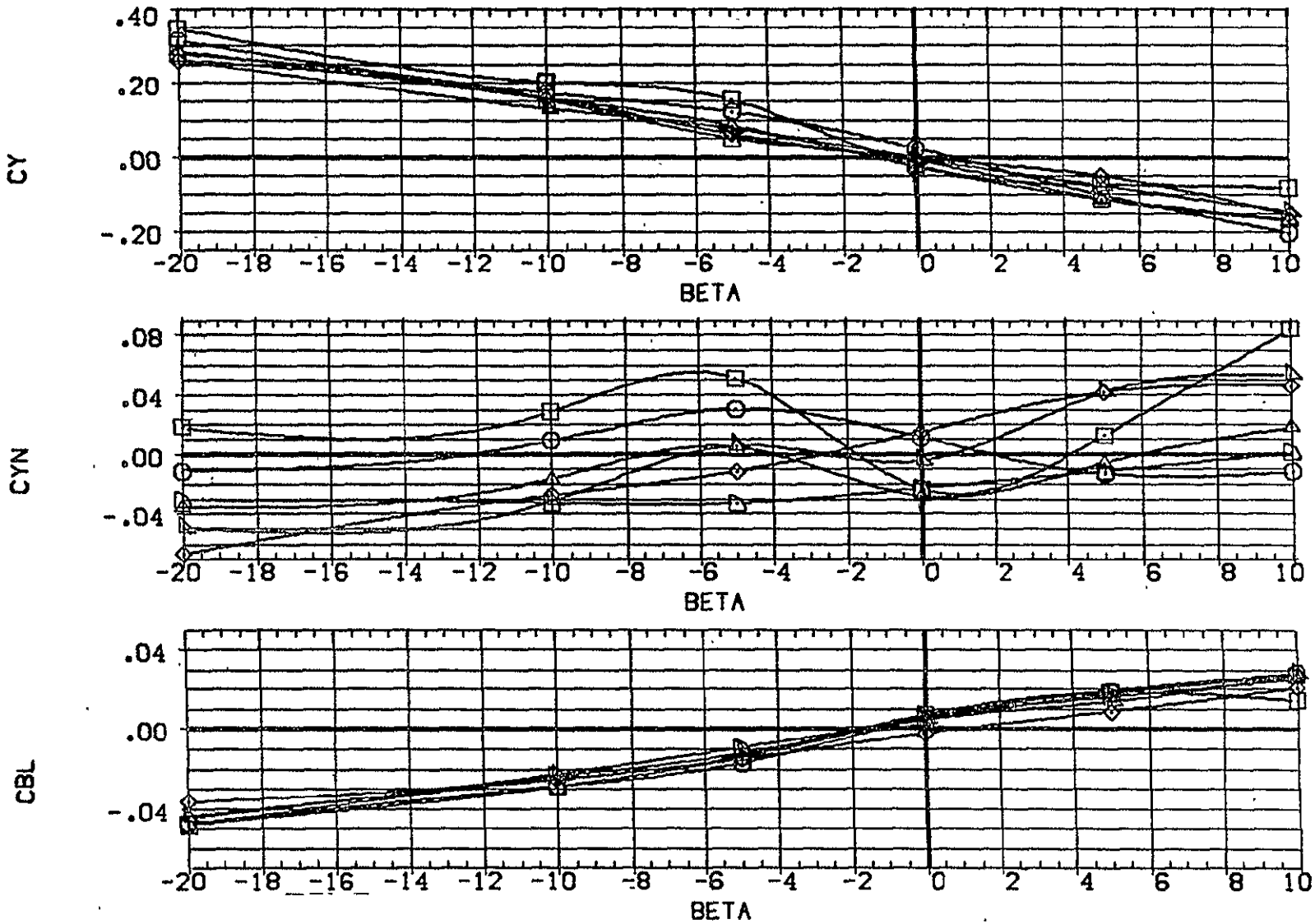

FIG. 9 EFFECT OF NOSE SHAPE FOR 2 REYN. NOS. AT VARIOUS ALPHAS, ZERO CON. SURF.

(A)ALPHA =-50.00

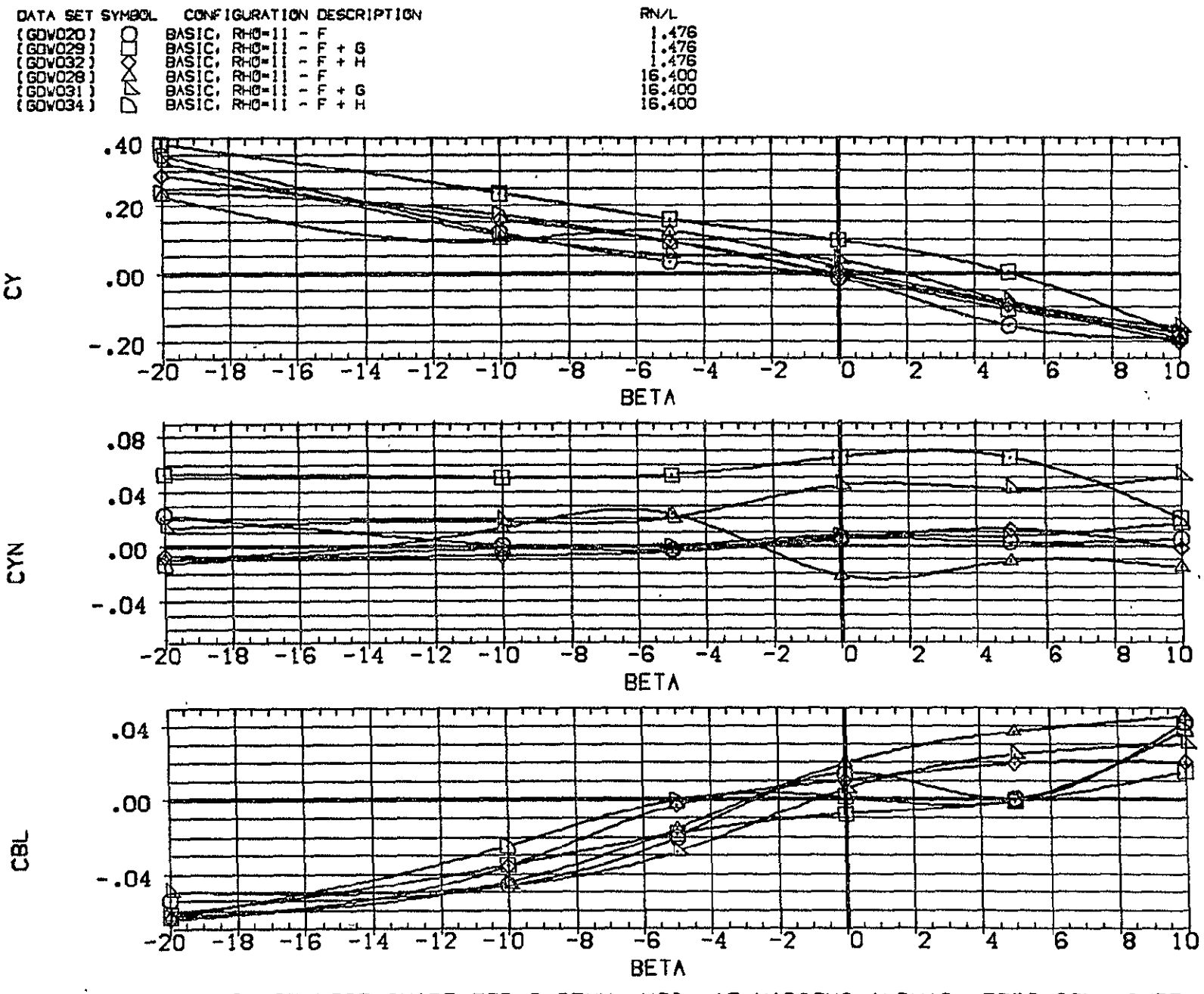

FIG. 9 EFFECT OF NOSE SHAPE FOR 2 REYN. NOS. AT VARIOUS ALPHAS, ZERO CON. SURF.

(B)ALPHA = -10 20

ORIGINAL PAGE IS
OF POOR QUALITY